Study of particle physics models with implication for dark matter and cosmic ray phenomenology

A thesis submitted in partial fulfillment of

the requirements for the degree of

Doctor of Philosophy

by

Gaurav Kumar Tomar

(Roll No. 11330006)

Under the guidance of

Prof. Subhendra Mohanty

Theoretical Physics Division

Physical Research Laboratory, Ahmedabad, India.

DISCIPLINE OF PHYSICS

INDIAN INSTITUTE OF TECHNOLOGY GANDHINAGAR

2015

To

My Family

Declaration

I declare that this written submission represents my ideas in my own words and where others' ideas or words have been included, I have adequately cited and referenced the original sources. I also declare that I have adhered to all principles of academic honesty and integrity and have not misrepresented or fabricated or falsified any idea/data/fact/source in my submission. I understand that any violation of the above can cause disciplinary action by the Institute and can also evoke penal action from the sources which have thus not been properly cited or from whom proper permission has not been taken when needed.

Gaurav Kumar Tomar

(Roll No: 11330006)

Date: July 19, 2016

CERTIFICATE

It is certified that the work contained in the thesis titled **"Study of particle physics models with implication for dark matter and cosmic ray phenomenology"** by **Mr. Gaurav Kumar Tomar** (Roll No. 11330006), has been carried out under my supervision and that this work has not been submitted elsewhere for a degree.

Prof. Subhendra Mohanty
(Thesis Supervisor)
Professor,
Theoretical Physics Division
Physical Research Laboratory,
Ahmedabad, India.

Date:

Acknowledgements

It has been a great prerogative to stay in Physical Research Laboratory for several years, where I got a research as well as homely atmosphere throughout my PhD tenure. It gives me a great pleasure to acknowledge all those who supported me directly or indirectly and made this thesis possible.

First and foremost, I wish to express my sincere gratitude to my supervisor, Prof. Subhendra Mohanty, for giving me guidance, encouragement and support throughout my PhD tenure that lead up to this thesis. It has always been a great pleasure to discuss with him in an open and frank atmosphere created by him. I am very thankful to him for keeping faith in me and giving me encouragement time to time, which was invaluable source of confidence. I am also grateful to him for introducing me to the interesting and challenging problems of the field, which will play an important role in my future research.

I am also thankful to my collaborator Prof. Sandip Pakvasa for his invaluable wisdom and insight.

I take the opportunity to thank Prof. Hiranmaya Mishra, Dr. Namit Mahajan, Prof. S. Goswami, Prof. R. Rangarajan, Prof. Jitesh Bhatt, Dr. B.K.Sahoo, Dr. Partha Konar and Prof. Mohanty for teaching several useful courses at various times during my Ph.D. I also thank the other faculty members of theory group : Prof. Sarkar, Prof. Joshipura, Prof. Rindani, Prof. Dilip Angom and Dr. N. Singh for creating a friendly, interactive atmosphere to work. I am especially thankful to Dr. Namit Mahajan and Dr. Partha Konar for useful discussions from which I learned a lot.

I would especially like to thank my seniors and collaborators Soumya Rao, Tanushree Basak and Ujjal Dey for their enthusiasm and stimulating discussions. The continuous company and support of Tanushree, Gaveshna, Ila, Ujjal, Naveen, and Yashpal has always kept me recharged. A very special thanks to my seniors Arvind Singh, Vimal Don, Vinni, Shashi Prabhakar, Sudip Haldar, and juniors Girish Kumar (aka Keju), Alok Tiwary and Arun Pandey for their continuous support and light moments. I thank all my batch-mates especially Naveen, Yashpal, Wageesh, Arko, Upendra, Gaurav Sharma, Reddy, Monojit, Gulab, Avdesh and Bhavya for cheering with me.

My special thanks to T.N. Soorya sir for his invaluable support, and giving me right-direction at the crucial moment of my life. I am also thankful to my precious friends Sunil Kumra, Hardeep Singh and Tarkeshwar Singh for making my life cheerful by putting ghatiya jokes or roaming around without any purpose. Thank you very much buddies!

I am also grateful to Razaa and Sujata ben for their sincere support and help whenever I asked.

Last, but not the least, I would be nowhere around here without the love and support of my family. Words cannot express my gratitude for my babuji, bhaiyya and didi. I am very thankful to Bhavya for her continuous and unconditional support and being with me whenever I felt alone and weak. I am also thankful to Bhavya's family for their support and faith in me. Finally, I must also acknowledge the love, support and blessings of friends, teachers, relatives and all known and unknown persons whom I met with or interacted with in life.

Gaurav Tomar

Abstract

There are many observations in particle physics and cosmology, which seek physics beyond standard model for their explanation. Some of them are : The excess of positron over cosmic ray background observed by AMS-02 experiment, the 3.6σ discrepancy between muon $(g-2)$ measurement by BNL and its standard model prediction, and the absence of Glashow-resonance in the PeV neutrino events at IceCube. As the thesis title indicates this work is about the study of particle physics models which not only explain the mentioned observations but also give a suitable candidate of dark matter with correct relic density.

In the work presented here we have proposed a gauged horizontal symmetry model for which we introduce a 4th generation of fermions into SM. We then introduce a $\mathrm{SU(2)_{HV}}$ vector gauge symmetry between the 4th generation leptons and muon families. The 4th generation right-handed neutrino is identified as dark matter which annihilates into leptons final state $(\mu^+\mu^-, \nu_\mu^c\nu_\mu)$ giving rise to correct relic density. In this model, dark matter is lephtophilic in nature, so it can explain AMS-02 positron excess remaining consistent with stringent bounds from antiproton. It is also possible to alleviate the discrepancy in muon $(g-2)$ from 4th generation charge lepton, $\mathrm{SU(2)_{HV}}$ gauge boson, and from neutral and charged scalars. In this way, both the signals, muon $(g-2)$ and the excess of positron can be explained simultaneously. We have also studied an alternative left-right model called dark left-right model, where it is possible to accommodate a suitable dark matter candidate. The second generation right-handed neutrino is identified as dark matter which dominantly annihilates into leptons final state. So it is possible to explain AMS-02 positron excess and lift the stringent bounds from antiproton. The singly and doubly charged scalars in dark left-right model also contribute to muon $(g-2)$ and so both the signatures can also be related in this model.

Another part of this thesis deals with the absence of Glashow resonance at IceCube PeV neutrino events. The IceCube collaboration has observed neutrino of very high energy which goes upto ~ 3 PeV, but did not see any events at Glashow resonance. The Glashow resonance gives rise to an enhanced cross-section for $\bar{\nu}_e$

at resonance energy 6.3 PeV which increases the detection rate of $\bar{\nu}_e$ by a factor of ~ 10. This implies that at least some of the events should have been observed at Glashow resonance, but none were. We proposed a new mechanism which can explain why neutrinos arising from astrophysical process may be suppressed. We assume a Lorentz violating higher dimensional operator, which modified dispersion relation of neutrinos (antineutrinos). As a result, pion and kaon decay widths get suppressed and we observe a cutoff in the neutrino spectrum which is consistent with IceCube data.

Keywords: Dark Matter, Beyond Standard Model, Relic abundance, Gauge extension, Muon magnetic moment, PeV neutrino events.

Contents

List of Figures

List of Tables

Chapter 1

Introduction

There are many observations in particle physics and cosmology, which require physics beyond the Standard Model (SM) for their explanation. The pattern of neutrino masses, the identity of Dark Matter (DM), and explanation of the observed matter-antimatter asymmetry are some of the well known open problems in particle physics.
Some specific experimental observations which call new physics for their explanation are :

- Observation of the excess of positron upto TeV energies at Alpha Magnetic Spectrometer (AMS-02) [1,2].

- The 3.6σ discrepancy between measurement of muon $(g-2)$ by Brookhaven National Laboratory (BNL) [3,4] and SM prediction.

- Non observation of Glashow-resonance in the PeV neutrino events at IceCube [5–8].

It is desirable to construct models of particle physics that can explain more than one experimental anomaly simultaneously. In addition a dark matter model, which explains the AMS-02 positron signal and muon $(g-2)$ anomaly must also be consistent with the dark matter relic density measured by Planck [9] and must evade the bounds from direct detection experiments [10–14] as well as other indirect signals of DM like γ-ray flux measured by Fermi-LAT [15] and HESS [16].

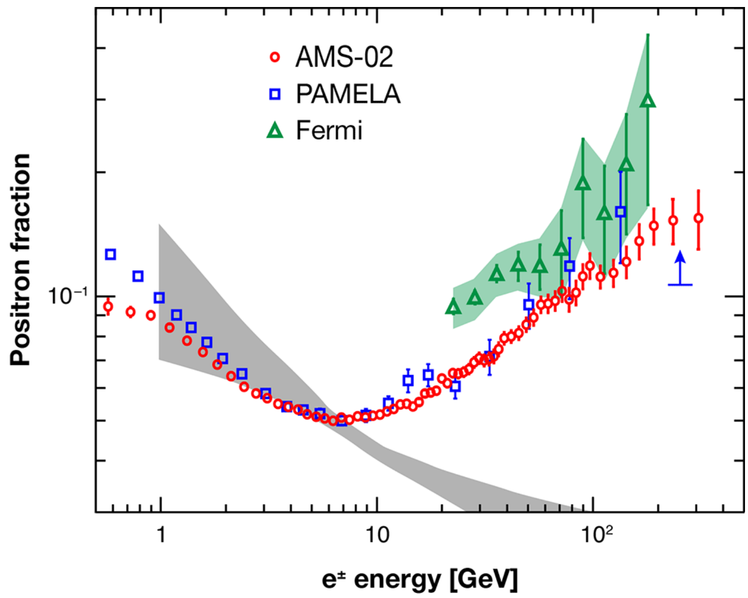

Figure 1.1: The excess of positron compared with the most recent measurements from AMS-02 [1, 2], Fermi-LAT [15] and PAMELA [17].

In the following, we list the known experimental properties of dark matter which all models constructed have to be consistent with.

1.1 AMS-02 positron excess

International space station based AMS-02 is one of the experiments, which is observing high energy cosmic rays. The new data from AMS-02 collaboration [1, 2] has confirmed the excess of positrons over cosmic ray background, which was observed first by PAMELA [17] followed by Fermi-LAT experiment [15]. But there is no antiproton excess over cosmic ray background as observed by AMS-02 experiment [18]. In Fig.(1.1), positron excess observed by these experiments over cosmic ray background is shown.

A population of nearby pulsars can provide an explanation [19–22] for the observed positron excess. However in the case of pulsars, an anisotropy is expected in the signal due to differing positions of individual contributing pulsars, which falls nearly an order of magnitude below the current constraints from both AMS-02 and the Fermi-LAT experiments [23]. Dark matter annihilation into SM particles can give a viable explanation for observed positron excess, but there exist stringent bounds from the absence of antiproton excess. If DM only couples to leptons (known as leptophilic DM [24–26]), it can not only explain the observed positron excess but also evade the stringent bounds from the absence of antiproton excess. It has been shown that to explain AMS-02 positron excess, the required cross-section into $\mu^+\mu^-$ final state is $\sigma v \sim 10^{-24}$ cm^{3}sec^{-1} [27, 28] for TeV scale DM, but such large cross-section is constrained by recent Planck results [29]. Therefore, a large astrophysical boost [30, 31] is necessarily required for explaining AMS-02 positron excess. Dark matter annihilation into other possible final states e.g. e^+e^- and $\tau^+\tau^-$, has also been considered [32–34]. In case of e^+e^- final state, a hard positron spectrum is expected which is not consistent with the observed data. For $\tau^+\tau^-$ final state, it is possible to satisfy the observed positron excess with somewhat high (compared to $\mu^+\mu^-$ final state) mass of DM [1]. In Section.2.2.2 and Section.3.2.1, we discuss leptophilic DM models that can explain the AMS-02 positron excess, keeping in agreement with antiproton absence over cosmic ray background. The decaying DM [2] with leptonic final states is another intriguing possibility used to explain AMS-02 positron excess [36, 37]. We now discuss in details the general properties of DM which are known and which the particle physics models have to be consistent with.

1.1.1 Dark Matter

DM constitutes around 84.5% of the total matter of the Universe. There are many direct and indirect methods by which dark matter can be searched. We review DM evidences, possible particle candidates, and its direct and indirect searches in the following sections.

Evidence of dark matter

In spite of its most compelling cosmological evidence, the first indication of dark matter existence dates back to 1930's. In 1933, Fritz Zwicky noticed that the

[1] The branching ratio of τ decay to e is only 17% in compared to μ, so the required dark matter mass for τ final state is larger than μ.

[2] Dark matter can also decay giving rise to SM particles, but its life-time should be larger than age of the Universe. For review see [35].

total amount of mass as deduced from the observation of Coma Cluster [38], did not match with the mass needed for explaining the rotation of galaxies around the Coma Cluster's halo. He credited this discrepancy to some mysterious massive component and christened it as "dark matter". After 50 years, using advanced technique of measurement of rotation curves, Rubin [39] and Albada [40] confirmed the existence of DM as apparent in Fig.(1.2).

According to Newtonian dynamics, the radial velocity of a galaxy should be falling as $1/\sqrt{r}$, but instead the rotation curve shows a roughly flat behavior as shown in Fig.(1.2). This observation suggests the existence of DM halo with $M(r) \propto r$,

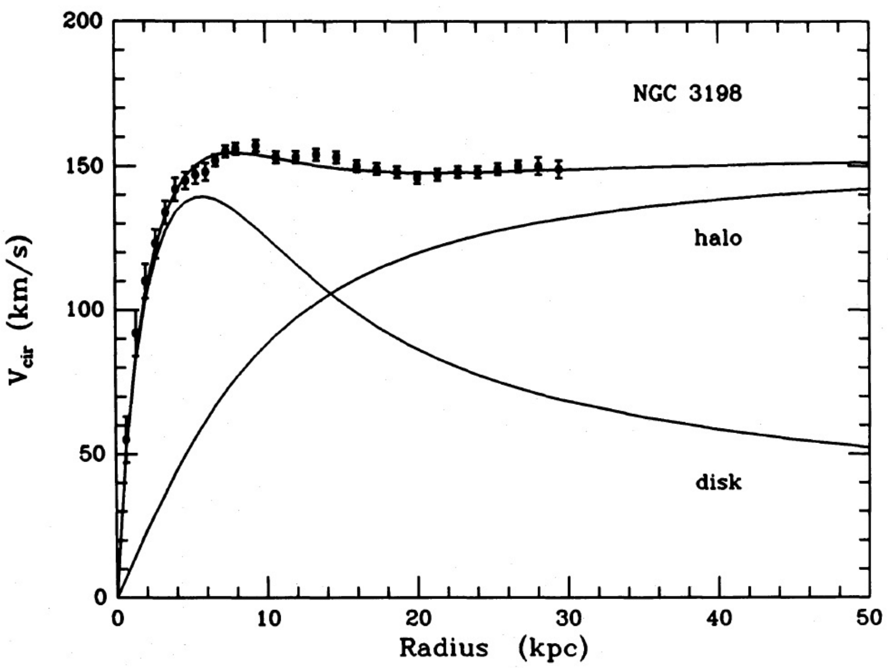

Figure 1.2: Rotation curve of NGC 3198 galaxy, which is fit by considering DM halo and exponential disk. The figure is extracted from [40].

where $M(r) = \int 4\pi\rho(r)r^2dr$ and $\rho(r)$ is the density profile. Therefore to account for the observed behavior of rotation curve, an unidentified dark mass is postulated to exist.

There are compelling evidences of DM at the scale of clusters, which emerge from gravitational lensing. According to Einstein's theory of general relativity, the presence of a massive object deforms the space-time curvature in its vicinity. Since the light rays follow geodesics, they get deflected by the gravitational field of the massive object. The deviation is proportional to the mass of the object that acts like a lens. As a result, light from distant clusters, galaxies and stars are gravitationally lensed by closer ones showing the evidence of gravitational lensing. In the context of DM, Bullet Cluster [41] shown in Fig.(1.3), is the most

Figure 1.3: Composite image of Bullet Cluster, obtained with gravitation lensing. The pink region shows the X-ray data related to the gas cloud and the blue region shows the lensing map. The clear septation between two regions proves that most of the matter in the clusters is collisionless dark matter.

famous example of gravitation lensing. Fig.(1.3) shows the collision between two clusters; lensing map (blue region) exhibits large amounts of DM which is not apparent in the X-ray gas map (pink region). Both the DM halos have passed each other through gas cloud and look like undisturbed after the collision. The gas clouds, which mostly consist of baryonic matter, have clearly exerted friction on each other during collision resulting in a bullet shape of the rightmost cluster. This shows that DM does not interact strongly either with the gas or itself, which points towards a collisionless, non-baryonic DM.

On large scale, the Universe gives rise to large and complex structures: galaxies formed clusters, clusters make superclusters and superclusters are parts of large scale sheets, filaments and voids. These type of patterns are disclosed by the large-scale surveys like 2dFGRS [42] and SDSS [43]. It is expected that these large-scale structures reflect the history of gravitational clustering of matter since the time of Big Bang. So, DM present at the time of structure formation, should have influence on the pattern of these structures, we see today. 'N-body' simulations of large scale cosmology [44–47] also reveal that, a large amount of DM is needed to account for the observed large-scale structure. Recent surveys indicate that total matter (dark plus visible matter) density in the Universe is $\Omega_m \approx 0.29$ [48]. The data from the Big Bang Nucleosynthesis, in short BBN, predict baryon density $\Omega_b \approx 0.04$. If we combine the measurements from large-scale structure and BBN, we find $\Omega_{remaining} \approx 0.25$, which must be identified as DM density.

The observation of angular anisotropies in the Cosmic Microwave Background (CMB) gives concrete evidence of DM. The nine-years Wilkinson Microwave Background Probe (WMAP) results show the existence of 25% of dark matter [49] in the Universe which is confirmed by PLANCK mission data [9]. According to the latest PLANCK data, the Universe contains $\Omega_\Lambda = 0.686 \pm 0.020$ and $\Omega_{\rm m}h^2 = 0.1423 \pm 0.0029$ by which $\Omega_{\rm b}h^2 = 0.02207 \pm 0.00033$ and $\Omega_{\rm dm}h^2 = 0.1196 \pm 0.0031$.

Dark Matter candidates

Before going into details of the possible candidates for DM, we review the minimum constraints [50–53], which should be fulfilled by a DM particle:

- Dark matter is optically dark, so its particles must have a very weak electromagnetic interactions. Since dark matter does not couple with the photon, it should be electrically neutral also.
- It should be non-relativistic at the time of decoupling from the radiation in order to be consistent with the observed density fluctuations at galactic scales. This characterizes DM to be cold.
- It should be long-lived, with life-time larger than age of the Universe, which is $\sim 10^{17}$ sec. DM should also be massive enough to be consistent with measured $\Omega_{\rm DM}$.
- It must be consistent with BBN, CMB observations and compatible with direct-indirect searches.

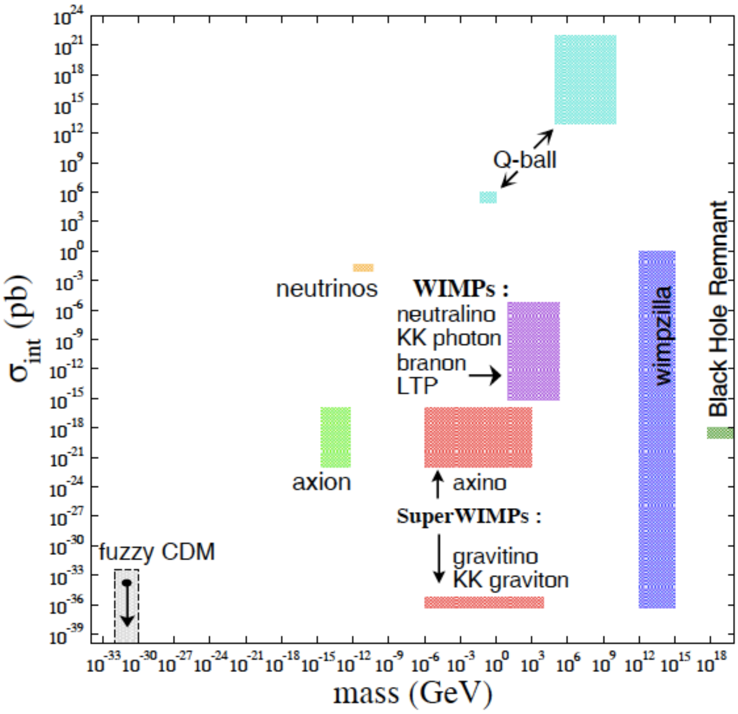

Figure 1.4: Dark matter candidates in their mass versus dark matter-nucleon interaction cross-section plot. This plot is extracted from [54]

In the SM, left-handed neutrinos can be dark matter candidate but large scale structure formation challenged their candidacy. So, it is not possible to accommodate a DM candidate, which satisfies all the requirements mentioned above. There are plenty of extensions of SM to accommodate dark matter. Out of many suitable candidates, Weakly Interacting Massive Particles (WIMPs) are the most popular and widely studied DM candidate. WIMPs interact with SM particles through weak force, which make them non-baryonic and electrically neutral by definition. WIMPs must have a conserved quantum number, making them stable on cosmological time scale. Examples of WIMPs include lightest neutralino in supersymmetry [55–58], the lightest Kaluza-Klein (KK) particle in extra-dimension models [59, 60], right-handed (RH) neutrino (see Section.2.2 and Section.3.2) and an additional scalars [61–63] etc. In addition to the cold dark matter discussed in this thesis, there may be warm dark matter which free-streams at the scale of galaxy-clusters. We do not study warm dark matter in this thesis.

In the literature, other than WIMPs there are many other candidates also proposed (for review see [51, 53, 57]). Some of the most relevant candidates are:

sterile neutrinos, gravitino, axions, axino and superheavy dark matter or wimpzillas; also shown in Fig.(1.4).

Thermal relics

Thermal relics are those particles whose relic abundance is set by their thermal production in the early Universe. WIMPs are supposed to be produced as thermal relics, which are byproducts of our hot Universe. In the early Universe, when temperature was very high ($T \gg m_\chi$; $m_\chi \equiv$ DM mass), DM particles were in thermal equilibrium with thermal plasma. In order to stay in thermal equilibrium, DM should annihilate enough. As the expansion rate of the Universe and corresponding dilution of WIMPs dominates over its annihilation rate, the number density of WIMPs becomes sufficiently small and they cease to interact with each other. This results the decoupling of WIMPs from the primordial particle soup which is called 'freeze-out'. Precisely, the effects of expansion and annihilation are described by the Boltzmann equation,

$$\frac{dn_\chi}{dt} + 3Hn_\chi = -\langle\sigma v\rangle (n_\chi^2 - n_{\chi,eq}^2), \tag{1.1}$$

where n_χ is the number density of WIMPs, H is the expansion rate of the Universe, and $\langle\sigma v\rangle$ is thermally averaged annihilation cross-section (multiplied by WIMPs relative velocity). At high temperature ($T \gg m_\chi$), WIMPs density is given by $n_{\chi,eq}$, but as the Universe expands, temperature goes down and number density falls exponentially. For sufficiently small value of n_χ, the annihilation rate becomes nugatory in comparison to Hubble expansion rate. As a consequence, the number density of WIMPs gets fixed and a thermal "freeze-out" takes place. The temperature at which WIMPs depart from the thermal equilibrium and freeze-out takes place is calculated by solving the Boltzmann equation numerically.
The WIMP relic abundance in the Universe today is approximately given by,

$$\Omega_\chi h^2 = 1.1 \times 10^9 \frac{x_f}{\sqrt{g^*} M_{pl} \langle\sigma v\rangle_{ann}} \mathrm{GeV}^{-1} \tag{1.2}$$

where $x_f = m_\chi / T_f$ and T_f is the freeze-out temperature. M_{Pl} is the Planck mass and g^* is the effective number of relativistic degree of freedom. After using

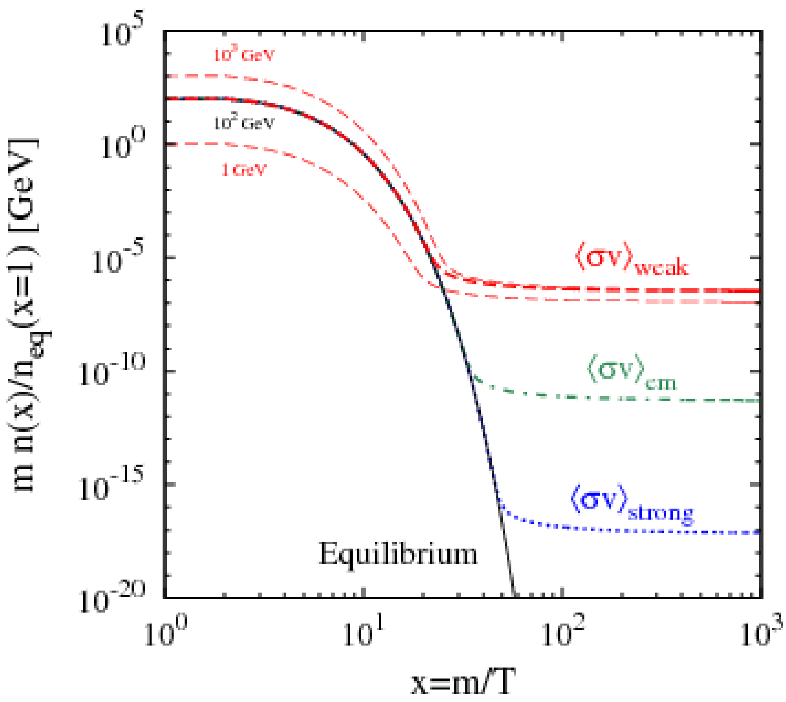

Figure 1.5: The Evolution of WIMPs abundance as a function of $x = m/T$. It is shown that for 100 GeV WIMPs, the cross-section for different SM interactions correspond to thermal "freeze-out" are, $\langle \sigma v \rangle_{\text{weak}} = 2 \times 10^{-26} \text{cm}^3\text{s}^{-1}$, $\langle \sigma v \rangle_{\text{em}} = 2 \times 10^{-21} \text{cm}^3\text{s}^{-1}$ and $\langle \sigma v \rangle_{\text{strong}} = 2 \times 10^{-15} \text{cm}^3\text{s}^{-1}$. The abundance evolution also shown for different masses of WIMPs considering weak interaction. The solid line correspond to evolution of equilibrium abundance for 100 GeV WIMPs (extracted from [64]).

$x_f = 20$ and $g^* = 100$ (considering g^* to be constant with temperature), the relic density can be expressed in a more popular form,

$$\Omega_\chi h^2 \approx 0.1 \left(\frac{2.2 \times 10^{-26} \text{cm}^3 \text{sec}^{-1}}{\langle \sigma v \rangle_{ann}} \right) \tag{1.3}$$

It is clear from Fig.(1.5) that after considering various SM interactions (weak, electromagnetic and strong), it is weak interaction, which gives the correct order of cross-section ($\sigma \sim \alpha^2/m_\chi^2$) required for getting correct relic density today. This similarity between the weak interaction cross-section and the value required (Eq.1.3) to generate the observed quantity of dark matter is known as "WIMP miracle".

WIMP dark matter searches

There are various direct and indirect experiments by which DM is actively searched. It is also possible to search dark matter through its production at colliders like LHC. In this section, we discuss these different possibilities in detail. First we discuss the direct detection techniques of dark matter, which is followed by indirect detection methods. Finally, we talk about collider limits on dark matter. In [65, 66], various DM searches are reviewed in details.

Direct Detection

WIMPs can be searched by looking at their scattering off some nuclei, when they pass through a detector. Recoils of nuclei by WIMP collision is the most promising way to detect dark matter directly. There are variety of experiments [10–14, 67–73] looking for dark matter with mass ranging from keV to $\sim \mathcal{O}(100)$ GeV. Some of them are shown in Fig.(1.6) with their different exclusion limits. The direct detection of dark matter is sensitive to its local density and velocity distribution. The

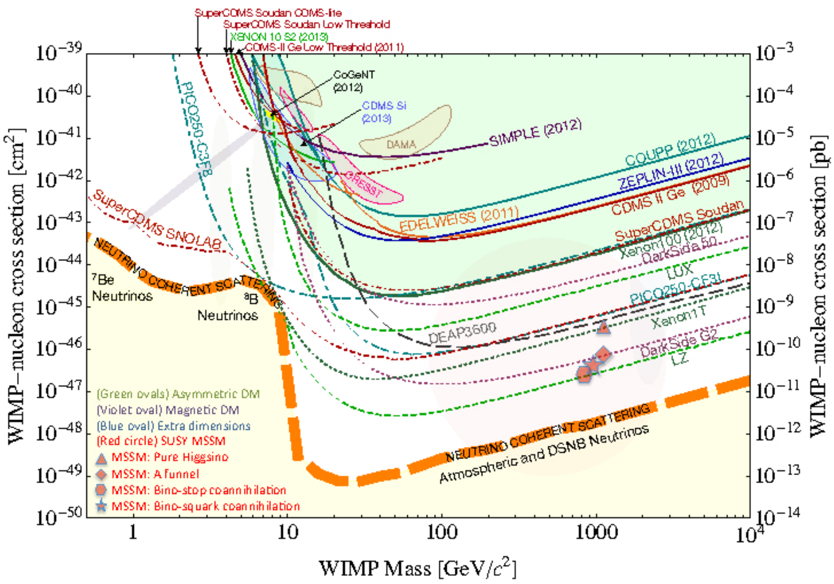

Figure 1.6: The constraints and future projections on dark matter spin-independent cross-section. The plot is taken from [74].

interaction cross-section between DM and nuclei are two types : spin-independent cross-section σ_{SI}, and spin-dependent one σ_{SD}. The interaction for σ_{SI} takes place between WIMPs and all nucleons, whereas for σ_{SD} the interaction only takes place to nuclei with net spin. The target nuclei with different isotopic compositions can be chosen for spin-dependent or spin-independent searches.

At present XENON100 collaboration sets the most stringent bound on spin-independent cross-section, which is $\sim 2 \times 10^{-45}\mathrm{cm}^2$ for $m_\chi \approx 55$ GeV [11]. Recently, LUX collaboration has pushed this limit by one more order i.e $\sim 7.6 \times 10^{-46}\mathrm{cm}^2$ for 33 GeV WIMP [13].

Indirect Detection

The indirect detection of WIMPs is possible through its annihilation or decay into SM particles. Basically indirect detection is focused on the primary and/or secondary products of DM annihilation/decay in the form of neutrinos, photons, positrons or other cosmic-rays (see Section.2.2.2 and Section.3.2.1). The popular place for searching WIMPs byproducts are those with large dark matter density and low astrophysical background. The Galactic Center (GC) is the most common target given its distance and significant amount of DM [75, 76]. Dwarf galaxies are also an important area for looking DM, because of their large DM contents and significantly low background [77, 78]. There are wide range of gamma-ray and cosmic-ray observations in space and ground currently searching for DM signals [2, 7, 15]. Recent study of gamma-ray emission from the region surrounding GC points out the excess of 1-3 GeV gamma-ray. This excess can be explained by $\sim 30 - 40$ GeV annihilating dark matter into $b\bar{b}$ final state [79], bringing up other indirect signal of dark matter.

Collider Searches

It is also possible that hadron colliders can produce dark matter, which can be detected in the form of "missing energy". But it is not possible to get the information of DM lifetime, as it passes through the collider in a fraction of second.

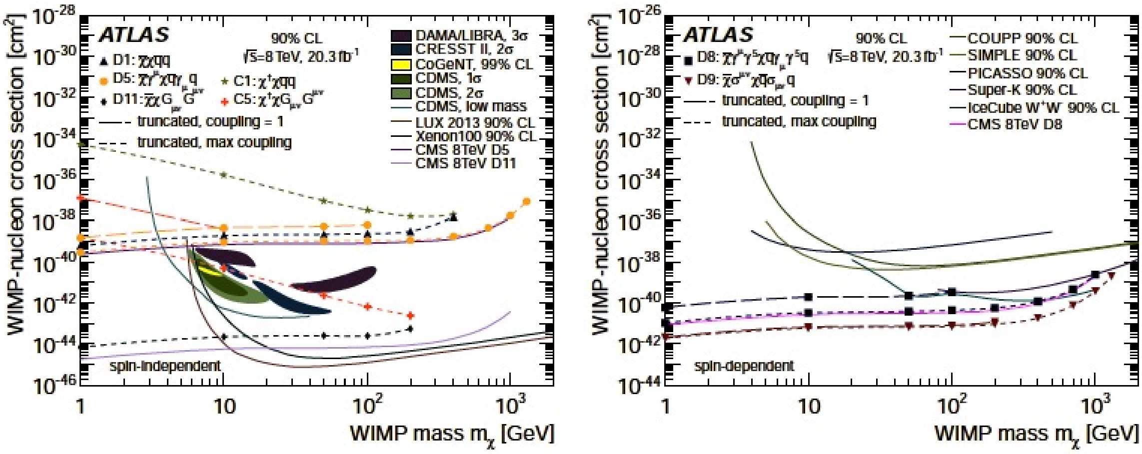

Figure 1.7: Spin-independent (left) and spin-dependent (right) WIMP-nucleon scattering cross-section as function of WIMP mass m_χ for different operators. Results from other direct detection experiments and CMS detector are shown for comparison. Plot is taken from [80].

In other words, although it is possible to produce dark matter in collider very efficiently but it is not possible to determine that new neutral particle basically constitutes the dark matter of the Universe. Mono-jet searches along with mono-photon, mono-W and mono-Z are the most important channels for searching dark matter in colliders [81, 82]. Even though, in comparison to direct detection experiments, collider bounds on spin-independent cross-section are weak [83], but it provides very stringent bounds on spin-dependent cross-section, as shown in Fig.(1.7).

1.1.2 Models for dark matter

Supersymmetric dark matter

In all possible extensions of SM, Supersymmetry (SUSY) is the most popular one (for review see [84–86]). SUSY not only provides the viable WIMP candidate, but also helps in solving the other shortcomings of SM. Basically, SUSY relates fermions to bosons in such a way that for each fermionic degree of freedom there is a bosonic degree of freedom. This extends the SM spectrum of particles such that each particle has a corresponding superpartner. In order to be a DM candidate, a SUSY particle must be stabled to prevent its decay into SM particles. This is achieved by R-parity, which has the following form,

$$R = (-1)^{3(B-L)+2s}, \tag{1.4}$$

where s is the particle's spin; B and L are the baryon and lepton numbers respectively. Therefore all SM particles have R-parity, $+1$ and all their SUSY partners has R-parity, -1.

Right-handed neutrino dark matter

In some of the extensions of SM, it is possible to identify right-handed neutrino as DM [87–89]. Right-handed neutrino as a SM singlet is a good candidate of DM, which interacts with the SM sector via singlet scalar Φ_s. Since the singlet scalar Φ_s mixes with the SM higgs doublet Φ, it is also known as higgs-portal DM [90].

Another intriguing possibility is sterile neutrinos : they are collisionless and can be long lived (due to small mixing with SM particles), which makes them a good candidate of DM [91–93]. Formally sterile neutrino is warm dark matter candidate, which interacts with the SM particles through the mixing with the neutrino. The mixing angle is tightly constrained $\sim \mathcal{O}(10^{-9})$ from the experimental data [94, 95], and so sterile neutrino decay via weak interaction is suppressed. But if they are DM, their lifetime should be larger than the age of the Universe. It is also possible to add an extra 4th generation lepton family into SM (one left-handed doublet and two right-handed singlet), which couples to muon family via a new symmetry called horizontal symmetry. The 4th generation right-handed neutrino is identified as DM and its stability is ensured by keeping it light in compare to charged lepton and horizontal symmetry gauge bosons. We consider this option in Chapter (2) in details.

In left-right symmetric models, right-handed neutrino can not be a DM candidate because of its gauge interactions, which makes its decay possible. But in left-right model, it is possible to identify the right-handed neutrino as DM by proposing a new U(1) global symmetry. In dark left-right model (DLRM) a new U(1) global symmetry S is proposed, which forbids right-handed neutrino from decaying and stabilizes it as DM. In Chapter (3), we discuss this possibility in details.

In Chapter (2) and (3), we considered models in which DM couples to only muons and it annihilates as, $\chi\chi \to \mu^+\mu^-$. In this way, it is possible to relate AMS-02 positron excess with the muon $(g-2)$ measurement. The particles through which DM annihilates also give an adequate contributions to muon $(g-2)$. In the following section, we will describe muon anomalous magnetic moment in detail.

1.2 Muon anomalous magnetic moment

Stern and Gerlach were the first, who measured gyromagnetic ratio (g) of electron, which was later combined with spin by Dirac in his relativistic equation. The magnetic moment $\vec{\mu}$ of an object is a measure of torque experienced by the object when put in a magnetic field. Subatomic particles have a magnetic moment due to their intrinsic spin; g relates these two quantities in the following way,

$$\vec{\mu} = g\left(\frac{e}{2m}\right)\vec{s}. \tag{1.5}$$

It is clear that g is 2 for charged leptons viz. electron, muon, and tau. Indeed the Dirac equation also predicts $g = 2$ for point like particle. But there is a small discrepancy observed by experiments, which is caused by corrections from higher order interactions described by quantum field theories.

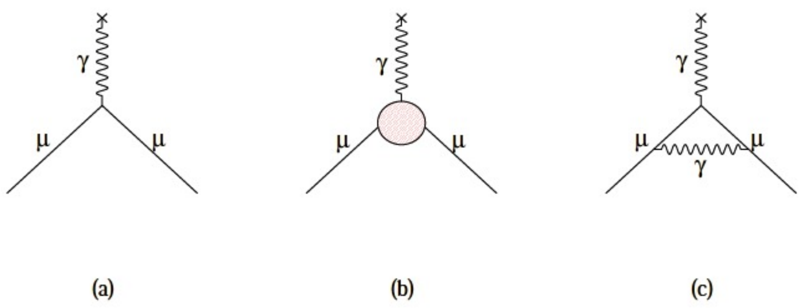

Figure 1.8: Feynman diagrams for muon magnetic moment, where (a) correspond to $g = 2$, (b) the general form of diagrams that give contributions to muon magnetic moment, and (c) correspond to Schwinger contribution.

The possible contributions to muon magnetic moment in short muon $(g-2)$

from quantum field theories are shown in Fig.(1.8). The diagram 1.8.(a) shows the coupling of muon to a photon from the external field, which corresponds to $g = 2$; the prediction of Dirac equation. The other two diagrams 1.8(b)-(c) correspond to higher order or radiative corrections. The virtual fields couplings lead to an anomalous part of the magnetic moment called a_μ and defined as,

$$a_\mu = \frac{(g-2)}{2}. \tag{1.6}$$

The dominant contribution to muon $(g-2)$ comes from the virtual photon as shown in digram 1.8.(c). This was first calculated by Schwinger [96], so this is known as Schwinger contribution which read,

$$a_\mu = \frac{\alpha}{2\pi} \approx 0.0016. \tag{1.7}$$

In SM, besides large QED contribution, a_μ also gets contributions from electroweak and strong interactions,

$$a_\mu^{SM} = a_\mu^{QED} + a_\mu^{Weak} + a_\mu^{Had}. \tag{1.8}$$

The summary of the Standard model contributions to muon $(g-2)$ is given in Table.(1.1). The BNL experiment E821 [3, 4] measured the following value for

	VALUES ($\times 10^{-11}$) UNITS
QED	$116\ 584\ 718.951 \pm 0.009 \pm 0.019 \pm 0.007 \pm 0.077$
HVP(lo) [97]	6923 ± 42
HVP(ho) [97]	-98.4 ± 0.7
HLbL	105 ± 26
EW	154 ± 1
Total SM [97]	$116\ 591\ 802 \pm 42_{\text{H-L-O}} \pm 26_{\text{H-H-O}} \pm 2_{\text{other}} (\pm 49_{\text{tot}})$

Table 1.1: Summary of the standard model contributions to muon anomaly.

muon $(g-2)$,

$$a_\mu^{\text{E821}} = (116\ 592\ 089 \pm 63) \times 10^{-11}, \tag{1.9}$$

which gives a difference of,

$$\Delta a_\mu(\text{E821 - SM}) = (287 \pm 80) \times 10^{-11} \quad [97]. \tag{1.10}$$

So there exists a discrepancy between experimental measurement [3, 4] and SM prediction [97–101] of muon $(g-2)$ at the level of 3.6σ. The deviation of 3.6σ is tantalizing and can be a hint of physics beyond standard model. There exist many models [102] which can explain muon $(g-2)$ discrepancy using new physics scenario.

In the popular extension of SM like Supersymmetry, there are neutralino-smuon and chargino-sneutrino loops, which give contributions to muon $(g-2)$ [103,104]. In supersymmetric models, to get an adequate contribution to muon $(g-2)$, we need a large tanβ ($\equiv \mathrm{v_d}/\mathrm{v_u}$) and light supersymmetry particles (few 100 GeV) in the loop. In constrained minimal supersymmetric standard models (CMSSM) [105–107] and nonuniversal higgs mass models (NUHM) [108–110], preferable parameter space of muon $(g-2)$ is in tension with 125 GeV higgs observed at LHC [111, 112], dark matter scenario [11] and flavor physics [113, 114]. To lift the tension, many nonuniversal models are proposed in the literature [115–118], which reconcile the SUSY explanations of observed muon $(g-2)$ with dark matter, higgs mass and flavor physics.

Basically, in all SUSY diagrams, which give rise to required muon $(g-2)$, there exists m_μ suppression i.e. $a_\mu^{\rm SUSY} \propto m_\mu^2/M_{\rm SUSY}^2$, where $M_{\rm SUSY}$ is proportional to the mass of SUSY particle in the loop. The mass suppression in $(g-2)$ can be evaded with a horizontal gauge symmetry like in [119], where mass suppression is lifted by proposing additional $U(1)_{L_\mu - L_\tau}$ symmetry. In the Section.2.1, we described a $\mathrm{SU(2)_{HV}}$ gauge horizontal symmetry model, which can lift the mass suppression in muon $(g-2)$ and have a viable candidate of dark matter. The dark matter in this model is leptophilic in nature, which is required (as described in Section.1.1) for explaining the AMS-02 positron excess [1, 2]. The muon anomalous magnetic moment and dark matter have also been related in other extensions of SM [120–122].

The other interesting scenarios to overcome the 3.6σ discrepancy are additional gauge bosons [123,124], anomalous gauge couplings [125], leptoquarks [126], extra dimensions [127, 128], muon substructure [129, 130], exotic flavor changing interactions [131], possible nonperturbative effect at the 1 TeV order [132], 4th generation leptons [133, 134], and the violation of CPT and Lorentz invariance [135]. Some of these models are in tension with current experimental data from colliders. This is also possible to explain the muon $(g-2)$ in left-right models, where again the contribution to muon magnetic moment is muon mass suppressed [136, 137]. In Chapter (3), we studied a variant of left-right model called dark left-right model, where in Section.3.3 we calculated its contribution to muon $(g-2)$. In this model, right-handed neutrino is identified as DM, which dominantly couples to leptons, giving rise to a connection between muon $(g-2)$ and AMS-02 positron excess.

1.3 IceCube neutrino events

Besides DM, various other intriguing properties of neutrinos are another important source of physics beyond standard model. Neutrino oscillation data suggests that neutrino has tiny mass, which does not have standard model explanation, and so physics beyond standard model is needed for that.

Neutrinos travel from the edge of the Universe without any absorption and deflection by magnetic fields. So high energy neutrinos may reach us unperturbed from cosmic distances. But due to their weakly interacting nature, it is very difficult to detect them, and so a ginormous particle detector is required to collect the significant events of neutrinos.

IceCube is a south pole based neutrino detector, which is on a continuous hunt of neutrinos since the year 2000. It is buried beneath the surface at the depth of about 2.5 Km. In the detector, there are optical modules attached to its 86 vertical strings, which are arrayed over a cubic kilometer at 1,450 meters to 2,450 meters depth. The set-up of the IceCube detector is shown in Fig.(1.9). Some of the high energy neutrinos interact with the nucleus of the constituents atoms of the ice molecules and create muons as well as electromagnetic and hadronic secondary particle showers. The charged secondary particles radiate Cherenkov light that can be detected by optical modules in the detector. There are other neutrino detectors e.g. BDUNT [138] and NESTOR [139] deployed in Lake Baikal

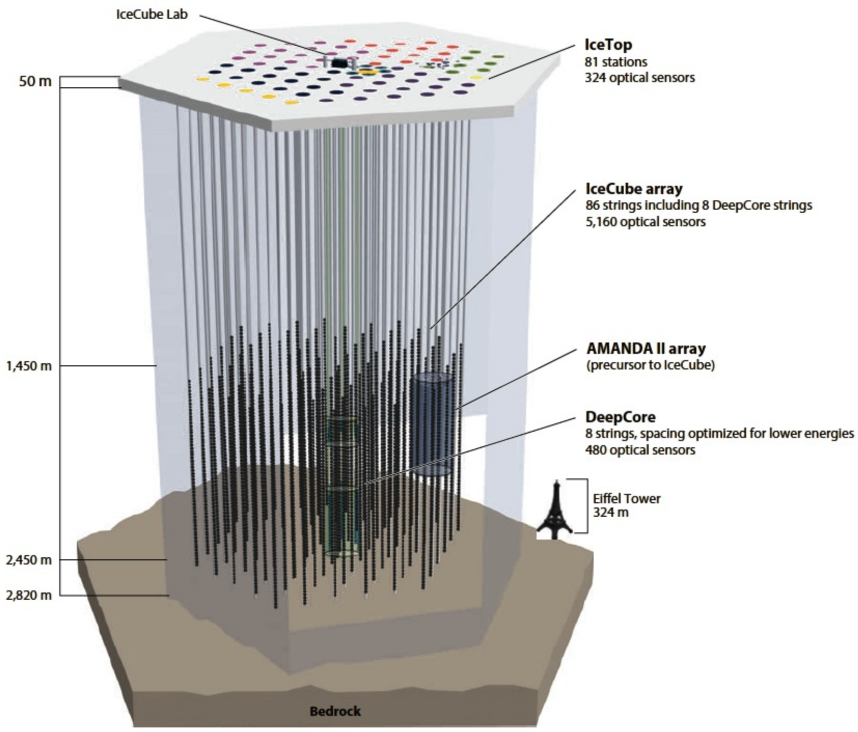

Figure 1.9: Artist's drawing of IceCube set-up. The former AMANDA detector is shown in blue and the deepcore subarray in green.

and Mediterranean sea respectively, which are also looking for high energy neutrino events.

Recently IceCube collaboration has observed very high energy neutrinos events with energy between 60 TeV to $\sim$ 3 PeV, in which four events are $\sim \mathcal{O}(1$ PeV) [5–8]. IceCube events as a function of deposited energy are shown in Fig.(1.10). It is clear from Fig.(1.10) that a purely atmospheric muons (red color) and/or neutrinos (dark blue color) explanation for these events is strongly disfavored (at the level of 5.7σ [7]). The energy expected from atmospheric neutrinos (coming from π/K decay) only competes upto 100 TeV [140], but IceCube observed events of much higher energies (upto $\sim$ 3 PeV). Even though charm decay can produce a hard spectrum for atmospheric neutrinos (their energies goes upto 1000 TeV as shown in Fig.(1.10)), but this possibility is also constrained by observed angular distribution of the events. Therefore astrophysical and/or new physics explanations have been pursued for the origin of these high energy neutrinos.

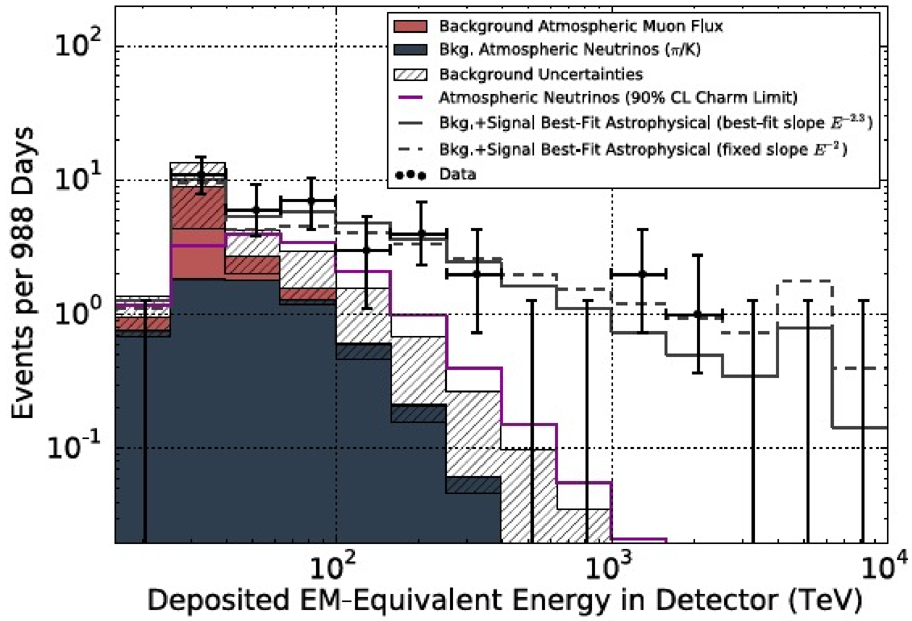

Figure 1.10: The plot of IceCube observed events with predictions. The patched region shows uncertainties in the background. Atmospheric muons and neutrinos background are shown in red and dark blue colors respectively. The plot is taken from [7].

The possible astrophysical sources of neutrino production are supernova remnants (SNR) [141–143], active galactic nuclei (AGN) [144–146] and gamma-ray bursts (GRB) [147]. All these sources have some specific neutrino emission spectra, which depend on their production environments. In a model independent analysis, the IceCube data in the energy range 60 TeV-2 PeV is consistent with E_ν^{-2} neutrino spectrum following $E_\nu^2 dN_\nu/dE_\nu \simeq 1.2\times10^{-8}$ GeVcm^{-2}s^{-1}sr^{-1} [6,7]. But spectrum sharper than $E^{-2.3}$ does not provide a good fit to the data [7]. It is not straightforward to fit the data using astrophysical sources, and extragalactic sources are required. The requirement of extragalactic sources is also supported by isotropic feature and galactic constraints [148–150].

Dark matter explanation of high energy neutrino events have also been investigated in various models, in which either dark matter decays into standard model particles that give energetic neutrinos [151–160], or it decays into some light dark matter particles which interact with nucleon and produce neutrino events [161, 162]. The neutrino flux produced from dark matter decay should be isotropic because DM contributes same at galactic as well as extragalactic scale.

Dark matter explanation of IceCube neutrino events predicts a sharp cutoff in the neutrino spectrum, and can also explain the possible energy gap between 400 TeV $\sim$ 1 PeV (although not statistically significant) in the data [7] motivating two component flux and leptophilic DM decay [163–166].

There is no neutrino events observed by IceCube above $\sim$ 3 PeV. In particular, Glashow resonance [167], $\bar{\nu}_e + e^- \to W^- \to$ shower, is absent which is otherwise expected at 6.3 PeV. As a result of Glashow resonance, the cross-section for $\bar{\nu}_e$ gets enhanced at neutrino energy $E = M_W^2/2m_e = 6.3$ PeV, which increases the detection rate of $\nu_e + \bar{\nu}_e$ by a factor of ~ 10 [6]. Taking into account the increment in detection rate and declination in the neutrino energy spectrum from E^{-2}, one would expect about 3 events at Glashow resonance. Even without Glashow resonance, there should be some events from the extension of E^{-2} spectra above 2.6 PeV. But there is none!

The Glashow resonance gives rise to multiple energy peaks at different energies [168]. The first one is at 6.3 PeV and others lie at the $E_{vis} = E - E_X$, where E_X is the energy in the W decay, which does not contribute to the visible shower [169]. The decay of W into hadrons goes as $W \to \bar{q}q$, giving rise to a peak at 6.3 PeV, while decay into leptons goes as $W \to \bar{\nu}l$, which means W boson will lose half of its energy and so a second peak at 3.2 PeV is expected. In case of τ lepton in the final state, a further decay takes place producing a neutrino and thus a third peak at 1.6 PeV. The events observed by IceCube [5–8] between 1 to $\sim$ 3 PeV range may be associated with the second (leptonic decay of W) and third (τ decay) peak, but non-appearance of Glashow resonance hadronic shower from $W \to \bar{q}q$ at 6.3 PeV (dominant peak) makes this idea less attractive. The non observation of the expected signature of Glashow resonance in IceCube data indicates a cutoff of neutrino energies between 2.6-6.3 PeV [169, 170].

We propose a mechanism (Section.4.1) which can explain why neutrinos above a certain energy may be suppressed in the astrophysical production processes like $\pi \to \mu\bar{\nu}_\mu$, $\mu \to e\bar{\nu}_e\nu_\mu$ etc. One explanation of the absence of Glashow resonance is the violation of Lorentz symmetry at high energies. The numerical relation,

$$m_\pi^2 - m_\mu^2 \sim \frac{\text{PeV}^3}{M_{Pl}}, \tag{1.11}$$

suggests that there may be an unique opportunity to test the Planck suppressed Lorentz violation via PeV neutrinos. We assume that Lorentz violating higher dimensional operators [171, 172] give rise to a modified dispersion relation for the neutrinos (antineutrinos) of the form $E^2 = p^2 + m_\nu^2 - (\xi_n/M_{pl}^{n-2})\ p^n$ with $n > 2$. Depending on the sign of ξ_n, the neutrinos (antineutrinos) can be either superluminal ($\xi_n < 0$) or subluminal ($\xi_n > 0$). In Chapter (4), we describe our proposal in detail following the derivation of modified neutrino dispersion and spinors relations of appendices A and B.

1.4 Aim of the thesis

There are many observations in particle physics and cosmology which seek theory beyond standard model for their explanations. The excess of positrons observed by AMS-02 experiment, the discrepancy between the SM value and experimental measurement of muon $(g-2)$, and absence of the Glashow resonance at IceCube are some of the important signatures which call for new physics for their explanations. So, it becomes quite important to construct the particle physics models, which not only explain these signals but can also find the relation between them. The aim of this thesis work is to study the particle physics models, which can explain and relate these signals.

1.5 Thesis overview

The thesis is organized as follows : Chapter (1) contains the basic introduction of DM with its properties, and possible candidates. The AMS-02 positron excess, and other experimental signatures viz. muon anomalous magnetic moment and IceCube high energy neutrino events are also discussed in details.

In Chapter (2), we discuss our newly proposed gauged horizontal symmetry model. We extend the SM with a 4th generation of fermions and propose a $SU(2)_{HV}$ horizontal gauge symmetry between the 4th generation leptons and muon families. We identify the 4th generation right-handed neutrino as DM and use it to explain the AMS-02 positron excess. As an artefact of $SU(2)_{HV}$

gauge symmetry, we have new contributions to muon $(g-2)$ from $\mathrm{SU(2)_{HV}}$ gauge boson and different scalars. In this chapter, we will discuss the phenomenological aspects of new model in details.

Chapter (3) focuses on dark left-right model. In left-right model, due to its gauge interactions, it is not possible to identify the right-handed neutrino as DM. But in other variant of left-right model called dark left-right model, it is possible to accommodate DM by proposing a new U(1) global symmetry. The new symmetry forbids the mass term connecting left to right-handed neutrino, and so stops the decay of right-handed neutrino. The right-handed neutrino is identified as DM (called scotino). The new particles in the model also give an adequate contribution to muon $(g-2)$. We discussed all these possibilities in details.

Chapter (4) is dedicated to the study of Lorentz invariance violation. IceCube collaboration has observed neutrinos of very high energies, which goes upto PeV arising from pion and muon decays. Through the numerical relation $m_\pi^2 - m_\mu^2 \sim \mathrm{PeV}^3/M_{pl}$, it is possible to test the Planck suppressed Lorentz violation operators via observations of PeV neutrinos. We discussed these possibilities in details. In the last Chapter (5) of the thesis, we provide the summary and scope for future work.

Chapter 2

Gauged horizontal symmetric model

The Standard Model (SM) is a theory of electromagnetic and weak interactions between leptons and quarks, and is based on the gauge group $\mathrm{SU(2)_L \times U(1)_Y}$. In combination with symmetry group $\mathrm{SU(3)_C}$, SM provides the unified framework for the electromagnetic, weak and strong forces. The spontaneous breaking of gauge theories generates masses of the W, Z gauge bosons and the three generations of quarks and leptons. In SM, each of the fermion family (both for leptons and quarks) is independently anomaly free. But there exists a pattern in the quarks and neutrinos mixing matrices which suggests a larger symmetry between their respective three generations. This set of evidence points towards the existence of a horizontal symmetry, which distinguish two left-handed doublets or singlets of quarks and leptons other than masses. The horizontal symmetry may be discrete [173], global [174] or a gauged [175] symmetry. The AMS-02 collaboration [1, 2] has recently observed positrons excess over cosmic ray background, and did not notice any significant excess of antiprotons over cosmic ray background. The dark matter (DM) explanation of the observed positron excess (remaining consistent with the absence of antiprotons excess over cosmic ray background) may require new interactions between DM and leptons, which can be achieved by gauging the leptons of different families. In this chapter, we introduce a gauged horizontal symmetric model which can explain muon $(g-2)$, measured at BNL [3, 4] and

the excess of positrons measured by AMS-02 [1, 2] simultaneously.
There is a discrepancy at 3.6σ level between the experimental measurement [3, 4] and the SM prediction [97–101] of muon anomalous magnetic moment,

$$\Delta a_\mu \equiv a_\mu^{\rm Exp} - a_\mu^{\rm SM} = (28.7 \pm 8.0) \times 10^{-10}, \tag{2.1}$$

where a_μ is the anomalous magnetic moment in the unit of $e/2m_\mu$. In SM, contribution of gauge bosons to the muon anomalous magnetic magnetic moment goes as $a_\mu^W \propto m_\mu^2/M_{W,Z}^2$ and we have $a_\mu^{\rm SM} = 19.48 \times 10^{-10}$ [176]. In minimal supersymmetric standard model (MSSM) [103, 104], we get contributions to muon $(g-2)$ from neutralino-smuon and chargino-sneutrino loops. In all MSSM diagrams there still exist the m_μ suppression in $(g-2)$, arising from the following cases:

- In case of bino in the loop, the mixing between the left and right handed smuons is $\propto m_\mu$.
- In case of wino-higgsino or bino-higgsino in the loop, the higgsino coupling with smuon is $\propto y_\mu$, so there is a m_μ suppression.
- In the case of chargino-sneutrino in the loop, the higgsino-muon coupling is $\propto y_\mu$, which again gives rise to m_μ suppression.

Therefore in MSSM $a_\mu^{\rm MSSM} \propto m_\mu^2/M_{\rm SUSY}^2$, where $M_{\rm SUSY}$ is proportional to the mass of the SUSY particle in the loop.
One can evade the muon mass suppression in $(g-2)$ with a horizontal gauge symmetry. A horizontal $U(1)_{L_\mu - L_\tau}$ symmetry was used to lift m_μ suppression [119]. Here muon $(g-2)$ is proportional to m_τ and $a_\mu \propto m_\mu m_\tau/m_{Z'}^2$, where $L_\mu - L_\tau$ gauge boson mass $m_{Z'} \propto 100$ GeV gives the required a_μ, but $m_{Z'}$ of $\sim \mathcal{O}(100)$ GeV is tightly constrained from flavor physics. The SM extension needed to explain muon $(g-2)$ can also be related to dark matter [120, 121] and the implication of this new physics in LHC searches has been studied [177]. The second experimental signal which we addressed in this chapter is the excess of positron over cosmic-ray background, which has been observed by AMS-02 experiment [1] upto energy ~ 425 GeV [2]. An analysis of AMS-02 data suggests that a dark

matter (DM) annihilation interpretation would imply that the annihilation final states are either μ or τ [28, 178]. The dark matter annihilation into $e^{\pm}$ pairs would give a peak in the positron signal, which is not seen in the positron spectrum. Since the branching ratio of τ decay to e is only 17% compared to μ, this makes μ as the preferred source of origin of high energy positrons. There is no excess of antiproton flux over cosmic-ray background observed by AMS-02 experiment [179, 180], which also indicates towards a leptophilic dark matter [26, 181].
In this chapter, we describe a gauged horizontal symmetric model. We introduce a 4th generation of fermions and a $\mathrm{SU(2)_{HV}}$ vector gauge symmetry between the 4th generation leptons and the muon family. In this model, the muon $(g-2)$ has a contribution from the 4th generation charged lepton μ', $\mathrm{SU(2)_{HV}}$ gauge boson θ^{+}, and from the neutral (h, A) and charged $H^{\pm}$ higgs. In all these cases, there is no quadratic suppression $\propto m_\mu^2$ because of the horizontal symmetry. By choosing parameters of the model without any fine tunning, we can obtain the required number $\Delta a_\mu = 2.87 \times 10^{-9}$ within 1σ.
In this model, we identify the 4th generation right-handed neutrino $\nu_{\mu' R}$, as dark matter. The dark matter annihilates to SM particles through the $\mathrm{SU(2)_{HV}}$ gauge boson θ_3 and with the only final states being $(\mu^+\mu^-)$ and $(\nu_\mu^c\ \nu_\mu)$. The stability of DM is maintained by taking the 4th generation charged lepton to be heavier than DM. To explain the AMS-02 signal [1, 2], one needs a cross-section (CS), $<\sigma v>_{\chi\chi\to\mu^+\mu^-} = 2.33 \times 10^{-25}\mathrm{cm}^3/\mathrm{sec}$, which is larger than the CS, $\sigma v_{\chi\chi\to SM} \sim 3 \times 10^{-26}\mathrm{cm}^3/\mathrm{sec}$, required to get the correct thermal relic density $\Omega h^2 = 0.1199 \pm 0.0027$ [9, 49]. In our model, the enhancement of annihilation CS of DM in the galaxy is achieved by the resonant enhancement mechanism [182–184], which we attain by taking $M_{\theta_3} \simeq 2m_\chi$.
This chapter is organized as follows : In the next section, we describe our proposed gauge horizontal symmetric model in detail. In section (2.2), we discuss about the dark matter candidate and then its phenomenology. The relic density and the fitting of AMS-02 positron data are discussed in the sections (2.2.1) and (2.2.2) respectively. We compute the muon $(g-2)$ contributions from this model in (2.3) and then we give our conclusion and outlook in section (2.4).

2.1 Model

We introduce the 4th generation of quarks (c', s') and leptons (ν'_μ, μ') (of both chiralities) in the SM. We also add three right-handed neutrinos and extend the gauge group of SM by horizontal symmetry denoted by $\mathrm{SU(2)_{HV}}$, between the 4th generation lepton and muon families. Addition of three right-handed neutrinos ensures that the model is free from SU(2) Witten anomaly [185]. We assume that the quarks of all four generations and the leptons of e and τ families are singlet of $\mathrm{SU(2)_{HV}}$ to evade the constraints from flavor changing processes. The $\mathrm{SU(2)_{HV}}$ symmetry can be extended to e and τ families by choosing suitable discrete symmetries, however for this work we have taken e and τ families to be singlet of $\mathrm{SU(2)_{HV}}$ for simplicity and discuss the most economical model, which can explain muon $(g-2)$ and AMS-02 positron excess at the same time.

We denote the left-handed muon and 4th generation lepton families by $\Psi_{Li\alpha}$ and their right-handed charged and neutral counterparts by $E_{R\alpha}$ and $N_{R\alpha}$ respectively (here i and α are the $\mathrm{SU(2)_L}$ and $\mathrm{SU(2)_{HV}}$ indices respectively and run through the values 1 and 2). The left-handed electron and tau doublets are denoted by ψ_{eLi} and $\psi_{\tau Li}$ and their right-handed counterparts by e_R and τ_R respectively. The gauge fields of $\mathrm{SU(2)_L \times U(1)_Y \times SU(2)_{HV}}$ groups are denoted by A^a_μ, B_μ and θ^a_μ $(a = 1, 2, 3)$ with gauge couplings g, g' and g_H respectively.

The leptons transformations under the gauge group, $\mathrm{SU(3)_c \times SU(2)_L \times U(1)_Y \times SU(2)_{HV}} \equiv \mathrm{G_{STD}}$ (SM gauge group) $\times\, \mathrm{SU(2)_{HV}}$ are shown in Table.(2.1). From the assigned quantum numbers, it is clear that the $\mathrm{SU(2)_{HV}}$ gauge bosons connect only the lepton pairs, $\psi_{\mu_L} \leftrightarrow \psi_{\mu'_L}$ and $(\mu_R, \nu_{\mu R}) \leftrightarrow (\mu'_R, \nu'_{\mu R})$. This assignment ensures the contribution of heavy lepton μ' to the muon $(g-2)$ as shown in Fig.(2.4). In our $\mathrm{G_{STD}} \times \mathrm{SU(2)_{HV}}$ model, the gauge couplings of the muon and 4th generation lepton families are,

$$\begin{aligned}\mathcal{L}_\psi = {} & i\bar{\Psi}_{Li\alpha}\gamma^\mu \left(\partial_\mu - \frac{i}{2} g\tau\cdot A_\mu + ig' B_\mu - \frac{i}{2} g_H \tau\cdot\theta_\mu\right)_{ij;\alpha\beta} \Psi_{Lj\beta} \\ & + i\bar{E}_{R\alpha}\gamma^\mu \left(\partial_\mu + i2g' B_\mu - \frac{i}{2} g_H \tau\cdot\theta_\mu\right)_{\alpha\beta} E_{R\beta} \\ & + i\bar{N}_{R\alpha}\gamma^\mu \left(\partial_\mu - \frac{i}{2} g_H \tau\cdot\theta_\mu\right)_{\alpha\beta} N_{R\beta} \end{aligned} \tag{2.2}$$

Particles	$\mathrm{G_{STD}} \times \mathrm{SU(2)_{HV}}$ Quantum numbers
$\psi_{eLi} \equiv (\nu_e, e)$	$(1, 2, -1, 1)$
$\Psi_{Li\alpha} \equiv (\psi_\mu, \psi_{\mu'})$	$(1, 2, -1, 2)$
$\psi_{\tau Li} \equiv (\nu_\tau, \tau)$	$(1, 2, -1, 1)$
$E_{R\alpha} \equiv (\mu_R, \mu'_R)$	$(1, 1, -2, 2)$
$N_{R\alpha} \equiv (\nu_{\mu R}, \nu_{\mu' R})$	$(1, 1, 0, 2)$
e_R, τ_R	$(1, 1, -2, 1)$
$\nu_{eR}, \nu_{\tau R}$	$(1, 1, 0, 1)$
ϕ_i	$(1, 2, 1, 1)$
$\eta^\beta_{i\alpha}$	$(1, 2, 1, 3)$
χ_α	$(1, 1, 0, 2)$

Table 2.1: Representation of the various fields in the model under the gauge group $\mathrm{G_{STD}} \times \mathrm{SU(2)_{HV}}$.

The "neutral-current" of $\mathrm{SU(2)_{HV}}$ contributes to the annihilation process, $(\nu_{\mu'}\nu_{\mu'}) \rightarrow \theta_3^* \rightarrow (\mu^+\mu^-), (\nu^c_\mu\ \nu_\mu)$, which is relevant for the AMS-02 and relic density calculations. The "charge-changing" vertex $\mu\mu'\theta^+$, contributes to the $(g-2)$ of the muon.

To evade the bounds on the 4th generation from the higgs production at LHC, we extend the higgs sector (in addition to ϕ_i) by a scalar $\eta^\beta_{i\alpha}$ (i and α are the $\mathrm{SU(2)_L}$ and $\mathrm{SU(2)_{HV}}$ indices respectively and run through the values 1 and 2), which is a doublet under SU(2) and triplet under $\mathrm{SU(2)_{HV}}$. As an SU(2) doublet $\eta^\beta_{i\alpha}$ evades 4th generation bounds from the overproduction of higgs in the same way as [186, 187], in that the 125 GeV mass eigenstate is predominantly η which has no Yukawa couplings with the quarks. As $\eta^\beta_{i\alpha}$ is a triplet under $\mathrm{SU(2)_{HV}}$, its Yukawa couplings with the muon and 4th generation lepton families split the masses of the muon and 4th generation leptons. We also introduce a $\mathrm{SU(2)_{HV}}$ doublet χ_α, which generates masses for $\mathrm{SU(2)_{HV}}$ gauge bosons. The quantum numbers of the scalars are shown in Table.(2.1). The general potential of this set of scalars $(\phi_i, \eta^\beta_{i\alpha}, \chi_\alpha)$ is given in [188]. Following [188], we take the vacuum expectation values (vevs) of these scalars as,

$$\begin{aligned} \langle\phi_i\rangle &= \langle\phi\rangle\delta_{i2}, \\ \langle\eta_{i\alpha}^{\beta}\rangle &= \langle\eta\rangle\delta_{i2}(\delta_{\alpha 1}\delta^{\beta 1} - \delta_{\alpha 2}\delta^{\beta 2}), \\ |\langle\chi\rangle|^2 &= |\langle\chi_1\rangle|^2 + |\langle\chi_2\rangle|^2, \end{aligned} \tag{2.3}$$

where $\langle\phi_i\rangle$ breaks $\mathrm{SU(2)_L}$, $\langle\chi_\alpha\rangle$ breaks $\mathrm{SU(2)_{HV}}$ and $\langle\eta_{i\alpha}^{\beta}\rangle$ breaks both $\mathrm{SU(2)_L}$ and $\mathrm{SU(2)_{HV}}$ and generate the TeV scale masses for $\mathrm{SU(2)_{HV}}$ gauge bosons. The mass eigenstates of the scalars will be a linear combination of $\phi_i, \eta_{i\alpha}^{\beta}$ and χ_α. We shall assume that the lowest mass eigenstate h_1 with the mass $\sim$ 125 GeV is primarily constituted by $\eta_{i\alpha}^{\beta}$. We shall also assume that the parameters of the higgs potential [188] are tuned such that mixing between h_1 and ϕ_i is small. The Yukawa couplings of 4th generation quarks are only with ϕ_i, therefore the 125 GeV Higgs will have very small contribution from the 4th generation quark loops. The gauge couplings of the scalar fields $\phi_i, \eta_{i\alpha}^{\beta}$ and χ_α are given by the Lagrangian,

$$\begin{aligned} \mathcal{L}_s = &|(\partial_\mu - \frac{i}{2}g\tau\cdot A_\mu - ig'B_\mu)\phi|^2 + |(\partial_\mu - \frac{i}{2}g\tau\cdot A_\mu - ig'B_\mu - ig_H T\cdot\theta_\mu)\eta|^2 \\ &+ |(\partial_\mu - \frac{i}{2}g_H\tau\cdot\theta)\chi|^2, \end{aligned} \tag{2.4}$$

where $\tau_a/2$ $(a = 1,2,3)$ are 2×2 matrix representation for the generators of $\mathrm{SU(2)_L}$ and T_a $(a = 1,2,3)$ are 3×3 matrix representation for the generators of $\mathrm{SU(2)_{HV}}$. After expanding $\mathcal{L}_s$ around the vevs defined in Eq.(2.3), the masses of gauge bosons come,

$$M_W^2 = \frac{g^2}{2}(2\langle\eta\rangle^2 + \langle\phi\rangle^2), \quad M_Z^2 = \frac{g^2}{2}\sec^2\theta_W(2\langle\eta\rangle^2 + \langle\phi\rangle^2), \quad M_A^2 = 0,$$

$$M_{\theta^+}^2 = g_H^2(4\langle\eta\rangle^2 + \frac{1}{2}\langle\chi\rangle^2), \quad M_{\theta_3}^2 = \frac{1}{2}g_H^2\langle\chi\rangle^2. \tag{2.5}$$

We tune the parameters in the potential such that the vevs of scalars are,

$$\begin{aligned} \sqrt{2\langle\eta\rangle^2 + \langle\phi\rangle^2} &= 174 \text{ GeV}, \\ \langle\chi\rangle &= 22.7 \text{ TeV}, \end{aligned} \tag{2.6}$$

for the generation of large masses for 4th generation leptons $\mu', \nu_{\mu'}$ and $\mathrm{SU}(2)_{\mathrm{HV}}$ gauge bosons θ^+, θ_3. The Yukawa couplings of the leptons are given by,

$$\begin{aligned}\mathcal{L}_Y = & -h_1\bar{\psi}_{eLi}\phi_i e_R - \tilde{h}_1\epsilon_{ij}\bar{\psi}_{eLi}\phi^j\nu_{eR} - h_2\bar{\Psi}_{Li\alpha}\phi_i E_{R\alpha} \\ & - \tilde{h}_2\epsilon_{ij}\bar{\Psi}_{Li\alpha}\phi^j N_{R\alpha} - k_2\bar{\Psi}_{Li\alpha}\eta^{\beta}_{i\alpha}E_{R\beta} - \tilde{k}_2\epsilon_{ij}\bar{\Psi}_{Li\alpha}\eta^{j\beta}_{\alpha}N_{R\beta} \\ & - h_3\bar{\psi}_{\tau Li}\phi_i\tau_R - \tilde{h}_3\epsilon_{ij}\bar{\psi}_{\tau Li}\phi^j\nu_{\tau R} + \text{h.c.}\end{aligned}$$

after corresponding scalars take their vevs as defined in Eq.(2.3), we obtain,

$$\begin{aligned}\mathcal{L}_Y = & -h_1\bar{\psi}_{eL2}\langle\phi\rangle e_R - \tilde{h}_1\bar{\psi}_{eL1}\langle\phi\rangle\nu_{eR} - \bar{\Psi}_{L2\alpha}[h_2\langle\phi\rangle + k_2\langle\eta\rangle(\delta_{\alpha 1} - \delta_{\alpha 2})]E_{R\alpha} \\ & - \bar{\Psi}_{L1\alpha}[\tilde{h}_2\langle\phi\rangle + \tilde{k}_2\langle\eta\rangle(\delta_{\alpha 1} - \delta_{\alpha 2})]N_{R\alpha} - h_3\bar{\psi}_{\tau L2}\langle\phi\rangle\tau_R - \tilde{h}_3\bar{\psi}_{\tau L1}\langle\phi\rangle\nu_{\tau R} \\ & - h_1\bar{\psi}_{eLi}\phi'_i e_R - \tilde{h}_1\epsilon_{ij}\bar{\psi}_{eLi}\phi'^j\nu_{eR} - \bar{\Psi}_{Li\alpha}[h_2\phi'_i\delta^{\beta}_{\alpha} + k_2\eta'^{\beta}_{i\alpha}]E_{R\beta} \\ & - \bar{\Psi}_{Li\alpha}[\tilde{h}_2\epsilon_{ij}\phi'^j\delta^{\beta}_{\alpha} + \tilde{k}_2\epsilon_{ij}\eta'^{j\beta}_{\alpha}]N_{R\beta} - h_3\bar{\psi}_{\tau Li}\phi'_i\tau_R - \tilde{h}_3\epsilon_{ij}\bar{\psi}_{\tau Li}\phi'^j\nu_{\tau R} + \text{h.c.}\end{aligned} \tag{2.7}$$

where ϕ'_i and $\eta'^{\beta}_{i\alpha}$ are the shifted fields. From Eq.(2.7), we see that the muon and 4th generation leptons masses get split and are given by,

$$\begin{aligned} & m_e = h_1\langle\phi\rangle, \quad m_\tau = h_3\langle\phi\rangle, \quad m_{\nu_e} = \tilde{h}_1\langle\phi\rangle, \quad m_{\nu_\tau} = \tilde{h}_3\langle\phi\rangle, \\ & m_\mu = h_2\langle\phi\rangle + k_2\langle\eta\rangle, \quad m_{\nu_\mu} = \tilde{h}_2\langle\phi\rangle + \tilde{k}_2\langle\eta\rangle, \\ & m_{\mu'} = h_2\langle\phi\rangle - k_2\langle\eta\rangle, \quad m_{\nu_{\mu'}} = \tilde{h}_2\langle\phi\rangle - \tilde{k}_2\langle\eta\rangle,\end{aligned} \tag{2.8}$$

Thus by choosing the suitable values of Yukawas, the required leptons masses can be generated.

2.2 Dark Matter Phenomenology

In this model, we identify the 4th generation right-handed neutral lepton ($\nu'_{\mu R} \equiv \chi$) as the dark matter, which is used to fit AMS-02 data [1,2]. The only possible channels for DM annihilation are into ($\mu^+\mu^-$) and ($\nu^c_\mu\ \nu_\mu$) pairs (Fig.2.1). In this scenario for getting the correct relic density, we use the Breit-Wigner resonant enhancement [182–184] and take $M_{\theta_3} \simeq 2m_\chi$. The thermally averaged annihilation CS can be tuned to be $\sim 10^{-26}\mathrm{cm}^3\mathrm{s}^{-1}$ with the resonant enhancement, which gives the observed relic density. In principle the dark matter can decay into the

Parameters	Numerical values
g_H	0.087
y_h	0.037
y_A	0.020
$y_{H^\pm}$	0.1
m_χ	700 GeV
$m_{\mu'}$	740 GeV
M_{θ_3}	1400 GeV
M_{θ^+}	1400 GeV
$m_{H^\pm}$	1700 GeV
m_h	125 GeV
m_A	150 GeV
δ	10^{-3}
γ	10^{-4}

Table 2.2: Bench mark set of values used in the model.

light leptons via $\mathrm{SU(2)_{HV}}$ gauge boson θ^+ and scalar $\eta^\beta_{i\alpha}$, but by taking the mass of 4th generation charged leptons μ' larger than χ, the stability of dark matter can be ensured.

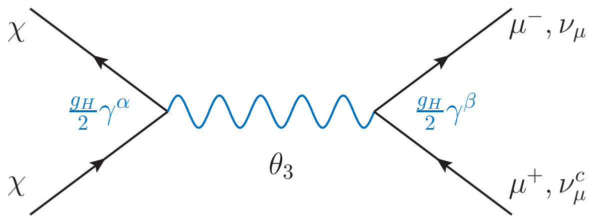

Figure 2.1: Feynman diagram of dark matter annihilation with corresponding vertex factor.

2.2.1 Relic density

The dark matter annihilation channels into SM particles are, $\chi\chi \to \theta_3^* \to \mu^+\mu^-, \nu^c_\mu\nu_\mu$. The annihilation rate of dark matter σv, for a single channel, in the limit of massless leptons, is given by

$$\sigma v = \frac{1}{16\pi} \frac{g_H^4 m_\chi^2}{(s - M_{\theta_3}^2)^2 + \Gamma_{\theta_3}^2 M_{\theta_3}^2} \tag{2.9}$$

where g_H is the horizontal gauge boson coupling, m_χ the dark matter mass, M_{θ_3} and Γ_{θ_3} are the mass and the decay width of $\mathrm{SU(2)_{HV}}$ gauge boson respectively. Since both of the final states (ν_μ, μ) contribute in the relic density, the cross-section of Eq.(2.9) is multiplied by a factor of 2 for relic density computation. The contributions to the decay width of θ_3 comes from the decay modes, $\theta_3 \to \mu^+\mu^-, \nu_\mu^c \nu_\mu$. The total decay width is given by,

$$\Gamma_{\theta_3} = \frac{2g_H^2}{48\pi} M_{\theta_3}. \tag{2.10}$$

In the non-relativistic limit, $s = 4m_\chi^2(1 + v^2/4)$, then by taking into account the factor of 2, Eq.(2.9) simplifies as,

$$\sigma v = \frac{2}{256\pi m_\chi^2} \frac{g_H^4}{(\delta + v^2/4)^2 + \gamma^2}, \tag{2.11}$$

where δ and γ are defined as $M_{\theta_3}^2 \equiv 4m_\chi^2(1-\delta)$, and $\gamma^2 \equiv \Gamma_{\theta_3}^2(1-\delta)/4m_\chi^2$. If δ and γ are larger than $v^2 \simeq (T/M_\chi)^2$, the usual freeze-out takes place, on the other hand if δ and γ are chosen smaller than v^2 then there is a resonant enhancement of the annihilation CS and a late time freeze-out. We choose $\delta \sim 10^{-3}$ and $\gamma \sim 10^{-4}$, so that we have a resonant annihilation of dark matter. The thermal average of annihilation rate is given as [182–184],

$$\langle \sigma v \rangle (x) = \frac{1}{n_{EQ}^2} \frac{m_\chi}{64\pi^4 x} \int_{4m_\chi^2}^{\infty} \hat{\sigma}(s) \sqrt{s} K_1 \left(\frac{x\sqrt{s}}{m_\chi} \right) ds, \tag{2.12}$$

where,

$$n_{EQ}^2 = \frac{g_i}{2\pi^2} \frac{m_\chi^3}{x} K_2(x), \tag{2.13}$$

$$\hat{\sigma}(s) = 2g_i^2 m_\chi \sqrt{s - 4m_\chi^2}\, \sigma v, \tag{2.14}$$

and where $x \equiv m_\chi/T$; $K_1(x)$, $K_2(x)$ represent the modified Bessel functions of second type and g_i is the internal degree of freedom of DM particle. Using Eq.(2.11), Eq.(2.13) and Eq.(2.14) in Eq.(2.12), it can be written as,

$$\langle \sigma v \rangle (x) = \frac{g_H^4}{512 m_\chi^2} \frac{x^{3/2}}{\pi^{3/2}} \int_0^\infty \frac{\sqrt{z}\, \exp[-xz/4]}{(\delta + z/4)^2 + \gamma^2} dz \tag{2.15}$$

where $z \equiv v^2$. We solve the Boltzmann equation for $Y_\chi = n_\chi/s$,

$$\frac{dY_\chi}{dx} = -\frac{\lambda(x)}{x^2}(Y_\chi^2(x) - Y_{\chi eq}^2(x)) \tag{2.16}$$

where

$$\lambda(x) \equiv \left(\frac{\pi}{45}\right)^{1/2} m_\chi M_{Pl} \left(\frac{g_{*s}}{\sqrt{g_*}}\right) \langle\sigma v\rangle(x) \tag{2.17}$$

and where g_* and g_{*s} are the effective degrees of freedom of the energy density and entropy density respectively, with $\langle\sigma v\rangle$ given in Eq.(2.15). We can write the $Y_\chi(x_0)$ at the present epoch as,

$$\frac{1}{Y_\chi(x_0)} = \frac{1}{Y_\chi(x_f)} + \int_{x_f}^{x_s} dx \frac{\lambda(x)}{x^2} \tag{2.18}$$

where the freeze-out x_f is obtained by solving $n_\chi(x_f)\langle\sigma v\rangle = H(x_f)$. We find that $x_f \sim 30$ and the relic density of χ is given by,

$$\Omega = \frac{m_\chi s_0 Y_\chi(x_0)}{\rho_c} \tag{2.19}$$

where $s_0 = 2890\ \mathrm{cm}^{-3}$ is the present entropy density and $\rho_c = h^2 1.9\times 10^{-29}\ \mathrm{gm/cm}^3$ is the critical density. We find that by taking $g_H = 0.087$, $\delta \sim 10^{-3}$ and $\gamma \sim 10^{-4}$ in Eq.(2.15), we obtain the correct relic density $\Omega h^2 = 0.1199 \pm 0.0027$, consistent with WMAP [49] and Planck [9] data. From g_H and γ we can fix $M_{\theta_3} \simeq 1400$ GeV and $m_\chi \simeq \frac{1}{2} M_{\theta_3} \simeq 700$ GeV. There is a large hierarchy between the fourth generation charged fermion mass and the other charged leptons masses. We do not have any underlying theory for the Yukawa couplings and we take the $m_{\mu'}$ mass which fits best the AMS-02 positron spectrum and muon $(g-2)$. A bench mark set of values used in this paper for the masses and couplings is given in Table.(2.2).

2.2.2 Comparison with AMS-02 and PAMELA data

The dark matter in the galaxy annihilates into $\mu^+\mu^-$ and the positron excess seen at AMS-02 [1,2] appears from the decay of muon. We use publicly available code PPPC4DMID [189,190] to compute the positron spectrum $\frac{dN_{e^+}}{dE}$ from the decay of μ pairs for 700 GeV dark matter. We then use the GALPROP code [191,192] for propagation, in which we take the annihilation rate $\sigma v_{\mu^+\mu^-}$, and the positron spectrum $\frac{dN_{e^+}}{dE}$ as an input to the differential injection rate,

$$Q_{e^+}(E,\vec{r}) = \frac{\rho^2}{2m_\chi^2}\langle\sigma v\rangle_{\mu^+\mu^-}\frac{dN_{e^+}}{dE} \tag{2.20}$$

where ρ denotes the density of dark matter in the Milky Way halo, which we take to be the NFW profile [44],

$$\rho_{\rm NFW} = \rho_0\frac{r_s}{r}\left(1+\frac{r}{r_s}\right)^{-2},\ \rho_0 = 0.4\ \text{GeV/cm}^3,\ r_s = 20\ \text{kpc}, \tag{2.21}$$

In GALPROP code [191, 192], we take the diffusion coefficient $D_0 = 3.6 \times 10^{28}\text{cm}^2\text{s}^{-1}$ and Alfven speed $v_A = 15\ \text{kms}^{-1}$. We choose, $z_h = 4$ kpc and $r_{max} = 20$ kpc, which are the half-width and maximum size for 2D galactic model respectively. We choose the nucleus spectral index to break at 9 GeV and spectral index above this is 2.36 and below is 1.82. The normalization flux of electron at 100 GeV is $1.25 \times 10^{-8}\text{cm}^{-2}\text{s}^{-1}\text{sr}^{-1}\text{GeV}^{-1}$ and for the case of electron, we take breaking point at 4 GeV and its injection spectral index above 4 GeV is $\gamma_1^{el} = 2.44$ and below $\gamma_0^{el} = 1.6$. After solving the propagation equation, GALPROP [191, 192] gives the desired positron flux.

To fit the AMS-02 data, the input annihilation CS required in GALPROP is, $<\sigma v>_{\chi\chi\to\mu^+\mu^-} = 2.33 \times 10^{-25}\text{cm}^3\text{s}^{-1}$. The annihilation CS for μ final state from Eq.(2.9) is, $\sigma v \approx 2.8 \times 10^{-25}\text{cm}^3\text{s}^{-1}$, which signifies that there is no extra "astrophysical" boost factor needed to satisfy AMS-02 data. The annihilation rate required for relic density was $\langle\sigma v\rangle \sim 3 \times 10^{-26}\text{cm}^3\text{s}^{-1}$, and the factor ~ 10 increase in σv at the present epoch is due to resonant enhancement by taking $m_\chi \simeq \frac{1}{2}M_{\theta_3}$. In Fig.(2.2), we plot the output of GALPROP code and compare it with the observed AMS-02 [1, 2] and PAMELA [17] data. We see that our positron spectrum fits the AMS-02 data very well. We also check the photon production from the decay of μ final state by generating the γ-ray spectrum called $\frac{dN_\gamma}{dE}$ from publicly available code PPPC4DMID [189, 190] and propagating it through the GALPROP code [191, 192]. We then compare the output with the observed Fermi-LAT data [193], as shown in Fig.(2.3), and find that the γ-ray does not exceed the observed limits. There is no annihilation to hadrons, so

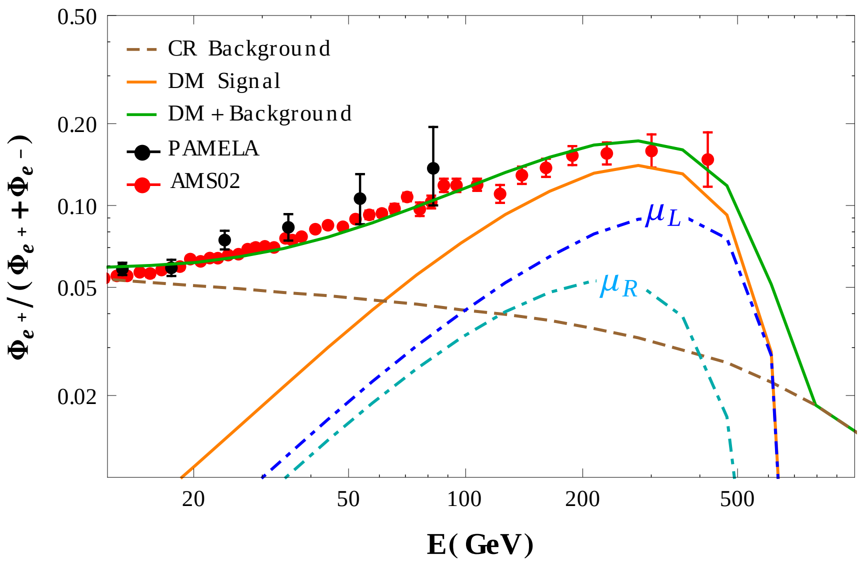

Figure 2.2: The positron flux spectrum compared with data from AMS-02 [1,2] and PAMELA [17]. The contributions of different channels (μ_L, μ_R) are shown for comparison.

no excess of antiprotons are predicted, consistent with the PAMELA [179] and AMS-02 [180] data.

2.3 Muon Magnetic Moment

The $\mathrm{SU(2)_{HV}}$ horizontal symmetry, which connects muon and 4th generation families, gives extra contributions to muon $(g-2)$. The diagrams that contribute to muon $(g-2)$ with $\mathrm{SU(2)_{HV}}$ charged gauge boson θ^+ and scalar $\eta^{\beta}_{i\alpha}$ are shown in Fig.(2.4).

We first calculate the contribution from $\mathrm{SU(2)_{HV}}$ gauge boson θ^+, which is shown in Fig.2.4(c). For this diagram the vertex factor of the amplitude $\mu(p')\Gamma_\mu\mu(p)\epsilon^\mu$ is,

$$\Gamma_\mu = \frac{eg_H^2}{2}\int\frac{d^4k}{(2\pi)^4}\gamma^\beta\frac{(\not{p}'+\not{k}+m_{\mu'})}{(p'+k)^2-m_{\mu'}^2}\gamma_\mu\frac{(\not{p}+\not{k}+m_{\mu'})}{(p+k)^2-m_{\mu'}^2}\gamma^\alpha\frac{g_{\alpha\beta}}{k^2-M_{\theta+}^2}. \tag{2.22}$$

We perform the integration and use the Gorden identity to replace,

$$\bar{u}(p')(p_\mu+p'_\mu)u(p) = \bar{u}(p')(2m_\mu\gamma_\mu - i\sigma^{\mu\nu}q_\nu)u(p), \tag{2.23}$$

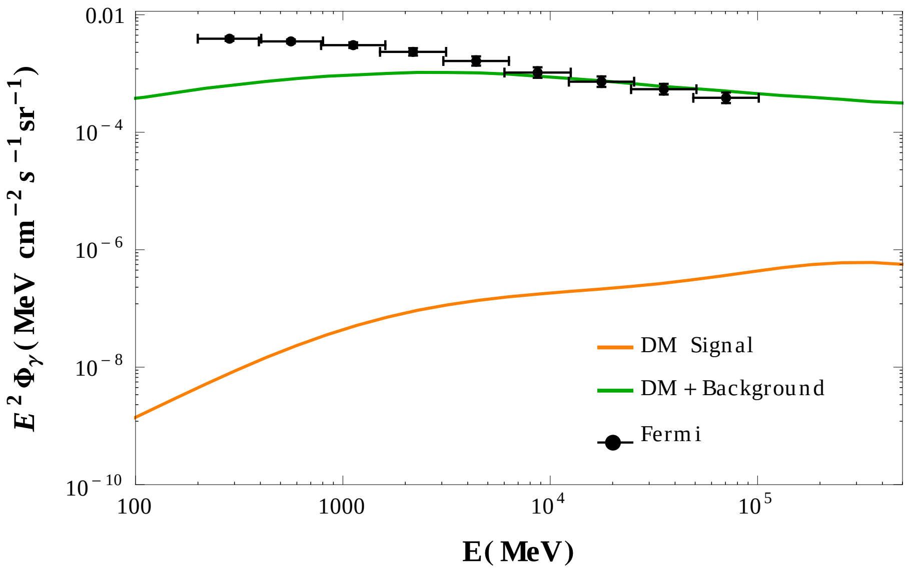

Figure 2.3: The γ-ray spectrum compared with data from Fermi Lat [193].

and identify the coefficient of the $i\sigma^{\mu\nu}q_\nu$ as the magnetic form factor. The contribution to Δa_μ is,

$$[\Delta a_\mu]_{\theta+} = \frac{m_\mu^2}{16\pi^2}\int_0^1 dx \frac{g_H^2\left(\frac{2m'_\mu}{m_\mu}(x-x^2)-(x-x^3)\right)}{(1-x)m_{\mu'}^2 - x(1-x)m_\mu^2 + xM_{\theta\pm}^2}. \tag{2.24}$$

In the limit of $M_{\theta+}^2 >> m_{\mu'}^2$, we get the anomalous magnetic moment,

$$[\Delta a_\mu]_{\theta+} = \frac{g_H^2}{8\pi^2}\left(\frac{m_\mu m_{\mu'} - 2/3m_\mu^2}{M_{\theta+}^2}\right), \tag{2.25}$$

we note that in Eq.(2.25), the first term is dominant which shows $m_\mu m_{\mu'}$ enhancement in the muon $(g-2)$.

In our model, the contribution from the neutral higgs η (CP-even h and CP-odd A) is shown in Fig.2.4. The $(g-2)$ contribution of this diagram is [194],

$$\begin{aligned}[\Delta a_\mu]_{h,A} = &\frac{m_\mu^2}{8\pi^2}\int_0^1 dx \frac{y_h^2(x^2 - x^3 + \frac{m_{\mu'}}{m_\mu}x^2)}{m_\mu^2 x^2 + (m_{\mu'}^2 - m_\mu^2)x + m_h^2(1-x)} \\ &+ \frac{m_\mu^2}{8\pi^2}\int_0^1 dx \frac{y_A^2(x^2 - x^3 - \frac{m_{\mu'}}{m_\mu}x^2)}{m_\mu^2 x^2 + (m_{\mu'}^2 - m_\mu^2)x + m_A^2(1-x)},\end{aligned} \tag{2.26}$$

where y_h, y_A represent the Yukawa couplings of neutral CP-even and -odd higgs respectively and their masses are denoted by m_h and m_A respectively. We shall calculate the contributions from the lightest scalars only, which give the larger

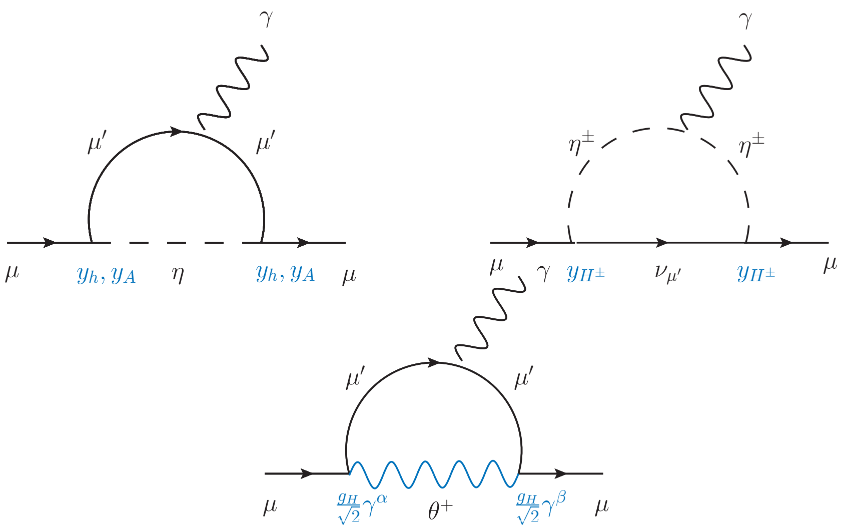

Figure 2.4: Feynman diagrams of scalar $\eta^\beta_{i\alpha}$ and SU(2)$_{\rm HV}$ gauge boson θ^+, which give contributions to muon $(g-2)$.

contributions in compare to heavy scalars. In the limits $m^2_{\mu'} \gg m^2_h$, $m^2_{\mu'} \gg m^2_A$, doing the integration in Eq.(2.26) we get the anomalous magnetic moment,

$$[\Delta a_\mu]_{h,A} = \frac{1}{8\pi^2}\left(\frac{3m_\mu m_{\mu'}(y_h^2 - y_A^2) + m_\mu^2(y_h^2 + y_A^2)}{6m^2_{\mu'}}\right). \tag{2.27}$$

In a similar way, the contribution from the mass eigenstate $H^\pm$ of charged higgs $\eta^\pm$, shown in Fig.2.4, is given by [194],

$$[\Delta a_\mu]_{H^\pm} = \frac{m_\mu^2}{8\pi^2}\int_0^1 dx \frac{y^2_{H^\pm}\left(x^3 - x^2 + \frac{m_{\nu_{\mu'}}}{m_\mu}(x^2 - x)\right)}{m_\mu^2 x^2 + (m^2_{H^\pm} - m^2_\mu)x + m^2_{\nu_{\mu'}}(1-x)}, \tag{2.28}$$

where $y_{H^\pm}$ and $m_{H^\pm}$ are the Yukawa coupling and mass of the charged higgs respectively. We perform the integration (Eq.2.28) in the limit $m^2_{H^\pm} \gg m^2_{\nu_{\mu'}}$, and get the anomalous magnetic moment,

$$[\Delta a_\mu]_{H^\pm} = -\frac{y^2_{H^\pm}}{8\pi^2}\left(\frac{3m_\mu m_{\nu_{\mu'}} + m_\mu^2}{6m^2_{H^\pm}}\right). \tag{2.29}$$

So the complete contribution to muon $(g-2)$ in our model is given as,

$$\Delta a_\mu = [\Delta a_\mu]_{\theta^+} + [\Delta a_\mu]_{h,A} + [\Delta a_\mu]_{H^\pm} \tag{2.30}$$

As discussed before, in our model the lightest CP-even scalar h_1 is mainly composed of η, so we can write,

$$y_h \sim k_2 \ \cos\alpha_1, \tag{2.31}$$

where α_1 is the mixing angle between CP-even mass eigenstate h_1 and gauge eigenstate η, and k_2 is the Yukawa coupling defined in Eq.(2.7). In a similar way, we assume that lightest pseudoscalar A and charged higgs $H^{\pm}$ are also mainly composed of η, so that we can write,

$$y_A \sim k_2 \ \cos\alpha_2, \quad y_{H^{\pm}} \sim \tilde{k}_2 \ \cos\alpha_3, \tag{2.32}$$

where α_2 is the mixing angle between CP-odd scalars and α_3 is the mixing angle between the charged scalars. $\tilde{k}_2$ denotes the Yukawa coupling defined in Eq.(2.7). In the SU(2)$_{\rm HV}$ gauge boson sector, we take $g_H = 0.087,\ M_{\theta^+} \approx 1400$ GeV ($M_{\theta_3} \approx M_{\theta^+}$), which are fixed from the requirement of correct relic density and we take $m_{\mu'} = 740$ GeV, coming from the stability requirement of dark matter ($m_{\mu'} > m_\chi$). After doing numerical calculation, we get $[\Delta a]_{\theta^+} = 3.61 \times 10^{-9}$. The contributions from (h, A) scalars depend on the parameter $k_2^2\ (\cos^2\alpha_1 - \cos^2\alpha_2)$, which we assume to be $\simeq 10^{-3}$ and obtain $[\Delta a_\mu]_{h,A} = 0.82 \times 10^{-9}$. For the charged scalar contribution, we assume $\tilde{k}_2\ \cos\alpha_3 = 0.1$ and $m_{H^{\pm}} = 1700$ GeV and obtain $[\Delta a_\mu]_{H^{\pm}} = -1.53 \times 10^{-9}$. Adding the contributions from θ^+, (h, A) and $H^{\pm}$, we get

$$\Delta a_\mu = 2.9 \times 10^{-9}, \tag{2.33}$$

which is in agreement with the experimental result [3, 4] within 1σ. To get the desired value of muon $(g-2)$, we have to consider a large hierarchy between the neutral higgs ($m_h \sim 125$ GeV, $m_A \sim 150$ GeV) and the charged higgs $m_{H^{\pm}} \sim 1700$ GeV. These masses have to arise by appropriate choices of the couplings in the higgs potential of $(\phi_i,\ \eta^{\beta}_{i\alpha},\ \chi_\alpha)$.

2.4 Conclusion and Outlook

In this chapter, we studied a 4th generation extension of the standard model, where the 4th generation leptons interact with the muon family via SU(2)$_{\rm HV}$ gauge bosons. The 4th generation right-handed neutrino is identified as the dark matter. We proposed a common explanation to the excess of positron seen at

AMS-02 [1,2] and the discrepancy between SM prediction [97–101] and BNL measurement [3,4] of muon $(g-2)$. The $\mathrm{SU(2)_{HV}}$ gauge boson θ^+ with 4th generation charged lepton μ' and charged higgs $H^{\pm}$, give the required contribution to muon $(g-2)$ to satisfy the BNL measurement within 1σ. The LHC constraints on 4th generation quarks is evaded by extending the higgs sector as in [186, 187].
In this horizontal $\mathrm{SU(2)_{HV}}$ gauge symmetry model, we also explain the preferential annihilation of dark matter to $\mu^+\mu^-$ channel over other leptons and predict that there is no antiproton excess, in agreement with PAMELA [179] and AMS-02 [180] data. Since the dark matter has gauge interactions only with the muon family at tree level, we can evade the bounds from direct detection experiments [11, 13] based on scattering of dark matter with the first generation quarks.

Chapter 3

Dark left-right gauge model

As we described in the previous chapter, there are two prominent experimental hints, which seek the extension of SM for their solutions; namely the AMS-02 positron excess [1, 2], and the discrepancy between the measured [3, 4] and the SM prediction [97–101] of muon $(g-2)$. It would be interesting to find an economic solution beyond SM to explain both the muon $(g-2)$ and AMS-02 positron measurements.

In this chapter, we examine another possibility for explaining the AMS-02 positron excess and muon $(g-2)$ simultaneously. We show that a variant of the left-right model called dark left-right gauge model (DLRM) [195, 196] has the ingredients to explain these two experimental signals. The alternative left-right symmetric model (ALRM) has been proposed in 1987 [197, 198]. One of the key advantages of ALRM over the standard/conventional left-right model (LRM) [199–203] is, it has no tree-level flavor changing neutral currents. Therefore, the $\mathrm{SU(2)_R}$ breaking scale can be low and hence allows a possibility for $W_R^{\pm}, Z'$ gauge bosons to be observable at collider experiments. Another variant of this ALRM is the dark left-right gauge model [195, 196], which has both the neutrino mass and a fermionic DM candidate. In DLRM, there exists a discrete R-parity. The neutral component of the right-handed lepton doublet n_R carries zero generalized lepton number $(\tilde{L})$ and is odd under the R-parity. Thus it can be made stable and a viable candidate for DM if it is the lightest R-odd particle in the spectrum. Additional higgs triplet (Δ_R) has been introduced to give mass to n_R. The annihilation of n_R into muonic final states takes place through the t-channel exchange of charged triplet higgs (Δ_R^+). One of the motivations of this work was to explain the positron excess seen by AMS-02 [1, 2] experiments through the annihilation of DM in the galactic halo. By choosing the $W_R^\pm, Z'$ bosons heavier than the Δ_R, we ensure that the DM is leptophilic which makes it ideal for explaining AMS-02 positron excess. But, the annihilation cross-section in this case is helicity suppressed. To overcome this suppression, we have considered the mechanism of internal bremsstrahlung (IB) [204] in the DM annihilation process. Also we need an astrophysical boost $\sim \mathcal{O}(10^3)$, to get the required cross-section for fitting AMS-02 data. A leading explanation of the observed positron excess comes from the annihilation of dark matter particles into leptonic final states which results in a soft positron spectrum which can account for the AMS-02 data quite well. A population of nearby pulsars can provide an alternative explanation [19–21] for the positron excess reported by AMS-02, PAMELA. However in case of pulsars, an anisotropy is expected in the signal contributions as a function of energy due to the differing positions of the individual contributing pulsars, which falls nearly an order of magnitude below the current constraints from both AMS-02 and the Fermi-LAT [23]. Another interesting aspect of this model is that the same Yukawa term $\Psi_R \Delta_R \Psi_R$, which produces muons from DM annihilation also gives rise to the muon $(g-2)$ through singly and doubly charged triplet higgs loop. We have shown that the same masses and couplings can be used to obtain both the relic abundance of DM and required $\Delta a_\mu = (2.87 \pm 0.8) \times 10^{-9}$ within 1σ of the experimental value [3, 4]. DLRM contains a number of singly and doubly charged scalars. The decay of $\Delta_R^{\pm\pm}$ into same sign di-leptons is an important signal from LHC perspective to test DLRM.

This chapter is organized as follows: In Section.3.1, we describe the details of the model; the dark matter part is discussed in Section.3.2. The explanation of AMS-02 positron excess has been dealt in Section.3.2.1 and contribution to muon $(g-2)$ has been calculated in in Section.3.3. After giving a brief discussion in Section.3.4, finally we conclude our result in Section.3.5.

3.1 Dark Left-Right Gauge model

We adopt the dark left-right gauge model [195,196], whose gauge group is given by, $\mathrm{SU(3)_C \times SU(2)_R \times SU(2)_L \times U(1)} \times S$. Here an additional global U(1)[1] symmetry S has been introduced such that after the spontaneous breaking of $\mathrm{SU(2)_R} \times S$ the generalized lepton number $\tilde{L}$ (defined as, $\tilde{L} = S - T_{3R}$) remains unbroken. The scalar sector of this model consists of a bi-doublet Φ, two doublets (Φ_L, Φ_R) and two hypercharge '+1' triplets (Δ_L, Δ_R), denoted as,

$$\Phi = \begin{pmatrix} \phi_1^0 & \phi_2^+ \\ \phi_1^- & \phi_2^0 \end{pmatrix}, \; \Phi_{L,R} = \begin{pmatrix} \phi_{L,R}^+ \\ \phi_{L,R}^0 \end{pmatrix} \text{ and } \Delta_{L,R} = \begin{pmatrix} \frac{\Delta_{L,R}^+}{\sqrt{2}} & \Delta_{L,R}^{++} \\ \Delta_{L,R}^0 & -\frac{\Delta_{L,R}^+}{\sqrt{2}} \end{pmatrix}.$$

The quantum numbers of the scalars under the DLRM gauge group and S are listed in Table 3.1. The fermionic sector (as shown in Table.3.2) consists of additional $\mathrm{SU(2)_R}$ lepton (Ψ_R) and quark doublet (Q_R). Also it contains a quark singlet (x_L), which carries a generalized lepton number, $\tilde{L} = 1$. The same structure follows for all three generations of fermion in SM.

Scalar	$\mathrm{SU(3)_C \times SU(2)_L \times SU(2)_R \times U(1)}$	S
Φ	$(1,2,2,0)$	$1/2$
$\tilde{\Phi}$	$(1,2,2,0)$	$-1/2$
Φ_L	$(1,2,1,1/2)$	0
Φ_R	$(1,1,2,1/2)$	$-1/2$
Δ_L	$(1,3,1,1)$	-2
Δ_R	$(1,1,3,1)$	-1

Table 3.1: Scalar content of DLRM model. Note that $\tilde{\Phi} = \sigma_2 \Phi^* \sigma_2$.

The scalar potential contains all allowed (by S-symmetry) singlet combination like,

$$\begin{aligned} V &= (m_1^2 \Phi^\dagger \Phi + m_2^2 \Phi_L^\dagger \Phi_L + m_3^2 \Phi_R^\dagger \Phi_R + m_4^2 \Delta_L^\dagger \Delta_L + m_5^2 \Delta_R^\dagger \Delta_R) + \\ &\quad \Phi_R^\dagger \Delta_R \tilde{\Phi}_R + \Phi_L^\dagger \Phi \Phi_R + \mathrm{Tr}(\tilde{\Phi}^\dagger \Delta_L \Phi \Delta_R^\dagger) + (quartic - terms). \end{aligned} \tag{3.1}$$

From the minimization condition of the potential it is evident that there exists a solution with $\langle \phi_1^0 \rangle \equiv v_1 = 0$. The leptons and the up type quarks get mass

[1]which is different from the dark left-right U(1) group.

Fermion	$SU(3)_C \times SU(2)_L \times SU(2)_R \times U(1)$	S	L
$\Psi_L = (\nu, e)_L$	(1,2,1,-1/2)	1	(1,1)
$\Psi_R = (n, e)_R$	(1,1,2,-1/2)	1/2	(0,1)
$Q_L = (u, d)_L$	(3,2,1,1/6)	0	(0,0)
$Q_R = (u, x)_R$	(3,1,2,1/6)	1/2	(0,1)
d_R	(3,1,1,-1/3)	0	0
x_L	(3,1,1,-1/3)	1	1

Table 3.2: Fermion content of DLRM model.

through the Yukawa terms $\bar{\Psi}_L \Phi \Psi_R$ and $\bar{Q}_L \tilde{\Phi} Q_R$ respectively, when the neutral component of the bi-doublet gets vacuum expectation value (vev), i.e., $\langle \phi_2^0 \rangle = v_2$. Similarly the down type quark gets mass through the interaction $\bar{Q}_L \Phi_L d_R$. The triplet higgses ($\Delta_{L,R}$) give masses to ν and n respectively. Due to S-symmetry, terms like $\bar{\Psi}_L \tilde{\Phi} \Psi_R$ and $\bar{Q}_L \Phi Q_R$ are forbidden, which also ensures the absence of flavor-changing neutral currents at the tree-level. In addition, a generalized R-parity (defined as, $R = (-1)^{3B+\tilde{L}+2j}$) is imposed on this model, since $\tilde{L}$ is broken to $(-1)^{\tilde{L}}$ when neutrinos acquire Majorana masses. This implies n, x, $W_R^\pm$, $\Phi_R^\pm$, $\Delta_R^\pm$ are odd under R-parity. One interesting feature of this model is that $W_R^\pm$-boson also carries generalized lepton number $\tilde{L} = \mp 1$, which forbids it from mixing with $W_L^\pm$-boson. This model also contains an extra Z'-boson, but we have neglected the $Z - Z'$ mixing, as the mass of the Z' is $\sim$ TeV and the mixing with Z is small.

3.2 Dark matter in DLRM

By virtue of the S-symmetry the Yukawa-term $\bar{\Psi}_L \tilde{\Phi} \Psi_R$ is forbidden thus n_R is not the Dirac mass partner of ν_L. n_R is termed as 'scotino' [195], i.e., dark fermion and the lightest one is treated as a viable dark matter candidate. The DM candidate is stable as an artifact of R-parity, under which it is odd. We choose $n_R^\mu \equiv \chi$, as the dark matter. The mass of DM is generated through the term $\Psi_R \Psi_R \Delta_R$. Here, we assume that $W_R^\pm, Z'$ gauge bosons are considerably

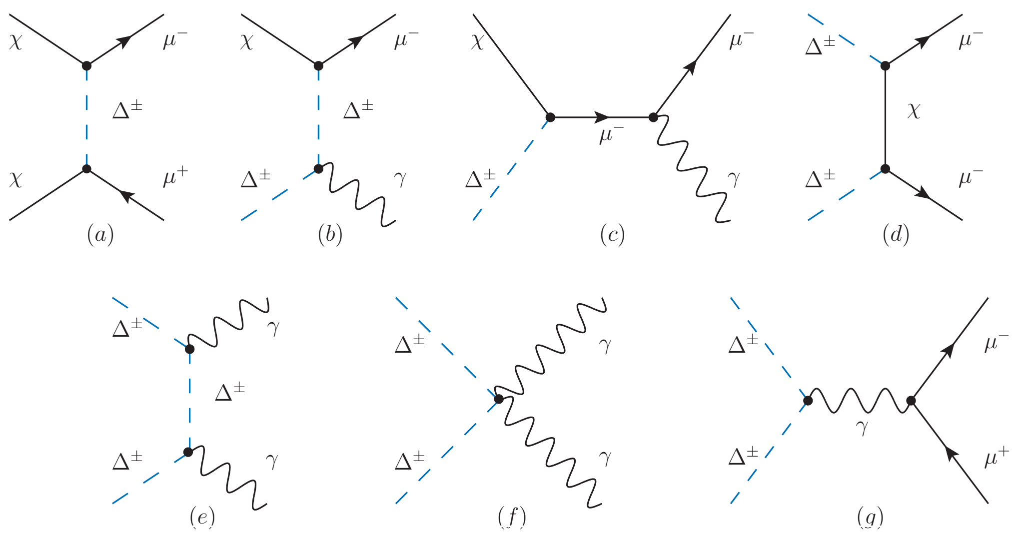

Figure 3.1: Feynman diagrams of all dominant annihilation and co-annihilation channels.

heavier than Δ_R^+. Therefore, the dominant annihilation channel of χ into leptonic final states (mainly $\mu^+\mu^-$) is through the t-channel exchange of $\Delta_R^\pm$ (as shown in Fig.3.1(a)). Since, the triplet higgs does not couple with the quarks, the dark matter in this model is mostly leptophilic. Also there is no constraint on DM cross-section from direct detection experiments [11, 13].

Using partial-wave expansion, the annihilation cross-section can be written as, $\langle \sigma v \rangle_{ann} \simeq a + 6b/x_f$ where, a and b are the s-wave and p-wave contribution respectively. The s-wave part is helicity suppressed and is given by [205, 206],

$$a \simeq \frac{c_d^4}{32\pi m_\chi^2} \frac{m_f^2}{m_\chi^2} \frac{1}{(1+z)^2}, \tag{3.2}$$

whereas the p-wave contribution can be expressed as [207],

$$b \simeq \frac{c_d^4}{48\pi m_\chi^2} \frac{(1+z^2)}{(1+z)^4}, \tag{3.3}$$

where, c_d is the Yukawa-coupling between χ, μ^- and Δ_R^+. The ratio of RH-charged triplet mass to DM mass is denoted by, $z \equiv (m_{\Delta_R^+}/m_\chi)^2$. Clearly, the s-wave contribution is negligible compared to the later part, which is velocity-suppressed today.

If the masses of dark matter and the charged higgs are nearly degenerate, i.e., $\delta m \sim T_f$ the coannihilations [205, 208, 209] become important and relic density

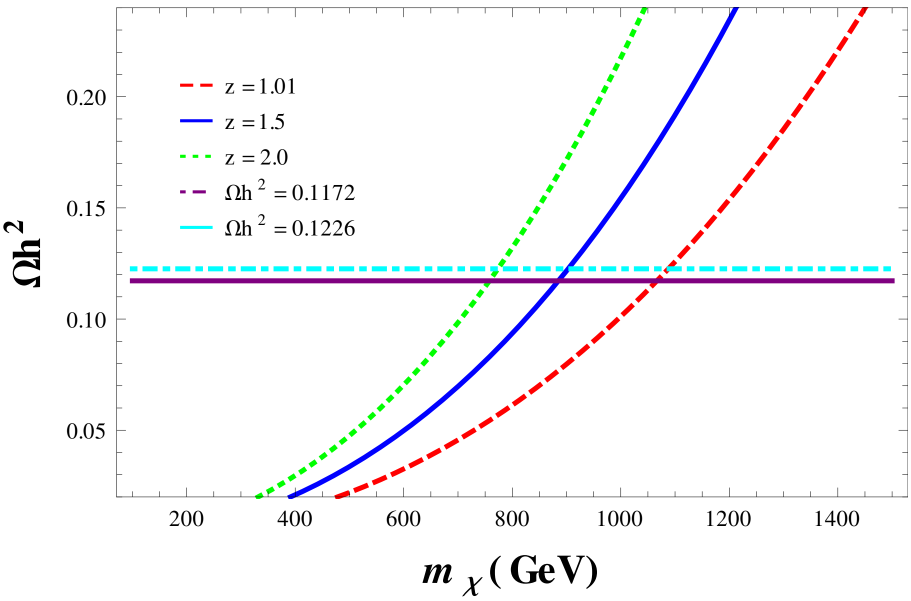

Figure 3.2: Plot of relic abundance as a function of DM mass, for $c_d = 1.6$ and with different values of $z = 1.01$ (red), 1.5 (blue), 2.0 (green). The straight lines show the present value of $\Omega h^2 = 0.1199 \pm 0.0027$ from Planck experiments [9].

is no longer produced by thermal freeze-out. We have to take into account cross-sections of processes like $\chi\Delta^+ \to \mu^+\gamma$, $\Delta^+\Delta^- \to \gamma\gamma$ and $\Delta^+\Delta^- \to \mu^+\mu^-$ (as shown in Fig.3.1(b-f)). However, the contributions from the diagrams shown as Fig.3.1(d) and Fig.3.1(g) are less important since those are helicity-suppressed. The effective cross-section is given by,

$$\sigma_{eff} v = \sum_{ij} \frac{n_i^{eq} n_j^{eq}}{(\sum_k n_k^{eq})^2} \sigma_{ij} v, \tag{3.4}$$

where, $n_i^{eq} = g_i(\frac{m_i T}{2\pi})^{3/2} e^{-m_i/T}$. The analytic expression of the relic abundance can be formulated as [210, 211]

$$\Omega_{_{CDM}} h^2 \simeq \frac{\langle \sigma_{ann} v \rangle}{\langle \sigma_{eff} v \rangle} \left(\frac{T_{f0}}{T_f} \right) \left(\frac{m_\chi^2}{c_d^4} \right) \frac{(1+z)^4}{1+z^2} \mathrm{GeV}^{-2}, \tag{3.5}$$

where, $T_{f0} \simeq m_\chi/20$ is the temperature at the time of freeze-out and $\langle \sigma_{ann} v \rangle$ is the annihilation cross-section without taking into account coannihilation. To produce the correct relic abundances, one can tune the coupling c_d and the ratio z. In Fig.(3.2), the relic abundance is plotted as a function of DM mass for $c_d = 1.6$ but with different values of $z = 1.01$ (red), 1.5 (blue), 2.0 (green). The straight lines (solid and dashed) show the latest PLANCK data i.e., $\Omega_{_{CDM}} h^2 = 0.1199 \pm 0.0027$

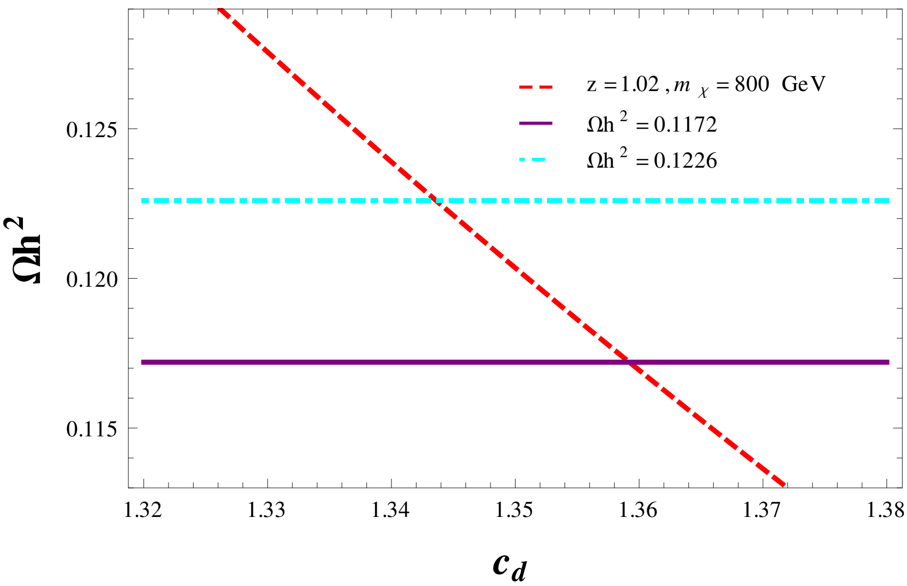

Figure 3.3: Plot of relic abundance as a function of coupling, for $m_\chi = 800$ GeV and $z = 1.02$.

[9]. We observe that as the ratio z is increased, one requires lower values of dark matter mass in order to satisfy correct relic abundance. We choose a specific set of benchmark point as, $m_\chi \sim 800$ GeV and $z = 1.02$. We plot relic abundance, as shown in Fig.(3.3), for this particular choice of benchmark set. We obtain a narrow allowed range of coupling, i.e., $1.343 < c_d < 1.36$, which is consistent with relic abundance [9].

3.2.1 Explanation of AMS-02 positron excess

It has been shown that AMS-02 positron excess [1, 2] can be explained by DM annihilation into $\mu^+\mu^-$ if the annihilation cross-section is $\sigma v \sim 10^{-24}\text{cm}^3\text{sec}^{-1}$ [27, 28] for a TeV scale DM. Such large cross-section needed to explain AMS-02 result through DM annihilation into 'radiation' is constrained by recent Planck results [29]. Therefore, the AMS-02 explanation necessarily requires an astrophysical boost [30, 31]. In DLRM, we have Majorana fermionic DM which implies that annihilation into fermionic final states is helicity suppressed by a factor of m_f^2/m_χ^2. As discussed earlier, the p-wave part of the annihilation cross-section is suppressed by the velocity squared of the galactic DM particles today, which is typically $v_{today} \sim 10^{-3}$. One of the possibilities to evade the suppression is to make use

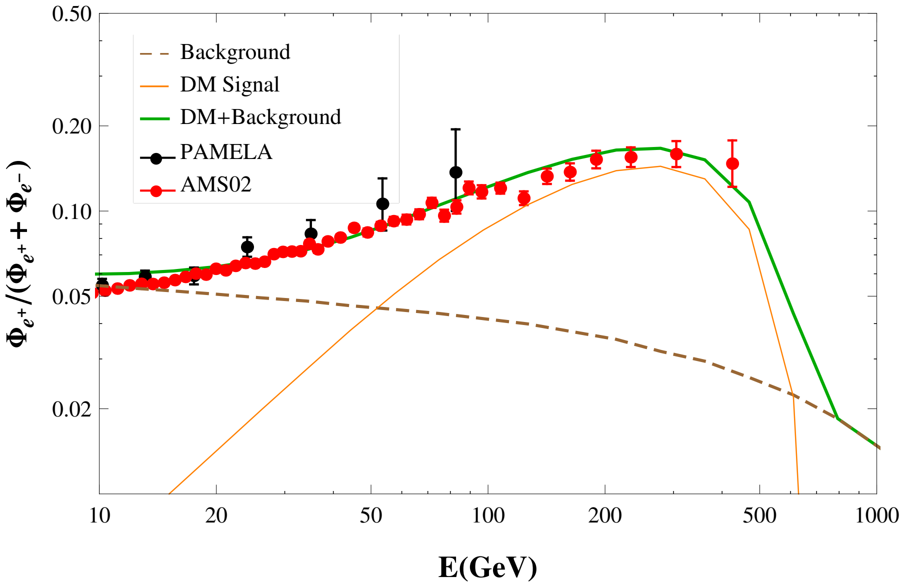

Figure 3.4: Prediction of the cosmic-ray positron fraction from dark matter annihilation into $\mu^+\mu^-$ final state. The positron fraction spectrum is compared with the data from AMS-02 [1,2] and PAMELA [17].

of the IB mechanism, where the emission of associated vector boson lifts the helicity suppression in the s-wave contribution to the annihilation cross-section [204, 212]. The process of IB incorporates both virtual internal bremsstrahlung (VIB) and the photons from final-state radiation (FSR). Therefore, we consider the annihilation of DM into $\chi\chi \to \mu^+\mu^-\gamma$ in the late universe (i.e. today), for which the cross-section is given by [204, 212],

$$\begin{aligned}\langle\sigma v\rangle_{\mu^+\mu^-\gamma} &\simeq \frac{\alpha_{em} c_d^4}{64\pi^2 m_\chi^2}\left\{(1+z)\left[\frac{\pi^2}{6} - \ln^2\left(\frac{z+1}{2z}\right) - 2\mathrm{Li}_2\left(\frac{z+1}{2z}\right)\right]\right. \\ &\left. + \frac{4z+3}{z+1} + \frac{4z^2-3z-1}{2z}\ln\left(\frac{z-1}{z+1}\right)\right\},\end{aligned} \tag{3.6}$$

where, α_{em} is the fine-structure constant and $\mathrm{Li}_2(x) = \sum_{k=1}^{\infty} x^k/k^2$. As described in previous chapter, for generating the positron spectrum, dN_e^+/dE from muon decay ($m_\chi \sim$ 800 GeV), we use the publicly available code PPPC4DMID [189, 190] and then we use GALPROP code [191, 192] for the propagation of charged particles in the galaxy. The differential rate of production of primary positron flux per unit energy per unit volume is given by,

$$Q_{e^+}(E,\vec{r}) = \frac{\rho^2}{2m_\chi^2}\langle\sigma v\rangle_{\mu^+\mu^-\gamma}\frac{dN_{e^+}}{dE}, \tag{3.7}$$

where $\langle\sigma v\rangle_{\mu^+\mu^-\gamma}$ is the annihilation cross-section and ρ denotes the density of dark matter particle in the Milky Way halo, which we assume to be described by NFW profile [44]. In GALPROP code [191, 192], we set $D_0 = 3.6 \times 10^{28}$ cm^{2}s^{-1}, $z_h = 4$ kpc and $r_{max} = 20$ kpc, which are the diffusion coefficient, the half-width and maximum size of 2D galactic model respectively. We choose the nucleus injection index breaking at 9 GeV and the values above and below its breaking are 2.36 and 1.82 respectively. Similarly in the case of electron, we choose injection index breaking at 4 GeV and its spectral index above and below are 5.0 and 2.44 respectively with normalization flux 1.25×10^{-8}cm^{-2}s^{-1}sr^{-1}GeV^{-1} at 100 GeV. Taking into account the chosen parameters, GALPROP [191, 192] solves the propagation equation, and we find the propagated positron flux.

In order to fit AMS-02 data [1, 2], the required annihilation cross-section in GALPROP code [191, 192] is $\langle\sigma v\rangle_{\mu^+\mu^-\gamma} = 8.8 \times 10^{-25}$cm^{3}s^{-1}. But the internal bremsstrahlung process ($\chi\chi \to \mu^+\mu^-\gamma$) gives the annihilation cross-section $\langle\sigma v\rangle_{\mu^+\mu^-\gamma} = 1.37 \times 10^{-28}$cm^{3}s^{-1}, using the benchmark set $m_\chi \sim 800$ GeV, $m_{\Delta_R^\pm} \sim 808$ GeV and $c_d \sim 1.36$. It has been proposed in Ref. [30, 31] that local clumping at scales of ~ 20 kpc can enhance the positron flux (which arise from distances < 20 kpc) without changing the γ-ray or anti-proton flux [213] significantly. We have assumed that local clumping provides a boost factor ~ 6400 to the positron flux, which is needed to fit the observed AMS-02 data. In Fig.(3.4), we plot the positron flux obtained from the GALPROP and compare it with observed AMS-02 [1, 2] and PAMELA data [17]. From Fig.(3.4), we observe that positron flux predicted from our model fits the data well. Since we are considering the internal bremsstrahlung process to lift the helicity suppression in the dark matter annihilation cross-section, there will be primary photons in the final state as well as secondary photons from muons. We also check the consistency of the predicted photon spectrum from this model with the observed data [214]. We have generated the γ-ray spectrum, i.e., dN_γ/dE using micrOMEGAs 3.3.9 code [218]. We compare the output γ spectrum with observed Fermi-LAT data [214], which is shown in Fig.(3.5). The required cross-section for fitting AMS-02 positron excess, obtained in this model is consistent with the latest Fermi-LAT 4-year measure-

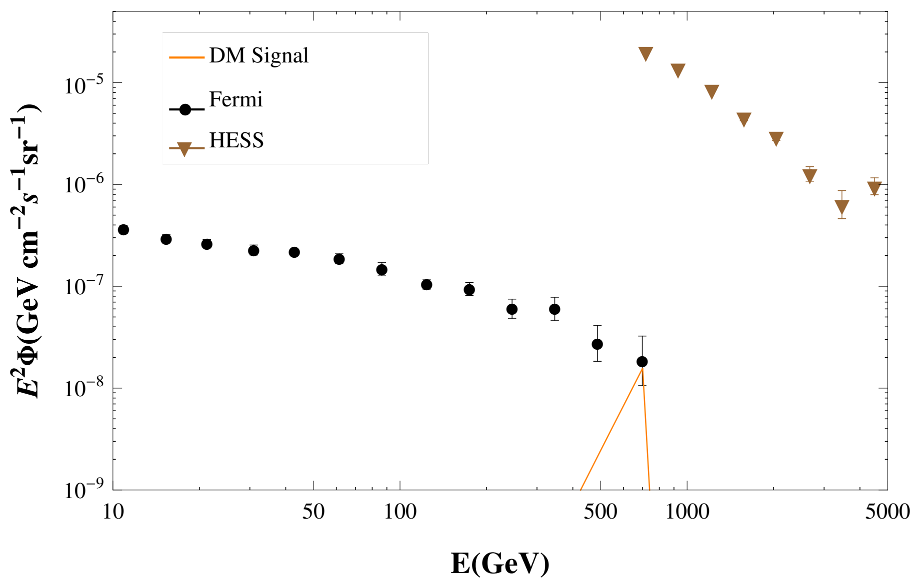

Figure 3.5: Predicted γ-ray spectrum is compared with Fermi LAT data [214]. HESS measurement [215,216] of $(e^+ + e^-)$ flux acts as upper bound on γ-ray flux in the 0.7-4 TeV range [217].

ment of the gamma-ray background (see Fig.8 of Ref. [214]). In Fig.(3.5), we have also shown the HESS measurement [215,216] of $(e^+ + e^-)$ flux, which acts as an upper bound on γ-ray flux [217] and clearly the γ-ray spectrum of our model is well below the upper limits. In this model, the dark matter does not annihilate into hadronic final states. Hence, there is no predicted excess of antiprotons, which makes it consistent with the PAMELA [179] and AMS-02 data [180].

3.3 Muon magnetic moment

The muon magnetic moment is calculated by the magnetic moment operator, which is given as

$$\mathcal{L}_{MDM} = \frac{e}{2m_\mu} F_2(q^2) \bar{\psi}_\mu \sigma_{\mu\nu} \psi_\mu F^{\mu\nu}, \tag{3.8}$$

where m_μ is the mass of the muon and $F_2(q^2)$ is the magnetic form factor. Here $\sigma_{\mu\nu} = \frac{i}{2}[\gamma_\mu, \gamma_\nu]$ and $F^{\mu\nu}$ is the field strength of the photon field. The anomalous magnetic moment is related to F_2 as $\Delta a_\mu = F_2(0)$ for on-shell muon.

In DLRM [195], there exist diagrams containing additional gauge bosons and charged triplet scalars which give contributions to the muon magnetic moment.

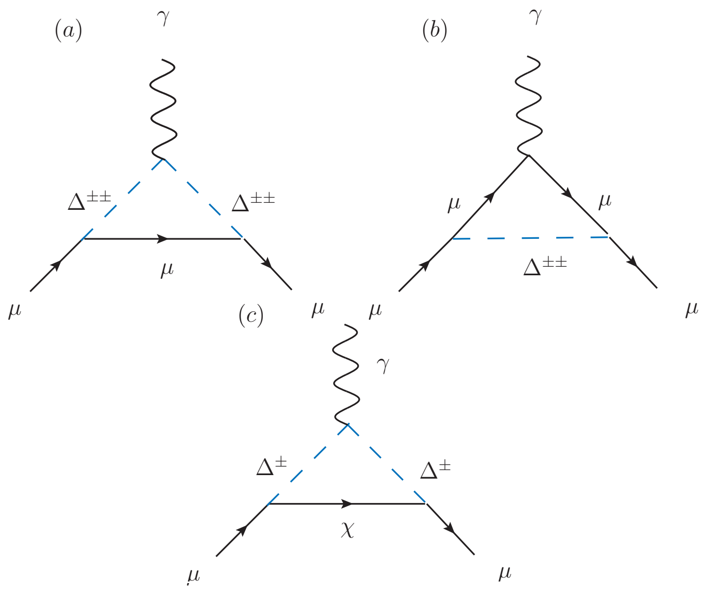

Figure 3.6: Dominant Feynman diagrams of singly (c) and doubly (a,b) charged triplet scalar loops contributing to muon $(g-2)$.

In the conventional left-right symmetric model [199–203] with $g_L = g_R$, there are stringent bounds from LHC on the masses of $\mathrm{SU(2)_R}$ gauge bosons $(W_R^{\pm}, Z')$, such that $M_{W_R^{\pm}} \sim 2.5$ TeV, $M_{Z'} \sim 3$ TeV [176]. Under these assumptions, the contributions of heavy gauge bosons to muon $(g-2)$, has been neglected in comparison to the charged scalars. Therefore, the interaction terms relevant to muon $(g-2)$ are $\psi_R\psi_R\Delta_R$ and $\psi_L\psi_L\Delta_L$. But, in the later term as the vev of Δ_L gives rise to neutrino masses, the Yukawa couplings are constrained to be sufficiently small. Whereas, the former interaction term has no such restriction on the Yukawa coupling. Thus, we only consider the contribution from $\Delta_R^+, \Delta_R^{++}$ loops to the anomalous magnetic moment of muon, as shown in Fig.(3.7).

The contribution from the doubly charged triplet higgs (as shown in Fig. 3.7(a)-3.7(b)) is given by [194],

$$[\Delta a_\mu]_{\Delta^{\pm\pm}} = 4 \times \left[\frac{2m_\mu^2}{8\pi^2} \int_0^1 dx \frac{f_{\mu s}^2 (x^3 - x) + f_{\mu p}^2 (x^3 - 2x^2 + x)}{m_\mu^2\,(x^2 - 2x + 1) + m_{\Delta^{\pm\pm}}^2 x} \right. \\ \left. - \frac{m_\mu^2}{8\pi^2} \int_0^1 dx \frac{f_{\mu s}^2 (2x^2 - x^3) - f_{\mu p}^2 x^3}{m_\mu^2\, x^2 + m_{\Delta^{\pm\pm}}^2 (1-x)} \right], \tag{3.9}$$

where $f_{\mu s}$ and $f_{\mu p}$ are the scalar and pseudoscalar couplings of charged triplet higgs with the muon respectively. The factor of four in eq.(3.9) is a symmetry factor coming from the presence of two identical field in the interaction term $(\psi_R\psi_R\Delta_R)$. Similarly, the contribution from singly charged triplet higgs $(\Delta_R^{\pm})$, which is shown in diagram 3.7.(c), given as [194],

$$[\Delta a_\mu]_{\Delta^\pm} = \frac{m_\mu^2}{8\pi^2}\int_0^1 dx \frac{f_{\mu s}^2(x^3 - x^2 + \frac{m_\chi}{m_\mu}(x^2 - x)) + f_{\mu p}^2(x^3 - x^2 - \frac{m_\chi}{m_\mu}(x^2 - x))}{m_\mu^2 x^2 + (m_{\Delta^\pm}^2 - m_\mu^2)x + m_\chi^2(1-x)}, \tag{3.10}$$

The choice of relevant parameters, in order to obtain the observed magnetic moment, has been depicted in Table.(3.3). Here, we would like to mention that the same set of parameters is also required to explain the positron excess observed by AMS-02 experiment [1,2] and relic abundance of dark matter. After adding

m_χ	$m_{\Delta^\pm}$	$m_{\Delta^{\pm\pm}}$	$f_{\mu s} \simeq f_{\mu p} \equiv c_d$
800 GeV	808 GeV	850 GeV	1.36

Table 3.3: Numerical values of the parameters.

the contributions from eq.(3.9) and eq.(3.10), we obtain

$$\Delta a_\mu = 2.9 \times 10^{-9}, \tag{3.11}$$

which is in agreement with the experimental result [3,4] within 1σ.

3.4 Discussion

In dark left-right model, for explaining the AMS-02 positron excess, an astrophysical boost factor of $\sim$ 6400 is required. The large boost factor of this order is quite constrained in cold dark matter models [219]. In [219], authors have studied the positron and γ flux from local dark matter clumps. They find that a local DM clump at 1 kpc distance with DM mass $\sim$ 650 GeV and luminosity $L = 3.4 \times 10^9$ $M_\odot^2$ pc^{-3} can explain the PAMELA positron excess (which is consistent with the AMS-02 positron excess). The calculated γ-flux $\Phi_\gamma = 10^{-6}$ cm^{-2}s^{-1} is an order of magnitude larger than Fermi-LAT observation, which is $\Phi_\gamma = 10^{-7}$ cm^{-2}s^{-1}. The γ-flux observation is highly directional dependent, whereas positron flux is isotropic. So the positrons from the 'point sources' of DM clusters will be observed but γ-rays can be missed if the telescope is not directed at the source. In this way it is possible to reconcile both the signals, but still the probability of such a large astrophysical boost factor is low as estimated from numerical simulation [219].

DLRM contains a number of singly and doubly charged scalars. According to the parameter space considered in this model, the dominant decay channel for $\Delta_R^{\pm\pm}$ is into same sign di-leptons, which is an important signal from the LHC perspective. The decay $\Delta_R^{\pm\pm} \to l^\pm l^\pm$, is constrained by CMS (ATLAS) collaboration, which exclude $m_{\Delta^{\pm\pm}}$ below 445 GeV (409 GeV) and 457 GeV (398 GeV) for $e^\pm e^\pm$ and $\mu^\pm\mu^\pm$ channels respectively [220, 221]. The singly charged scalar ($\Delta_R^\pm$) mass below 600 GeV (assuming, $BR : \Delta^+ \to \tau^+\nu_\tau = 1$) is ruled out at 95% confidence level [222, 223]. We considered $m_{\Delta^{\pm\pm}} \sim 808$ GeV and, $m_{\Delta^{\pm\pm}} \sim 850$ GeV for our calculations, which is above the exclusion limits.

Z' decays into SM fermions; $Z' \to \ell^+\ell^-$ $(\ell = e, \mu)$ have been searched by CMS (ATLAS) collaboration, which put $M_{Z'}$>2.6 TeV (2.9 TeV) [224,225]. In DLRM, $M_{Z'}$ and $M_{W_R^\pm}$ are related as [195],

$$M_{W_R}^2 > \frac{(1-2x)}{2(1-x)}\, M_{Z'}^2 + \frac{x}{2(1-x)^2}\, M_{W_L}^2, \tag{3.12}$$

which gives, M_{W_R}>1.5 TeV (1.7 TeV). Therefore, the contributions of heavy gauge bosons to relic density and muon $(g-2)$ will be small in comparison to charged scalars. By choosing the coupling of Δ^{++} to e^-e^- to be much smaller than the coupling with $\mu^-\mu^-$, we can evade the precession constraints from LEP [226]. We have assumed no flavor mixing through Δ_R, otherwise it will give rise to large contribution to $\mu \to e\gamma$ and $\mu \to eee$ process, which is not observed [176]. In this chapter, we have claimed that we can accommodate both relic abundance and observed magnetic moment of muon in the same benchmark set. In Fig.3.7, we have shown the contours of muon $(g-2)$ and relic abundance in the plane of m_χ and m_{Δ^+} for $c_d = 1.36$. The choice of particular coupling c_d has been obtained from Fig.3.2, where we have imposed constraints from relic abundance. The contours of correct relic abundance, consistent with PLANCK result [29], shows the allowed range of masses of m_χ and m_{Δ^+}. Now we observe that the contours of $g-2$ (within 1σ) falls in the narrow band of parameter space favoured by relic

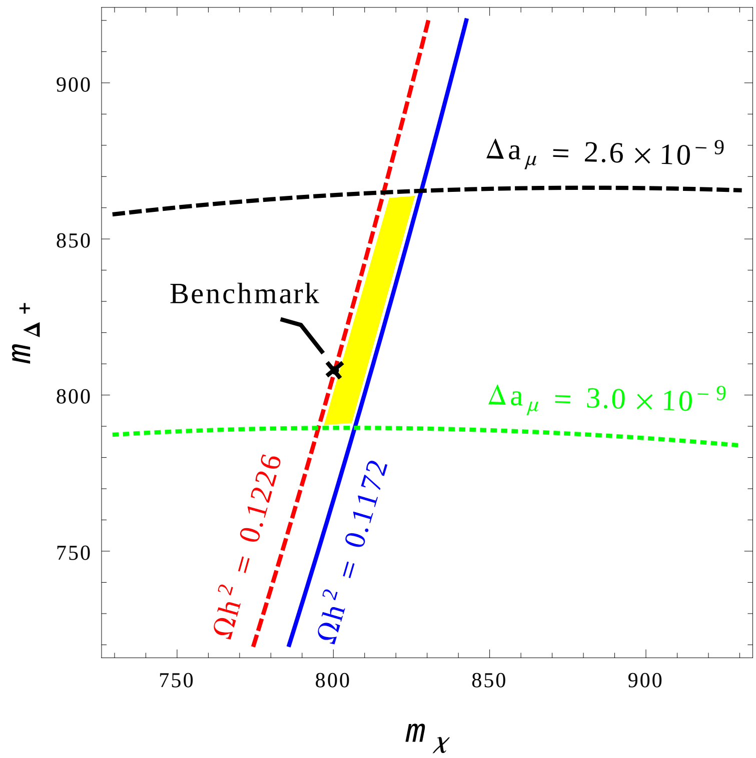

Figure 3.7: Contours of $(g-2)$ and relic abundance in the plane of m_χ and m_{Δ^+} for $c_d = 1.36$.

density of dark matter. Therefore, we find that there exist a common parameter region (the shaded region in the middle as shown in Fig.3.7) of interest consistent with both relic abundance and anomalous magnetic moment. We have chosen a benchmark set, shown as a cross-mark, within the allowed region. However, the cross-section required to fit the AMS-02 positron excess narrows the parameter space as it requires $m_\chi \sim 800$ GeV.

3.5 Conclusion and Outlook

We studied the DLRM model, in which the neutral component of RH-lepton doublet is the dark matter candidate. The Majorana fermionic DM candidate is stable as a consequence of a generalized R-parity. In this model, we explain simultaneously the two experimental signatures *viz.* AMS-02 positron excess and muon $(g-2)$ anomaly. The correct relic abundance of dark matter is obtained through the coannihilation of the DM and the charged triplet higgs. But the annihilation cross-section is helicity suppressed by a factor of m_f^2/m_χ^2. Therefore we use the mechanism of internal bremsstrahlung to lift the helicity suppression. In order to explain AMS-02 positron excess, we have considered the annihilation of the dark matter into $\mu^+\mu^-\gamma$ with an additional astrophysical boost factor ~ 6400. Here we would like to mention that the constraints from distant objects such as dwarf galaxies, and distant epochs such as the cosmic microwave background have been evaded by virtue of having a small underlying cross section and relying on a large local boost factor. The prediction of positron excess of this model is in good agreement with PAMELA and AMS-02 data. We also obtain the required contribution to muon $(g-2)$ through the additional charged triplet higgs loops by using the same set of parameters. We predict a downturn in the AMS-02 positron spectrum and a cut-off around 500 GeV. In addition as a signature of internal bremsstrahlung there is a peak in the gamma rays spectrum at ~ 0.8 TeV which is consistent with both Fermi-LAT gamma ray observations and HESS upper bound.

Chapter 4

IceCube neutrino events and Lorentz invariance violation

General relativity and quantum field theory are two fundamental tenets of physics, which are still unrelated, because general relativity is not perturbatively renormalizable. However, it is speculated that at the Planck scale ($\sim 10^{19}$ GeV) both gravity and other three fundamental forces may be unified. In order to provide a UV complete theory of general relativity, many quantum gravity theories are proposed in literature, which modify space-time structure at the Planck scale [227, 228]. Lorentz symmetry violation is one of the interesting ideas proposed as a result of modified space-time structure. There are many scenarios where Lorentz symmetry violation is explored, like in string theory [229], Hořava-Lifshitz gravity [230], loop quantum gravity and doubly special relativity [231, 232].

The invincible gap between Planck scale and accelerators energies has made it impossible to test Lorentz invariance violation (LIV) directly, but many lower energy effects have been predicted that can be tested with the help of a high precision measurement.

There are various astrophysical observations using X-ray, γ-ray and cosmic-ray data that have been used to study Lorentz violation [232]. The diffuse flux of high energy neutrinos produced in both our galaxy and intergalactic space is another important probe to study Lorentz violation. But low energy neutrinos would be swamped by cosmic-ray neutrinos that have been produced by cosmic-ray interactions in the atmosphere [233]. Until now there were no reported high energy neutrino events; but recently IceCube collaboration has observed neutrino events of very high energies. IceCube has observed neutrinos at PeV energies arising from pion and muon decays at AGNs and Blazers. The numerical relation $m_\pi^2 - m_\mu^2 \sim \text{PeV}^3/M_{pl}$ suggests that there may be an unique opportunity to test the Planck suppressed Lorentz violation operators via observations of PeV neutrinos. Basically 988-days IceCube data reveals 37 events, out of which 28 belongs to cascades and 9 are track events with energy between 60 TeV and 2 PeV [5–7]. Recently a new track event with energy ~ 3 PeV is observed by the collaboration [8].

The IceCube data in the energy range 60 TeV to ~ 3 PeV is consistent with E_ν^{-2} neutrino spectrum following $E_\nu^2 dN_\nu/dE_\nu \simeq 1.2 \times 10^{-8}$ GeVcm^{-2}s^{-1}sr^{-1} [6, 7]. A neutrino spectrum sharper than $E_\nu^{-2.3}$ does not give a good fit to the data [7]. There are no neutrino events observed above ~ 3 PeV.

In particular, there is no evidence of Glashow resonance [167], $\bar{\nu}_e + e^- \to W^- \to$ shower, which is expected at $E_\nu = 6.3$ PeV. Glashow resonance gives rise to an enhanced cross-section for $\bar{\nu}_e$ at resonance energy $E_\nu = M_W^2/2m_e = 6.3$ PeV, which increases the detection rate of $\nu_e + \bar{\nu}_e$ by a factor of ~ 10 [6]. This implies that at least three events should have been observed at Glashow resonance, but none were.

The Glashow resonance gives rise to multiple energy peaks at different energies [168]. The first one is at 6.3 PeV and others lie at the $E_{vis} = E - E_X$, where E_X is the energy in the W decay, which does not contribute to the visible shower [169]. The decay of W into hadrons goes as $W \to \bar{q}q$, giving rise to a peak at 6.3 PeV, while decay into leptons goes as $W \to \bar{\nu}l$, which means W boson will lose half of its energy and so a second peak at 3.2 PeV is expected. In case of τ lepton in the final state, a further decay takes place producing a neutrino and thus a third peak at 1.6 PeV. The events observed by IceCube [5–7] between 1 PeV to ~ 3 PeV range may be associated with the second (leptonic decay of W) and third peak (τ decay), but non-appearance of Glashow resonance hadronic shower from $W \to \bar{q}q$ at 6.3 PeV (dominant peak) makes this idea less attractive. The non-observation of the expected signature of Glashow resonance in the IceCube data indicates a cutoff of neutrino energies between 2-6.3 PeV [169, 234].

In this chapter, we propose a mechanism which can explain why neutrinos above a certain energy may be suppressed in the astrophysical production processes like $\pi \to \mu\nu_\mu$, $K \to \mu\nu_\mu$ etc. We assume that Lorentz violating higher dimensional operators [171, 172] give rise to a modified dispersion relation for the neutrinos (antineutrinos) of the form $E^2 = p^2 + m_\nu^2 - (\xi_n/M_{pl}^{n-2})\ p^n$ with $n > 2$. Depending on the sign of ξ_n, the neutrinos (antineutrinos) can be either superluminal ($\xi_n < 0$) or subluminal ($\xi_n > 0$). For the superluminal case, it has been shown [170, 235] that the presence of the extra terms in the dispersion results in a suppression of π and K decay widths. The phase space suppression for both the subluminal and superluminal dispersions for meson decay and the Cerenkov process $\nu \to \nu e^+ e^-$ has been noticed in [171, 236–239] with limits on Lorentz violation parameters from IceCube events. A comprehensive listing of Lorentz and CPT violating operators and their experimental constraints is given in [240]. In this chapter, we calculate the π, K, μ and n decay processes in a fixed frame (the frame chosen being the one in which the CMBR is isotropic; although the Earth moves at a speed $v_{Earth} \sim 300$ km/sec with respect to the CMBR, the Lorentz correction to the neutrino energy is small as $\beta_{Earth} \sim 10^{-3}$), where the neutrinos (antineutrinos) dispersion relation is $E^2 = p^2 + m_\nu^2 - (\xi_3/M_{pl})\ p^3$ [172, 241–243]. We will have $\xi_3 > 0$ for neutrinos and $\xi_3 < 0$ for antineutrinos. In the π^+ decay, we find that the spin averaged amplitude square $\overline{|M|^2}$, is suppressed at neutrino energy E_ν, where $m_\pi^2 - m_\mu^2 \simeq (\xi_3/M_{pl})\ p_\nu^3$. This implies that for the leading order Planck suppression ($n = 3$) taking $\xi_3 \sim 0.05$, the π^+ decay is suppressed at $E_\nu \sim 1.3$ PeV. Similarly K^+ decay will be cutoff at $E_\nu \sim 2$ PeV with $m_K^2 - m_\mu^2 \sim (\xi_3/M_{pl})p^3$ and neutron decay will be cutoff for p, where $(m_n - m_p)^2 \sim (\xi_3/M_{pl})p^3$, which is lower than the Glashow resonance energy. For the π^- decay the $\overline{|M|^2}$ is enhanced but the phase space is suppressed and therefor $\pi^- \to \mu^-\nu_\mu$ is also suppressed. In the case of $\mu^- \to e^-\bar{\nu}_e\nu_\mu$ decay, $\overline{|M|^2}$ is enhanced whereas the phase space suppression is not significant, so the μ^- decay rate is enhanced (while $\mu^+ \to e^+\nu_e\bar{\nu}_\mu$

decay rate is suppressed). This enhancement is significant at μ^- energies ~ 2 PeV but since the primary source of μ^- is π^- decay which is already cutoff, there will be no observable effect of this enhancement in the neutrino spectrum seen at IceCube. Neutrinos from $K^- \to \mu^- \bar{\nu}_\mu$ and $K^+ \to \mu^+ \nu_\mu$ decays will be cutoff at slightly higher energies. Radiative $\pi^\pm$ decay with a single neutrino in the outgoing state are also suppressed. The three body kaon decay rate is determined by the ξ_3 dependence of $\overline{|M|^2}$ and we find that $K^+ \to \pi^0 \mu^+ \nu_\mu$ decay is suppressed but $K^- \to \pi^0 \mu^- \bar{\nu}_\mu$ decay is enhanced. Neutron beta-decay $n \to p^+ e^- \bar{\nu}_e$ gets suppressed in the same way as μ^+ decay. If the source of $\bar{\nu}_e$ is neutron beta-decay [244] then the mechanism proposed in this paper can be used for explaining the absence of Glashow resonance [167] at IceCube.

The rest of the chapter is organized as follows. In the upcoming section 4.1, we discuss about the neutrino velocity with modified dispersion relation. In section 4.2, we calculate the leptonic decay widths of pions and kaons using modified dispersion relation of neutrino and compare them with their standard model counterparts. In section 4.3, we study $\mu^- \to e^- \bar{\nu}_e \nu_\mu$, $K^+ \to \pi^0 e^+ \nu_e$ and $n \to p^+ e^- \bar{\nu}_e$ processes with modified neutrino dispersion. We then give conclusion and outlook in section 4.4.

4.1 Neutrino velocity with modified dispersion

To calculate the decay widths of pion, kaon and muon, we use the following dispersion relation,

$$E^2 = p^2 + m_\nu^2 - \frac{\xi_n}{M_{pl}^{n-2}}\, p^n, \tag{4.1}$$

which is motivated by Lorentz violating higher dimensional operators [171, 172]. We will take $\xi_n > 0$ for neutrinos and $\xi_n < 0$ for antineutrinos. We use this modified dispersion relation to get the neutrino (antineutrino) velocity, which becomes

$$v = \frac{\partial E}{\partial p} = 1 - \frac{n-1}{2}\,\frac{\xi_n}{M_{pl}^{n-2}}\, p^{n-2}. \tag{4.2}$$

This is clear from eq.(4.2) that we have a subluminal neutrinos and superluminal antineutrinos. In this work, we considered the leading order Planck suppressed

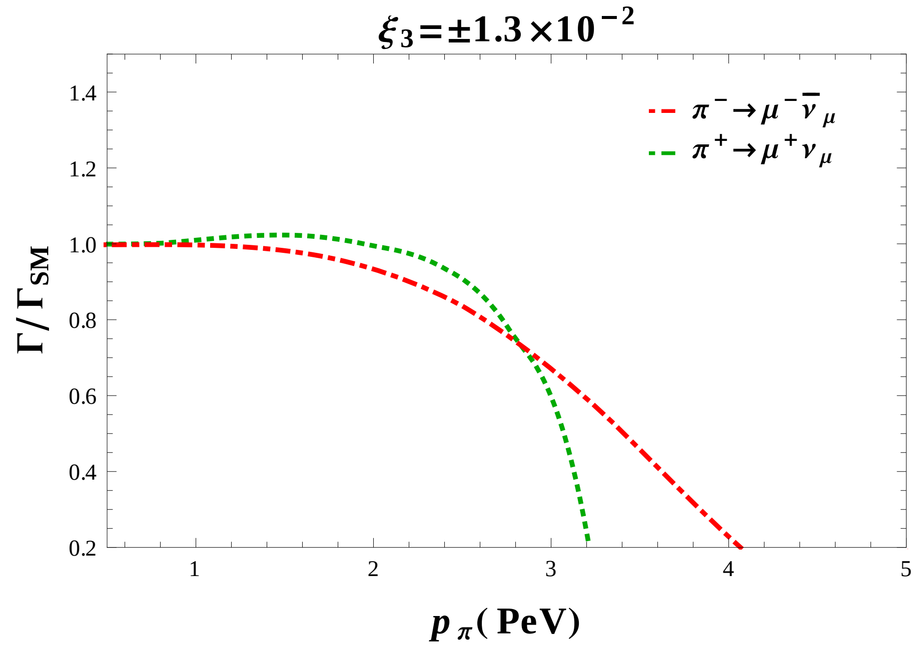

Figure 4.1: The ratio Γ/Γ_{SM} for $\pi^+ \to \mu^+\nu_\mu$ and $\pi^- \to \mu^-\bar{\nu}_\mu$ processes in Lorentz invariance violating framework to its SM prediction for superluminal $\bar{\nu}_\mu$ ($\xi_3 < 0$) and subluminal ν_μ ($\xi_3 > 0$) final states as a function of pion momentum p_π. We considered $\xi_3 = +1.3 \times 10^{-2}$ for neutrino and $\xi_3 = -1.3 \times 10^{-2}$ for antineutrino.

dispersion relation $E^2 = p^2 + m_\nu^2 - (\xi_3/M_{pl})\, p^3$ to compute the primary decay processes, which produce neutrinos and antineutrinos. In appendix.(A), we obtained modified dispersion relations for neutrinos and antineutrinos using dimension-5 operator.

4.2 Two body decays

4.2.1 Pion Decay

We calculate the pion decay width using the modified dispersion relation for neutrino by taking $n = 3$ case. The amplitude calculation of pion decay process $\pi^+(q) \to \mu^+(p)\nu_\mu(k)$ gives

$$M = f_\pi V_{ud}\, q^\mu \bar{u}(k)\frac{G_F}{\sqrt{2}}\gamma_\mu(1-\gamma_5)v(p), \tag{4.3}$$

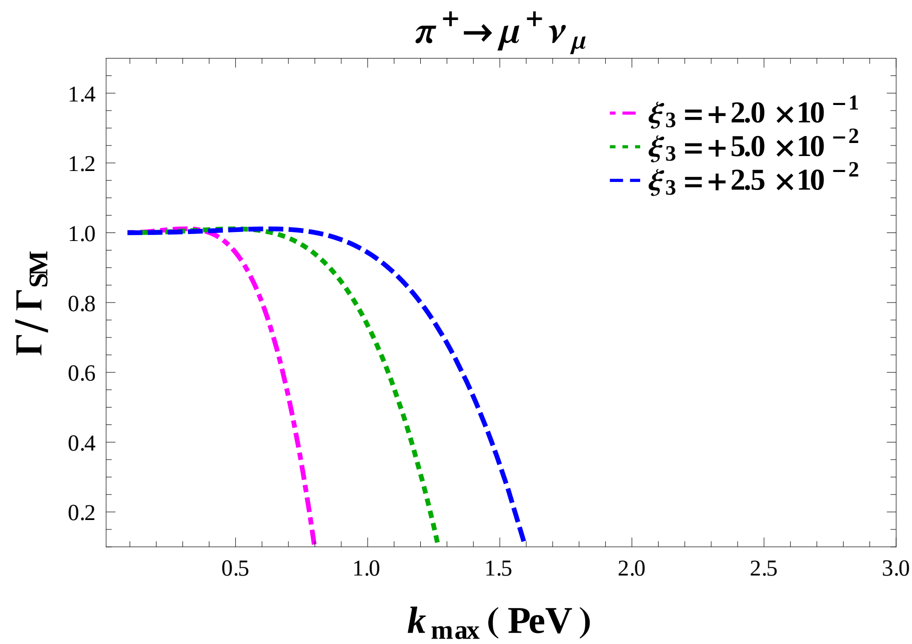

Figure 4.2: The ratio Γ/Γ_{SM} of $\pi^+ \to \mu^+\nu_\mu$ process in Lorentz invariance violating framework to its SM prediction for subluminal neutrino ($\xi_3 > 0$) as a function of neutrino energy k_{max} with different values of ξ_3.

where $f_\pi \equiv f(m_\pi^2)$ is a constant factor, V_{ud} is the CKM matrix element and G_F is the Fermi constant. The spin averaged amplitude squared is,

$$\overline{|M|^2} = 2G_F^2 f_\pi^2 |V_{ud}|^2 m_\mu^2 F(k) \left[m_\pi^2 - m_\mu^2 - \xi_3' k^3 \left(\frac{m_\pi^2}{m_\mu^2} + 2 \right) \right], \tag{4.4}$$

where $\xi_3' \equiv \xi_3/M_{pl}$ and the $F(k)$ factor comes from the modified spinor relation of neutrino, as described in eq.(B.9). The decay width of pion is then given by

$$\Gamma = \frac{G_F^2 f_\pi^2 |V_{ud}|^2 m_\mu^2 F(k)}{8\pi E_\pi} \int \frac{k^2\, dk\, d\cos\theta}{E_\nu \sqrt{|\vec{q}-\vec{k}|^2 + m_\mu^2}} \delta(E_{\nu_\mu} - E_\pi + \sqrt{|\vec{q}-\vec{k}|^2 + m_\mu^2})$$
$$\times \left[m_\pi^2 - m_\mu^2 - \xi_3' k^3 \left(\frac{m_\pi^2}{m_\mu^2} + 2 \right) \right], \tag{4.5}$$

after using $E_{\nu_\mu} = F(k)k$, and writing $|\vec{p}| = |\vec{q}-\vec{k}|^2 = k^2 + q^2 - 2kq\cos\theta$, our expression of eq.(4.5) takes the following form

$$\Gamma = \frac{G_F^2 f_\pi^2 |V_{ud}|^2 m_\mu^2}{8\pi E_\pi} \int \frac{k\, dk\, d\cos\theta}{\sqrt{|\vec{q}-\vec{k}|^2 + m_\mu^2}} \delta(E_{\nu_\mu} - E_\pi + \sqrt{|\vec{q}-\vec{k}|^2 + m_\mu^2})$$
$$\times \left[m_\pi^2 - m_\mu^2 - \xi_3' k^3 \left(\frac{m_\pi^2}{m_\mu^2} + 2 \right) \right], \tag{4.6}$$

from the argument of the delta function in eq.(4.6), we have

$$\sqrt{|\vec{q}-\vec{k}|^2+m_\mu^2} = E_\pi - E_{\nu_\mu}, \tag{4.7}$$

which gives,

$$\cos\theta = \frac{\left(m_\mu^2 - m_\pi^2 + 2E_\pi k - E_\pi k^2 \xi_3' + k^3 \xi_3'\right)}{2kq}. \tag{4.8}$$

We reduce the δ-function in E_{ν_μ} to a δ-function in $\cos\theta$ by taking,

$$\left|\frac{d}{d\cos\theta}(E_{\nu_\mu} - E_\pi + \sqrt{|\vec{q}-\vec{k}|^2+m_\mu^2})\right| = \frac{kq}{\sqrt{k^2+q^2-2kq\cos\theta+m_\mu^2}}, \tag{4.9}$$

and substituting in eq.(4.6). We get the pion decay width,

$$\Gamma = \frac{G_F^2 f_\pi^2 |V_{ud}|^2 m_\mu^2}{8\pi E_\pi}\int \frac{dk}{q}\left[m_\pi^2 - m_\mu^2 - \xi_3' k^3\left(\frac{m_\pi^2}{m_\mu^2}+2\right)\right]. \tag{4.10}$$

We solve the integration in the limits of k, which are fixed by taking $\cos\theta = \pm 1$ in eq.(4.8),

$$k_{max} = \frac{m_\pi^2 - m_\mu^2 + \xi_3' k_{max}^2 (E_\pi - k_{max})}{2(E_\pi - q)}, \tag{4.11}$$

$$k_{min} = \frac{m_\pi^2 - m_\mu^2 + \xi_3' k_{min}^2 (E_\pi - k_{min})}{2(E_\pi + q)}, \tag{4.12}$$

solving these equations numerically, we get the allowed limits of neutrino momentum. We solve eq.(4.10) and then compare our result with the SM result of pion decay in a moving frame, which is

$$\Gamma_{SM}(\pi \to \mu\nu) = \frac{G_F^2 f_\pi^2 |V_{ud}|^2 m_\mu^2 m_\pi^2}{8\pi E_\pi}\left(1 - \frac{m_\mu^2}{m_\pi^2}\right)^2. \tag{4.13}$$

We compute the pion decay rate numerically for superluminal $\bar{\nu}_e$ ($\xi_3 < 0$) and subluminal ν_e ($\xi_3 > 0$) final states and obtain the following :

- For subluminal neutrino final state ($\xi_3 > 0$), the allowed phase space (eq.4.11-eq.4.12) goes up but the $\overline{|M|^2}$ (eq.4.4) is suppressed. There is a net suppression in $\Gamma(\pi^+ \to \mu^+\nu_\mu)$ as shown in Fig.(4.1) for $\xi_3 = 1.3 \times 10^{-2}$.

- For superluminal antineutrino final state ($\xi_3 < 0$), the phase space (eq.4.11-eq.4.12) is suppressed but the $\overline{|M|^2}$ is enhanced. The net effect however is a suppression in the $\Gamma(\pi^- \to \mu^-\bar{\nu}_\mu)$ for this case also [235], as shown in Fig.(4.1) for $\xi_3 = -1.3 \times 10^{-2}$.

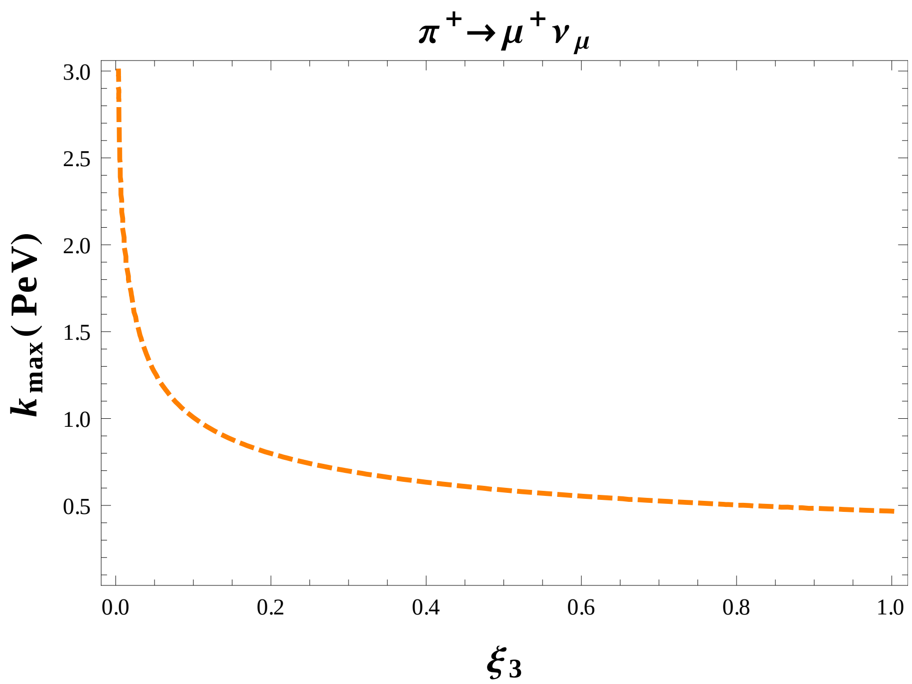

Figure 4.3: The maximum neutrino energy, k_{max} as a function of Lorentz invariance violation parameter ξ_3.

In Fig.(4.2), for the process $\pi^+ \to \mu^+\nu_\mu$, we show the maximum neutrino energy for different values of ξ_3 using the solution for q in terms of k_{max} and k_{min} from eq.(4.11-4.12) in eq.(4.10). We see that for $\xi_3 = 5.0 \times 10^{-2}$, the neutrino spectrum cutoff is at $k_{max} = 1.3$ PeV. The upper limit of observed neutrino energy provides bound on the Lorentz invariance violation parameter ξ_3. In Fig.(4.3), we show the maximum neutrino energy k_{max}, as a function of Lorentz invariance violation parameter ξ_3. This is clear from Fig.(4.3) that k_{max} goes down as ξ_3 increases.

4.2.2 Kaon Decay

In the similar way like pion decay, we calculate the kaon decay width for the process $K^+(q) \to \mu^+(p)\nu_\mu(k)$, using the modified dispersion relation for neutrinos by taking $n = 3$ case. We get the kaon decay width,

$$\Gamma = \frac{G_F^2 f_K^2 |V_{us}|^2 m_\mu^2}{8\pi E_K} \int \frac{dk}{q} \left[m_K^2 - m_\mu^2 - \xi_3' k^3 \left(\frac{m_K^2}{m_\mu^2} + 2 \right) \right] . \tag{4.14}$$

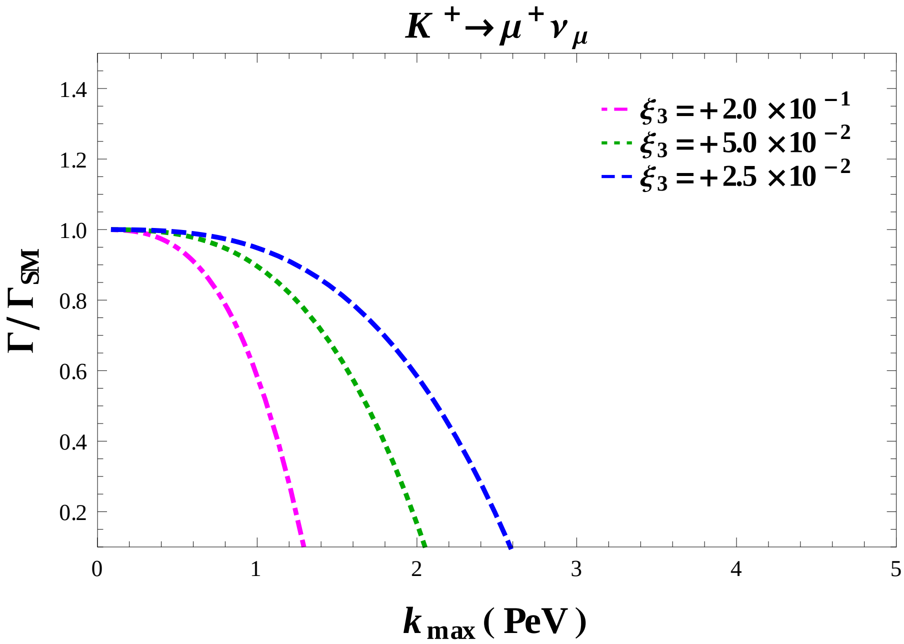

Figure 4.4: The ratio Γ/Γ_{SM} of $K^+ \to \mu^+\nu_\mu$ process in Lorentz invariance violating framework to its SM prediction for subluminal neutrino ($\xi_3 > 0$) as a function of neutrino energy k_{max} with different values of ξ_3.

Similar to the case of pion, we solve the integration in the limits of k by taking $\cos\theta = \pm 1$ which gives,

$$k_{max} = \frac{m_K^2 - m_\mu^2 + \xi_3' k_{max}^2 (E_K - k_{max})}{2(E_K - q)}, \tag{4.15}$$

$$k_{min} = \frac{m_K^2 - m_\mu^2 + \xi_3' k_{min}^2 (E_K - k_{min})}{2(E_K + q)}, \tag{4.16}$$

solving these equations numerically, we get the allowed limits of neutrino momentum. We solve eq.(4.14) and then compare our result with the standard model result of kaon decay in a moving frame, which is

$$\Gamma_{SM}(K \to \mu\nu) = \frac{G_F^2 f_K^2 |V_{us}|^2 m_\mu^2 m_K^2}{8\pi E_K} \left(1 - \frac{m_\mu^2}{m_K^2}\right)^2. \tag{4.17}$$

In Fig.(4.4), we show the maximum neutrino energy for different values of ξ_3 using the solution for q in terms of k_{max} and k_{min} from eq.(4.15-4.16) in eq.(4.14). We see that for $\xi_3 = 5.0 \times 10^{-2}$ the neutrino spectrum cutoff is at $k_{max} = 2$ PeV.

4.3 Three body decays

4.3.1 Muon Decay

We compute the muon decay width with subluminal neutrino and superluminal antineutrino in the final state, assuming the dispersion relation for the neutrino (antineutrino), $E_\nu^2 = k^2 - \xi_3' k^3$, where $\xi_3 > 0$ and $\xi_3 < 0$ correspond to subluminal neutrino and superluminal antineutrino respectively. We assume identical ξ_3 for all the species of ν (and $\bar{\nu}$) to avoid an extra source for neutrino oscillations which is not observed [239, 245]. The amplitude for the process $\mu^-(p) \to e^-(k')\bar{\nu}_e(k)\nu_\mu(p')$ is given as,

$$M = \frac{G_F}{\sqrt{2}}[\bar{u}(k')\gamma^\mu(1-\gamma_5)v(k)][\bar{u}(p')\gamma_\mu(1-\gamma_5)u(p)]. \tag{4.18}$$

After squaring amplitude and solve it using trace technology, we get the spin averaged amplitude,

$$\overline{|M|^2} = 64 G_F^2 (p\cdot k)(p'\cdot k'). \tag{4.19}$$

The differential decay width of muon is,

$$d\Gamma = \frac{d^3p'}{(2\pi)^3 2E_{\nu_\mu}}\frac{d^3k'}{(2\pi)^3 2E_e}\frac{d^3k}{(2\pi)^3 2E_{\bar{\nu}_e}}\frac{\overline{|M|^2}}{2E_\mu}(2\pi)^4\delta^4(p-p'-k'-k), \tag{4.20}$$

using the squared amplitude from eq.(4.19), we get

$$d\Gamma = \frac{32\ G_F^2}{8(2\pi)^5 E_\mu}\frac{d^3k'}{E_e}\frac{d^3p'}{E_{\nu_\mu}}\frac{d^3k}{E_{\bar{\nu}_e}}\delta^4(p-p'-k'-k)(p\cdot k)(p'\cdot k'), \tag{4.21}$$

First we write the decay width in eq.(4.21) as,

$$\Gamma = \frac{32\ G_F^2}{8(2\pi)^5 E_\mu}\int \frac{d^3k'}{E_e} p^\alpha k'^\beta I_{\alpha\beta}(p-k'), \tag{4.22}$$

where

$$I_{\alpha\beta}(p-k') \equiv \int \frac{d^3k}{E_{\bar{\nu}_e}}\frac{d^3p'}{E_{\nu_\mu}}\delta^4(p-p'-k'-k)k_\alpha p'_\beta, \tag{4.23}$$

and then to find out $I_{\alpha\beta}(p-k')$, we use the generic phase space integral formula,

$$\begin{aligned} I_{\alpha\beta} &\equiv \int \frac{d^3p}{\sqrt{m_2^2+\vec{p}\cdot\vec{p}}}\frac{d^3q}{\sqrt{m_1^2+\vec{q}\cdot\vec{q}}}\delta^4(k-p-q)p_\alpha q_\beta \\ &= \frac{I}{12k^4}(k^2[k^2-(m_1-m_2)^2][k^2-(m_1+m_2)^2]g_{\alpha\beta} \\ &+ 2[k^4+k^2(m_1^2+m_2^2)-2(m_1^2-m_2^2)^2]k_\alpha k_\beta), \end{aligned} \tag{4.24}$$

where

$$I = \frac{2\pi}{k^2}\sqrt{[k^2-(m_1-m_2)^2][k^2-(m_1+m_2)^2]}. \tag{4.25}$$

Applying this to our scenario by putting $m_1^2 = m_{\bar{\nu}_e}^2 = \xi_3' k^3$, $m_2^2 = m_{\nu_\mu}^2 = -\xi_3' p'^3$ and taking $k = p'/2 \sim p/4$, we find,

$$\begin{aligned} I_{\alpha\beta}(p-k') = \frac{\pi}{6}\left[1+\frac{7}{64}\frac{\xi_3' p^3}{(p-k')^2}\right]([(p-k')^2 + \frac{7}{32}\xi_3' p^3] g_{\alpha\beta} \\ + 2\left[1-\frac{7}{64}\frac{\xi_3' p^3}{(p-k')^2}\right](p-k')_\alpha (p-k')_\beta), \end{aligned} \tag{4.26}$$

after contracting $I_{\alpha\beta}$ with the muon and electron momentums which respectively are p and k', we get,

$$\begin{aligned} p^\alpha k'^\beta I_{\alpha\beta}(p-k') = \frac{\pi}{6}\left[1+\frac{7}{64}\frac{\xi_3' p^3}{(p-k')^2}\right]([(p-k')^2 \\ + \frac{7}{32}\xi_3' p^3](p\cdot k') \\ + 2\left[1-\frac{7}{64}\frac{\xi_3' p^3}{(p-k')^2}\right](p\cdot p - p\cdot k')(p\cdot k' - k'\cdot k')) \end{aligned} \tag{4.27}$$

where,

$$\begin{aligned} p\cdot p &= m_\mu^2, \\ k'\cdot k' &= m_e^2 \approx 0, \\ p\cdot k' &= \vec{k}'(E_\mu - \vec{p}\cos\theta), \\ (p-k')^2 &= m_\mu^2 - 2\vec{k}'(E_\mu - \vec{p}\cos\theta). \end{aligned} \tag{4.28}$$

The decay width from eq.(4.22) can be written as,

$$\Gamma = \frac{32G_F^2}{8(2\pi)^5}\frac{(2\pi)}{E_\mu}\int_{-1}^{1} d\cos\theta \int_0^{m_\mu^2/2(E_\mu - k\cos\theta)} k' dk' p^\alpha k'^\beta I_{\alpha\beta}, \tag{4.29}$$

after solving it, we finally get,

$$\Gamma = \frac{G_F^2 m_\mu^4}{192\pi^3 E_\mu}\left(m_\mu^2 + \frac{17}{80}\xi_3' p^3\right). \tag{4.30}$$

We compare our result with the standard model prediction of muon decay in a moving frame, which is

$$\Gamma_{SM}(\mu \to e\bar{\nu}_e\nu_\mu) = \frac{G_F^2 m_\mu^5}{192\pi^3}\frac{m_\mu}{E_\mu}. \tag{4.31}$$

We compute the muon decay rate for subluminal neutrino ($\xi_3 > 0$) and superluminal antineutrino ($\xi_3 < 0$) and obtain the following:

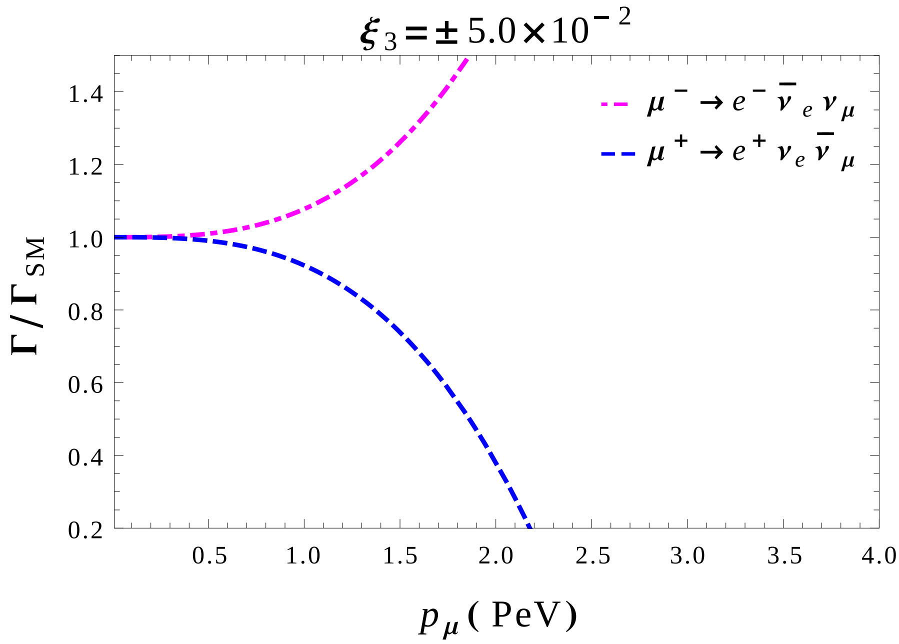

Figure 4.5: The ratio Γ/Γ_{SM} of $\mu^+ \to e^+\nu_e\bar{\nu}_\mu$ and $\mu^- \to e^-\bar{\nu}_e\nu_\mu$ processes in Lorentz invariance violating framework to its SM prediction for superluminal antineutrino ($\xi_3 < 0$) and subluminal neutrino ($\xi_3 > 0$) final states as a function of muon momentum p_μ. We considered $\xi_3 = +5.0 \times 10^{-2}$ for neutrino and $\xi_3 = -5.0 \times 10^{-2}$ for antineutrino.

- The decay rate of the process $\Gamma(\mu^- \to e^-\bar{\nu}_e\nu_\mu)$ is enhanced, as shown in Fig.(4.5) for $\xi_3 = +5.0 \times 10^{-2}$ for neutrino, and $\xi_3 = -5.0 \times 10^{-2}$ for antineutrino.

- The decay rate of the process $\Gamma(\mu^+ \to e^+\nu_e\bar{\nu}_\mu)$ is reduced, as shown in Fig.(4.5) for $\xi_3 = +5.0 \times 10^{-2}$ for neutrino, and $\xi_3 = -5.0 \times 10^{-2}$ for antineutrino.

4.3.2 Kaon Decay

We also calculate 3-body kaon decay width using the modified dispersion relation for neutrino by taking $n = 3$ case. The amplitude calculation of kaon decay process $K^+(p_K) \to \pi^0(p_\pi)e^+(p_e)\nu_e(p_\nu)$ gives,

$$\overline{|M|^2} = 16G_F^2|V_{us}|^2 f_+^2[m_K^2(p_K \cdot p_\nu + p_\pi \cdot p_\nu) - 2(p_K \cdot p_\nu)(p_K \cdot p_\pi) - 2(p_K \cdot p_\nu)(p_K \cdot p_\nu) - m_K^2\xi_3' p_\nu^3], \tag{4.32}$$

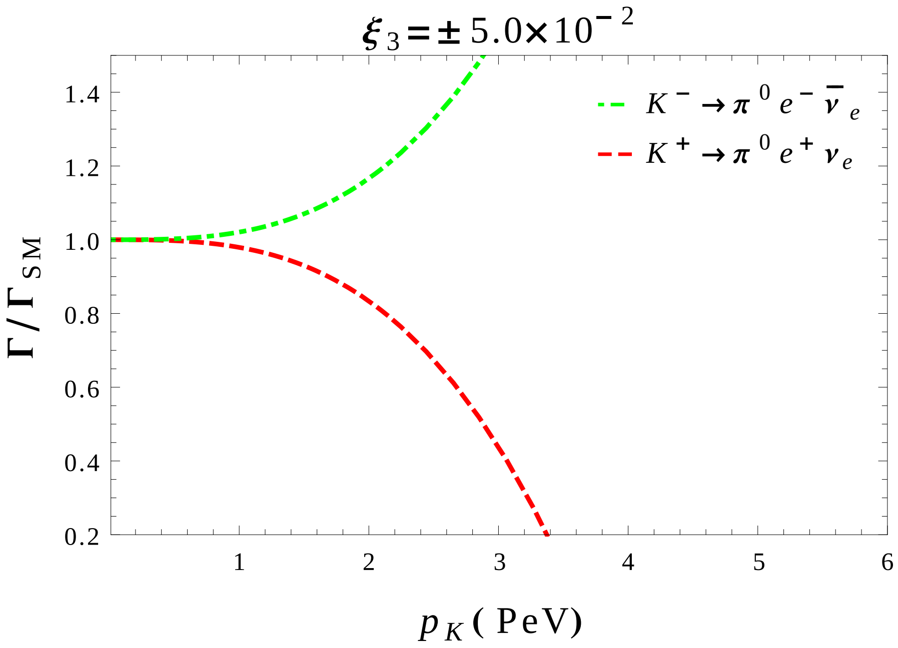

Figure 4.6: The ratio Γ/Γ_{SM} for $K^+ \to \pi^0 e^+ \nu_e$ and $K^- \to \pi^0 e^- \bar{\nu}_e$ processes in Lorentz invariance violating framework to its SM prediction for superluminal $\bar{\nu}_e$ ($\xi_3 < 0$) and subluminal ν_e ($\xi_3 > 0$) final states as a function of kaon momentum p_K. We considered $\xi_3 = +5.0 \times 10^{-2}$ for neutrino and $\xi_3 = -5.0 \times 10^{-2}$ for antineutrino.

where f_+ is the kaon form factor. The differential decay width of kaon is,

$$d\Gamma = \frac{d^3p_\pi}{(2\pi)^3 2E_\pi} \frac{d^3p_{\nu_e}}{(2\pi)^3 2E_{\nu_e}} \frac{d^3p_e}{(2\pi)^3 2E_e} \frac{\overline{|M|^2}}{2E_K} (2\pi)^4 \delta^4(p_K - p_\pi - p_{\nu_e} - p_e), \tag{4.33}$$

which gives,

$$\Gamma \simeq \frac{G_F^2 |V_{us}|^2 f_+^2 m_K^4}{768\pi^3 E_K} \left[m_K^2 \left(1 - \frac{8m_\pi^2}{m_K^2}\right) - \frac{4}{9} p_K^3 \xi_3' \left(1 - \frac{m_\pi^4}{m_K^4}\right)\right]. \tag{4.34}$$

It is clear from eq.(4.34) that the $K^+(K^-)$ decay rate goes down (up) as kaon momentum p_K increases, which is shown in Fig.(4.6) for $\xi_3 = +5.0 \times 10^{-2}$ for neutrino and $\xi_3 = -5.0 \times 10^{-2}$ for antineutrino..

4.3.3 Neutron Decay

In the similar way like muon decay, we also calculate the neutron beta decay width using the modified dispersion relation for antineutrino. The spin averaged amplitude squared for the neutron decay process $n(p) \to p^+(k) e^-(k') \bar{\nu}_e(p')$ comes,

$$\overline{|M|^2} = 64 G_F^2 (p \cdot p')(k \cdot k') \tag{4.35}$$

using eq.(4.35), we get the following differential decay width of neutron,

$$d\Gamma = \frac{32\ G_F^2}{8(2\pi)^5 E_n} \frac{d^3k}{E_p} \frac{d^3k'}{E_e} \frac{d^3p'}{E_{\bar{\nu}_e}} \delta^4(p - k - k' - p')(p \cdot p')(k \cdot k') \tag{4.36}$$

we solve eq.(4.36) in the similar way like muon decay using generic phase space integral formula (eq.4.24). Then we solve the final integral over the electron energy, for which the minimum energy is the rest energy m_e of the electron while the maximum energy is approximately,

$$E_{max} \approx m_n - m_p \tag{4.37}$$

which finally gives,

$$\Gamma \sim \frac{G_F^2 (m_n - m_p)^3 m_n}{15\pi^3 E_n} \left[(m_n - m_p)^2 - \frac{5}{16} \xi_3' p^3 \right]. \tag{4.38}$$

For $\xi_3 = 0.05$ the neutron decay width goes down at neutrino momentum $p \simeq 0.1$ PeV. This implies that antineutrino production from neutron decay will be suppressed, and so in our model it is also possible to explain the absence of Glashow resonance [167]. The decay rate of the charge conjugate process $\bar{n} \rightarrow \bar{p} e^+ \nu_e$ is enhanced, but since only neutrons are produced in the $p + \gamma \rightarrow \Delta \rightarrow n + \pi^+$ processes at the source, the enhanced decay of $\bar{n}$ is not relevant to the IceCube events.

4.4 Conclusion and Outlook

In this chapter, we have provided a mechanism by which one can account for the lack of antineutrino events at Glashow resonance (6.3 PeV) at IceCube. We have shown that if the neutrino (antineutrino) dispersion is modified by leading order Planck scale suppression $E^2 = p^2 - (\xi_3 / M_{Pl}) p^3$ (where $\xi_3 > 0$ correspond to neutrinos and $\xi_3 < 0$ correspond to antineutrino), then there is a suppression of the π^+ decay width and corresponding neutrinos will be cutoff at energies $E_\nu = 1.3$ PeV (with $\xi_3 = 0.05$). The neutrinos from kaon decay $K^+ \rightarrow \mu^+ \nu_\mu$ will be cutoff at 2 PeV.

- Three body decays like $\mu^- \rightarrow e^- \bar{\nu}_e \nu_\mu$ and $K^- \rightarrow \pi^0 e^- \bar{\nu}_e$ get enhanced due to different ξ_3 dependence in their $\overline{|M|^2}$, whereas three body decay widths of μ^+ and K^+ get suppressed.

- Neutron decay $n \to p^+ e^- \bar{\nu}_e$ gets suppressed in the similar way as μ^+ decay. So if the source of $\bar{\nu}_e$ is neutron beta-decay then the mechanism proposed in this paper can be used to explain the absence of Glashow resonance at IceCube.

- Radiative three body decays like $\pi^\pm \to e^\pm \nu \gamma$ and $\pi^\pm \to \mu^\pm \nu \gamma$ are factorized to the $\overline{|M|^2}$ for two body decays $\pi^\pm \to e^\pm \nu$ and $\pi^\pm \to \mu^\pm \nu$ times α_{em} [176, 246] and these are also suppressed like two body decay processes.

The enhancement in μ^- decay will be significant at muon energies of 2 PeV and if the primary source of μ^- is π^- decay then there will be no observable consequence of this in IceCube events. However such enhancement of the μ^- decay rate would be observable for μ^- produced not from π^- decay but e.g. via pair production like in $e^+e^- \to \mu^+\mu^-$. The precise numerical values depend on the choice of the parameter ξ_3, but obviously a cutoff between ~ 3 PeV and 6.3 PeV can be easily obtained in this model. We conclude that if neutrinos at Glashow resonance energies are not observed at IceCube then explanations in terms of new physics such as Lorentz violating modified neutrino dispersion relation become attractive. The fact that neutron decay into $p + e + \bar{\nu}_e$ is suppressed has the following implications. The conventional π/K decay neutrinos from astrophysical sources have the cutoff in the range of ~ 3 PeV. However the B-Z (Beresinsky-Zatsepin) neutrinos [247] which arise in GZK (Greisen-Zatsepin-Kuzmin) process ($\gamma + p \to \Delta^+ \to p + \pi^0$; $\gamma + p \to \Delta^+ \to n + \pi^+$) [248, 249] have two components [250], which are from pion (higher energies) and neutron (lower energies) decays; the higher energy neutrinos from π/K will be more suppressed compared to the lower energy n decay to $\bar{\nu}_e$. But both components of GZK process will be suppressed at $E_\nu > 3$ PeV. Future observations at IceCube will provide an important arena for testing theories of Lorentz violation at high energies.

Chapter 5

Future Directions and Discussion

The excess of the positron over cosmic ray background, discrepancy between the SM value and experimental measurement of muon $(g-2)$, and non observation of Glashow resonance in the PeV neutrino events at IceCube are some of the experimental signals, which require theory beyond SM for their explanation. In this thesis, we explored new particle physics models, which not only accommodate a suitable DM candidate addressing the observed positron excess, but also give an adequate contribution to muon $(g-2)$. We also discussed about the lack of Glashow resonance events at IceCube by considering a Lorentz invariance violation model of particle physics.

Recently, international space station based AMS-02 experiment has observed significant positron excess over cosmic ray background, but did not observe any antiproton excess. There may be an astrophysical explanation of this positron excess. For instance, it has been shown that the nearest pulsars can account for the positrons between 100 to 400 GeV seen at the AMS-02 [19–22]. But in the case of pulsars, an anisotropy is anticipated in the signal due to their different positions, which falls nearly an order of magnitude below the current constraints from both the AMS-02 and the Fermi-LAT experiments [23]. The leptophilic dark matter can not only explain the observed positron excess but also remain consistent with the absence of antiproton over cosmic ray background. We constructed a $SU(2)_{HV}$ horizontal symmetry model, where we identified 4th generation right-handed neutrino (cold relics) as DM. Our model not only accounts for the observed positron excess but also gives an adequate contribution to muon $(g-2)$ through $\mathrm{SU(2)_{HV}}$ gauge boson and scalars. We added a 4th generation fermion family to SM, and connected it to the muon family through a horizontal symmetry. As an artefact of $\mathrm{SU(2)_{HV}}$ horizontal symmetry between 4th generation leptons and muon families, DM can only annihilate into leptonic $(\mu^+\mu^-, \nu_\mu^c\nu_\mu)$ final states and so lifts the constraints from antiproton absence over cosmic ray background. In future, we wish to study the supersymmetric version of this model and implement it in the numerical codes like micrOMEGAs [218] and SARAH [251], which would enable us to study other DM and collider related phenomenology.

In left-right model, it is not possible to accommodate a dark matter candidate. Even though right-handed neutrino can be a good candidate, but it is not stable due to gauge interactions. In dark left-right model, a new global symmetry S is proposed which makes right-hand neutrino stable, and so a suitable candidate of DM. We studied DLRM in details and employed it for explaining the AMS-02 positron excess and the discrepancy in muon $(g-2)$ measurement. In this model, we assume the right-handed gauge bosons $(W_R^\pm, Z_R')$ to be heavy enough (~ 2 TeV), so that DM annihilation dominantly takes place through the charged scalar $(\Delta^\pm)$. As a result, DM annihilates into leptons and remains consistent with stringent bounds from observed antiproton flux. We also find that the charged scalars $(\Delta^\pm, \Delta^{\pm\pm})$ give adequate contributions to muon $(g-2)$.

Recently, the CMS collaboration has observed an excess of $eejj$ [252]. Even though the significance of the excess is small (2.8σ), but this can be a signal of physics beyond SM. We are working on a variant of left-right model, in which we can not only accommodate DM but also explain the observed $eejj$ signature. Here it is important to mention that in our $\mathrm{SU(2)_{HV}}$ horizontal symmetry model, it is not possible to accommodate the observed $eejj$ excess. In the variant of left-right model, it is possible to explain the flavor anomalies [253], which is reported from the LHCb [254], BaBar [255] and Belle collaborations [256]. But in $\mathrm{SU(2)_{HV}}$ horizontal symmetry model, there are no additional interactions present between quarks, so the flavor anomalies can not be addressed in this model.

IceCube detector has observed the neutrino events of very high energy, which goes upto PeV. The highest event observed by IceCube is ~ 3 PeV, but IceCube collaboration has not seen Glashow resonance which is expected at $E_\nu = 6.3$ PeV. Glashow resonance gives rise to an enhanced cross-section for $\bar{\nu}_e$ at resonance energy 6.3 PeV, which increase the detection rate of $\bar{\nu}_e$ by a factor of ~ 10. The non-observation of this expected signature indicates a cutoff in the neutrino spectrum, which lies between $2.6-6.3$ PeV. In this thesis, we propose a mechanism, by which it is possible to explain why neutrinos above certain energies may be suppressed in the astrophysical process like $\pi \to \mu\bar{\nu}_\mu, K \to \bar{\nu}_\mu$ etc. We consider the Lorentz violating higher dimensional operator, which gives rise to a modified dispersion relation for neutrinos (antineutrinos) of the form $E^2 = p^2 + m_\nu^2 - (\xi_n/M_{pl}^{n-2})$ with $n > 2$. The presence of extra term in dispersion results in a suppression of π and K decay widths and so a cutoff in the neutrino spectrum is expected. In this way, we can explain the absence of Glashow resonance at IceCube. In future, we are planning to study the Lorentz invariance violation in charged lepton sector, which can transfer from neutrino to charged lepton sector through loop processes.

In future we would like to construct particle physics models, which can address some of the recent observations in the context of DM : (1) Gamma-ray emission from the galactic center and inner galaxy regions as observed in Fermi-LAT data and can be explained by 31-40 GeV DM annihilation into $b\bar{b}$ final state [79, 257–259], (2) X-ray line signal at about 3.5 KeV from the analysis of XMN-Newton observatory data of Andromeda galaxy and Perseus galaxy cluster [260, 261], and (3) The alternative explanation of IceCube PeV neutrino event using dark matter (for example see Ref. [152, 153, 156, 262]) or using new particles produced on shell like leptoquarks [263, 264].

Appendix A

Neutrino modified dispersion relation

The cubic dispersion relation we used for neutrinos and antineutrinos can be obtained from the dimension 5 operator [171, 172],

$$\mathcal{L}_{LV} = \frac{1}{M_{pl}} \bar{\psi}(\eta_1 \not{n} + \eta_2 \not{n} \gamma_5)(n \cdot \partial)^2 \psi, \tag{A.1}$$

where n_μ is a fixed four vector that specifies the preferred frame. Both the vector and axial-vector terms in eq.(A.1) are CPT violating in addition to being Lorentz violating. The Lagrangian gives the equation of motion,

$$i\not{\partial}\psi = -\frac{1}{M_{pl}}(\eta_1 \not{n} + \eta_2 \not{n} \gamma_5)(n \cdot \partial)^2 \psi, \tag{A.2}$$

where we have taken $E \gg m$. This leads to the following dispersion relation for left and right handed particles ψ,

$$E^2 = p^2 + 2(\eta_1 \pm \eta_2)\frac{p^3}{M_{pl}}, \tag{A.3}$$

where $+$ and $-$ signs correspond to ψ_R and ψ_L respectively. Now taking the charge conjugation of eq.(A.1), we find

$$\mathcal{L}_{LV} = \frac{1}{M_{\rm pl}} \bar{\psi}^c(-\eta_1 \not{n} + \eta_2 \not{n} \gamma_5)(n \cdot \partial)^2 \psi^c, \tag{A.4}$$

where we used charge conjugation properties viz. $C^{-1}\gamma_\mu C = -\gamma_\mu$ and $C^{-1}\gamma_\mu\gamma_5 C = \gamma_\mu\gamma_5$. The operator (eq.A.4) gives the following dispersion relation for left and right handed antiparticle ψ^c,

$$E^2 = p^2 + 2(-\eta_1 \pm \eta_2)\frac{p^3}{M_{pl}}, \tag{A.5}$$

where the + sign is for ψ^c_R and − sign is for ψ^c_L. Therefor for the case of left-handed neutrinos ν_L, we will have the dispersion relation,

$$E^2 = p^2 + 2(\eta_1 - \eta_2)\frac{p^3}{M_{pl}}, \tag{A.6}$$

and for antineutrinos ν^c_R we have,

$$E^2 = p^2 - 2(\eta_1 - \eta_2)\frac{p^3}{M_{pl}}\ . \tag{A.7}$$

We have dispersion relation for neutrinos and antineutrinos $E^2 = p^2 - (\xi_3/M_{pl})p^3$, where $\xi_3 = -2(\eta_1 - \eta_2)$ for neutrinos and $\xi_3 = 2(\eta_1 - \eta_2)$ for antineutrinos.

Appendix B

Neutrino modified spinors relation

We assume that all the particles expect neutrinos follow the standard energy-momentum relation i.e,

$$E_i = \sqrt{p_i^2 + m_i^2}, \tag{B.1}$$

where m_i and p_i are the mass and momentum of different particles ($i = e, \mu, \tau\ etc$). The neutrinos follow the modified dispersion relation given in eq.(4.1). There exist very stringent bounds [245], which suggest that neutrino flavor is independent of their dispersion relation, so we assumed the universal dispersion relation for different flavor of neutrinos. We also define,

$$F(p) \equiv \frac{E}{p} = 1 - \frac{\xi_n p^{n-2}}{2M_{pl}^{n-2}}, \tag{B.2}$$

where the function $F(p)$ is the measure of the deviation of neutrino dispersion relation from the standard one [265]. In this framework, the modified Dirac equation for neutrino can be written as,

$$(i\gamma^0\partial_0 - iF(p)\vec{\gamma}\cdot\vec{\partial})\psi(x) = 0, \tag{B.3}$$

where we have neglected the neutrino mass for simplification. Now we replace the Dirac field ψ in terms of the linear combination of plane waves i.e,

$$\psi(x) = u(p)e^{-ip\cdot x}, \tag{B.4}$$

using it, we get the following form of Dirac equation,

$$(\gamma^0 E - F(p)\vec{\gamma} \cdot \vec{p})u(p) = 0. \tag{B.5}$$

Clearly, the positive energy solution of this equation will satisfy,

$$E(p) = F(p)p, \tag{B.6}$$

we used these results in the derivation of the spinors sum of neutrinos, which comes,

$$\sum_{s=1,2} u^s(p)\bar{u}^s(p) = \begin{pmatrix} 0 & \tilde{p} \cdot \sigma \\ \tilde{p} \cdot \bar{\sigma} & 0 \end{pmatrix}, \tag{B.7}$$

where we assumed neutrino to be massless and defined $\tilde{p} = (E, F(p)p)$. Following the Dirac algebra, we get the following result for spinor sum,

$$\sum_{s=1,2} u^s(p)\bar{u}^s(p) = \gamma^\mu \tilde{p}_\mu \equiv F(p)\gamma^\mu p_\mu, \tag{B.8}$$

where we used the result of eq.(B.6) for further simplification. For antiparticle when $m = 0$, there is an overall negative sign in eq.(B.5) and following the same procedure we obtain the same result,

$$\sum_{s=1,2} v^s(p)\bar{v}^s(p) = F(p)\gamma^\mu p_\mu. \tag{B.9}$$

Bibliography

[1] **AMS** Collaboration, M. Aguilar et al., *First Result from the Alpha Magnetic Spectrometer on the International Space Station: Precision Measurement of the Positron Fraction in Primary Cosmic Rays of 0.5-350 GeV*, *Phys.Rev.Lett.* **110** (2013) 141102.

[2] **AMS** Collaboration, L. Accardo et al., *High Statistics Measurement of the Positron Fraction in Primary Cosmic Rays of 0.5-500 GeV with the Alpha Magnetic Spectrometer on the International Space Station*, *Phys.Rev.Lett.* **113** (2014) 121101.

[3] **Muon g-2** Collaboration, G. Bennett et al., *Final Report of the Muon E821 Anomalous Magnetic Moment Measurement at BNL*, *Phys.Rev.* **D73** (2006) 072003, [hep-ex/0602035].

[4] **Muon (g-2)** Collaboration, G. Bennett et al., *An Improved Limit on the Muon Electric Dipole Moment*, *Phys.Rev.* **D80** (2009) 052008, [arXiv:0811.1207].

[5] **IceCube** Collaboration, M. Aartsen et al., *First observation of PeV-energy neutrinos with IceCube*, *Phys.Rev.Lett.* **111** (2013) 021103, [arXiv:1304.5356].

[6] **IceCube** Collaboration, M. Aartsen et al., *Evidence for High-Energy Extraterrestrial Neutrinos at the IceCube Detector*, *Science* **342** (2013) 1242856, [arXiv:1311.5238].

[7] **IceCube** Collaboration, M. Aartsen et al., *Observation of High-Energy Astrophysical Neutrinos in Three Years of IceCube Data*, *Phys.Rev.Lett.* **113** (2014) 101101, [arXiv:1405.5303].

[8] The IceCube collaboration, *http://icrc2015.nl.*

[9] **Planck** Collaboration, P. Ade et al., *Planck 2013 results. XVI. Cosmological parameters*, *Astron.Astrophys.* **571** (2014) A16, [arXiv:1303.5076].

[10] **XENON1T** Collaboration, E. Aprile, *The XENON1T Dark Matter Search Experiment*, *Springer Proc. Phys.* **148** (2013) 93–96, [arXiv:1206.6288].

[11] **XENON100** Collaboration, E. Aprile et al., *Dark Matter Results from 225 Live Days of XENON100 Data*, *Phys.Rev.Lett.* **109** (2012) 181301, [arXiv:1207.5988].

[12] **XENON100** Collaboration, L. S. Lavina, *Latest results from XENON100 data*, in *24th Rencontres de Blois on Particle Physics and Cosmology Blois, Loire Valley, France, May 27-June 1, 2012*, 2013. arXiv:1305.0224.

[13] **LUX** Collaboration, D. Akerib et al., *First results from the LUX dark matter experiment at the Sanford Underground Research Facility*, *Phys.Rev.Lett.* **112** (2014) 091303, [arXiv:1310.8214].

[14] R. Bernabei, P. Belli, F. Cappella, V. Caracciolo, S. Castellano, et al., *Final model independent result of DAMA/LIBRA-phase1*, *Eur.Phys.J.* **C73** (2013), no. 12 2648, [arXiv:1308.5109].

[15] **Fermi-LAT** Collaboration, M. Ackermann et al., *Fermi LAT Search for Dark Matter in Gamma-ray Lines and the Inclusive Photon Spectrum*, *Phys.Rev.* **D86** (2012) 022002, [arXiv:1205.2739].

[16] **HESS** Collaboration, A. Abramowski et al., *Search for Photon-Linelike Signatures from Dark Matter Annihilations with H.E.S.S.*, *Phys.Rev.Lett.* **110** (2013) 041301, [arXiv:1301.1173].

[17] **PAMELA** Collaboration, O. Adriani et al., *An anomalous positron abundance in cosmic rays with energies 1.5-100 GeV*, *Nature* **458** (2009) 607–609, [arXiv:0810.4995].

[18] AMS-02 Collaboration, *talks at the AMS Days at CERN, April 15-17, 2015.*

[19] M. Pato, M. Lattanzi, and G. Bertone, *Discriminating the source of high-energy positrons with AMS-02*, *JCAP* **1012** (2010) 020, [arXiv:1010.5236].

[20] S. H. Lee, T. Kamae, L. Baldini, F. Giordano, M. H. Grondin, L. Latronico, M. Lemoine-Goumard, C. Sgr, T. Tanaka, and Y. Uchiyama, *Explaining the cosmic-ray $e^+/(e^- + e^+)$ and anti-p/p ratios using a steady-state injection model*, *Astropart. Phys.* **35** (2011) 211–222, [arXiv:1010.3477].

[21] P. D. Serpico, *Astrophysical models for the origin of the positron 'excess'*, *Astropart. Phys.* **39-40** (2012) 2–11, [arXiv:1108.4827].

[22] P.-F. Yin, Z.-H. Yu, Q. Yuan, and X.-J. Bi, *Pulsar interpretation for the AMS-02 result*, *Phys. Rev.* **D88** (2013), no. 2 023001, [arXiv:1304.4128].

[23] T. Linden and S. Profumo, *Probing the Pulsar Origin of the Anomalous Positron Fraction with AMS-02 and Atmospheric Cherenkov Telescopes*, *Astrophys. J.* **772** (2013) 18, [arXiv:1304.1791].

[24] P. J. Fox and E. Poppitz, *Leptophilic Dark Matter*, *Phys. Rev.* **D79** (2009) 083528, [arXiv:0811.0399].

[25] N. F. Bell, Y. Cai, R. K. Leane, and A. D. Medina, *Leptophilic dark matter with Z interactions*, *Phys. Rev.* **D90** (2014), no. 3 035027, [arXiv:1407.3001].

[26] P. S. B. Dev, D. K. Ghosh, N. Okada, and I. Saha, *Neutrino Mass and Dark Matter in light of recent AMS-02 results*, *Phys.Rev.* **D89** (2014) 095001, [arXiv:1307.6204].

[27] M. Cirelli, M. Kadastik, M. Raidal, and A. Strumia, *Model-independent implications of the e+-, anti-proton cosmic ray spectra on properties of Dark Matter*, *Nucl.Phys.* **B813** (2009) 1–21, [arXiv:0809.2409].

[28] A. De Simone, A. Riotto, and W. Xue, *Interpretation of AMS-02 Results: Correlations among Dark Matter Signals*, *JCAP* **1305** (2013) 003, [arXiv:1304.1336].

[29] Planck collaboration, *http://www.insu.cnrs.fr/node/5108.*

[30] D. T. Cumberbatch and J. Silk, *Local dark matter clumps and the positron excess*, *Mon. Not. Roy. Astron. Soc.* **374** (2007) 455–465, [astro-ph/0602320].

[31] J. Lavalle, J. Pochon, P. Salati, and R. Taillet, *Clumpiness of dark matter and positron annihilation signal: computing the odds of the galactic lottery*, *Astron. Astrophys.* **462** (2007) 827–848, [astro-ph/0603796].

[32] J. Kopp, *Constraints on dark matter annihilation from AMS-02 results*, *Phys. Rev.* **D88** (2013) 076013, [arXiv:1304.1184].

[33] Y.-H. Chen, K. Cheung, and P.-Y. Tseng, *Dark Matter with Multi-Annihilation Channels and AMS-02 Positron Excess and Antiproton*, arXiv:1505.00134.

[34] V. C. Spanos, *The Price of a Dark Matter Annihilation Interpretation of AMS-02 Data*, arXiv:1312.7841.

[35] A. Ibarra, D. Tran, and C. Weniger, *Indirect Searches for Decaying Dark Matter*, *Int. J. Mod. Phys.* **A28** (2013) 1330040, [arXiv:1307.6434].

[36] K.-Y. Choi, B. Kyae, and C. S. Shin, *Decaying WIMP dark matter for AMS-02 cosmic positron excess*, *Phys. Rev.* **D89** (2014), no. 5 055002, [arXiv:1307.6568].

[37] A. Ibarra, A. S. Lamperstorfer, and J. Silk, *Dark matter annihilations and decays after the AMS-02 positron measurements*, *Phys. Rev.* **D89** (2014), no. 6 063539, [arXiv:1309.2570].

[38] F. Zwicky, *Die Rotverschiebung von extragalaktischen Nebeln*, *Helv. Phys. Acta* **6** (1933) 110–127.

[39] V. C. Rubin, N. Thonnard, and W. K. Ford, Jr., *Rotational properties of 21 SC galaxies with a large range of luminosities and radii, from NGC 4605 /R = 4kpc/ to UGC 2885 /R = 122 kpc/*, *Astrophys. J.* **238** (1980) 471.

[40] T. S. van Albada, J. N. Bahcall, K. Begeman, and R. Sancisi, *The Distribution of Dark Matter in the Spiral Galaxy NGC-3198*, *Astrophys. J.* **295** (1985) 305–313.

[41] D. Clowe, M. Bradac, A. H. Gonzalez, M. Markevitch, S. W. Randall, et al., *A direct empirical proof of the existence of dark matter*, *Astrophys.J.* **648** (2006) L109–L113, [astro-ph/0608407].

[42] **2DFGRS** Collaboration, M. Colless et al., *The 2dF Galaxy Redshift Survey: Spectra and redshifts*, *Mon. Not. Roy. Astron. Soc.* **328** (2001) 1039, [astro-ph/0106498].

[43] **SDSS** Collaboration, M. Tegmark et al., *The 3-D power spectrum of galaxies from the SDSS*, *Astrophys. J.* **606** (2004) 702–740, [astro-ph/0310725].

[44] J. F. Navarro, C. S. Frenk, and S. D. M. White, *The Structure of cold dark matter halos*, *Astrophys. J.* **462** (1996) 563–575, [astro-ph/9508025].

[45] V. Springel et al., *Simulating the joint evolution of quasars, galaxies and their large-scale distribution*, *Nature* **435** (2005) 629–636, [astro-ph/0504097].

[46] J. Diemand, M. Kuhlen, and P. Madau, *Dark matter substructure and gamma-ray annihilation in the Milky Way halo*, *Astrophys. J.* **657** (2007) 262–270, [astro-ph/0611370].

[47] V. Springel, J. Wang, M. Vogelsberger, A. Ludlow, A. Jenkins, A. Helmi, J. F. Navarro, C. S. Frenk, and S. D. M. White, *The Aquarius Project: the subhalos of galactic halos*, *Mon. Not. Roy. Astron. Soc.* **391** (2008) 1685–1711, [arXiv:0809.0898].

[48] **SDSS** Collaboration, W. J. Percival et al., *Baryon Acoustic Oscillations in the Sloan Digital Sky Survey Data Release 7 Galaxy Sample*, *Mon. Not. Roy. Astron. Soc.* **401** (2010) 2148–2168, [arXiv:0907.1660].

[49] **WMAP** Collaboration, G. Hinshaw et al., *Nine-Year Wilkinson Microwave Anisotropy Probe (WMAP) Observations: Cosmological Parameter Results*, *Astrophys.J.Suppl.* **208** (2013) 19, [arXiv:1212.5226].

[50] E. A. Baltz, *Dark matter candidates*, *eConf* **C040802** (2004) L002, [astro-ph/0412170].

[51] G. Bertone, D. Hooper, and J. Silk, *Particle dark matter: Evidence, candidates and constraints*, *Phys. Rept.* **405** (2005) 279–390, [hep-ph/0404175].

[52] M. Taoso, G. Bertone, and A. Masiero, *Dark Matter Candidates: A Ten-Point Test*, *JCAP* **0803** (2008) 022, [arXiv:0711.4996].

[53] L. Bergstrom, *Dark Matter Candidates*, *New J. Phys.* **11** (2009) 105006, [arXiv:0903.4849].

[54] S. Gardner and G. Fuller, *Dark Matter Studies Entrain Nuclear Physics*, *Prog. Part. Nucl. Phys.* **71** (2013) 167–184, [arXiv:1303.4758].

[55] J. R. Ellis, J. S. Hagelin, D. V. Nanopoulos, K. A. Olive, and M. Srednicki, *Supersymmetric Relics from the Big Bang*, *Nucl. Phys.* **B238** (1984) 453–476.

[56] K. Griest, M. Kamionkowski, and M. S. Turner, *Supersymmetric Dark Matter Above the W Mass*, *Phys. Rev.* **D41** (1990) 3565–3582.

[57] G. Jungman, M. Kamionkowski, and K. Griest, *Supersymmetric dark matter*, *Phys. Rept.* **267** (1996) 195–373, [hep-ph/9506380].

[58] N. Arkani-Hamed, A. Delgado, and G. F. Giudice, *The Well-tempered neutralino*, *Nucl. Phys.* **B741** (2006) 108–130, [hep-ph/0601041].

[59] H.-C. Cheng, J. L. Feng, and K. T. Matchev, *Kaluza-Klein dark matter*, *Phys. Rev. Lett.* **89** (2002) 211301, [hep-ph/0207125].

[60] G. Servant and T. M. P. Tait, *Is the lightest Kaluza-Klein particle a viable dark matter candidate?*, *Nucl. Phys.* **B650** (2003) 391–419, [hep-ph/0206071].

[61] L. Lopez Honorez, E. Nezri, J. F. Oliver, and M. H. G. Tytgat, *The Inert Doublet Model: An Archetype for Dark Matter*, *JCAP* **0702** (2007) 028, [hep-ph/0612275].

[62] P. Agrawal, E. M. Dolle, and C. A. Krenke, *Signals of Inert Doublet Dark Matter in Neutrino Telescopes*, *Phys. Rev.* **D79** (2009) 015015, [arXiv:0811.1798].

[63] E. Nezri, M. H. G. Tytgat, and G. Vertongen, *e+ and anti-p from inert doublet model dark matter*, *JCAP* **0904** (2009) 014, [arXiv:0901.2556].

[64] G. Steigman, B. Dasgupta, and J. F. Beacom, *Precise Relic WIMP Abundance and its Impact on Searches for Dark Matter Annihilation*, *Phys. Rev.* **D86** (2012) 023506, [arXiv:1204.3622].

[65] R. Bernabei et al., *Dark matter search*, *Riv. Nuovo Cim.* **26N1** (2003) 1–73, [astro-ph/0307403].

[66] G. B. Gelmini, *TASI 2014 Lectures: The Hunt for Dark Matter*, in *Theoretical Advanced Study Institute in Elementary Particle Physics: Journeys Through the Precision Frontier: Amplitudes for Colliders (TASI 2014) Boulder, Colorado, June 2-27, 2014*, 2015. arXiv:1502.01320.

[67] **CoGeNT** Collaboration, C. E. Aalseth et al., *Results from a Search for Light-Mass Dark Matter with a P-type Point Contact Germanium Detector*, *Phys. Rev. Lett.* **106** (2011) 131301, [arXiv:1002.4703].

[68] C. E. Aalseth et al., *Search for an Annual Modulation in a P-type Point Contact Germanium Dark Matter Detector*, *Phys. Rev. Lett.* **107** (2011) 141301, [arXiv:1106.0650].

[69] **CDMS-II** Collaboration, Z. Ahmed et al., *Results from a Low-Energy Analysis of the CDMS II Germanium Data*, *Phys. Rev. Lett.* **106** (2011) 131302, [arXiv:1011.2482].

[70] **CDMS** Collaboration, R. Agnese et al., *Silicon Detector Dark Matter Results from the Final Exposure of CDMS II*, *Phys. Rev. Lett.* **111** (2013), no. 25 251301, [arXiv:1304.4279].

[71] **SuperCDMS** Collaboration, R. Agnese et al., *Search for Low-Mass Weakly Interacting Massive Particles with SuperCDMS*, *Phys. Rev. Lett.* **112** (2014), no. 24 241302, [arXiv:1402.7137].

[72] **COUPP** Collaboration, E. Behnke et al., *First Dark Matter Search Results from a 4-kg CF_3I Bubble Chamber Operated in a Deep Underground Site*, *Phys.Rev.* **D86** (2012), no. 5 052001, [arXiv:1204.3094].

[73] **ZEPLIN-III** Collaboration, V. N. Lebedenko et al., *Limits on the spin-dependent WIMP-nucleon cross-sections from the first science run of the ZEPLIN-III experiment*, *Phys. Rev. Lett.* **103** (2009) 151302, [arXiv:0901.4348].

[74] J. L. Feng et al., *Planning the Future of U.S. Particle Physics (Snowmass 2013): Chapter 4: Cosmic Frontier*, in *Community Summer Study 2013: Snowmass on the Mississippi (CSS2013) Minneapolis, MN, USA, July 29-August 6, 2013*, 2014. arXiv:1401.6085.

[75] **Fermi-LAT** Collaboration, V. Vitale and A. Morselli, *Indirect Search for Dark Matter from the center of the Milky Way with the Fermi-Large Area Telescope*, in *Fermi gamma-ray space telescope. Proceedings, 2nd Fermi Symposium, Washington, USA, November 2-5, 2009*, 2009. arXiv:0912.3828.

[76] **HESS** Collaboration, F. Acero, *Localising the VHE gamma-ray source at the Galactic Centre*, *Mon. Not. Roy. Astron. Soc.* **402** (2010) 1877–1882, [arXiv:0911.1912].

[77] L. Pieri, A. Pizzella, E. M. Corsini, E. D. Bonta', and F. Bertola, *Could the Fermi-LAT detect gamma-rays from dark matter annihilation in the dwarf galaxies of the Local Group?*, *Astron. Astrophys.* **496** (2009) 351, [arXiv:0812.1494].

[78] G. D. Martinez, J. S. Bullock, M. Kaplinghat, L. E. Strigari, and R. Trotta, *Indirect Dark Matter Detection from Dwarf Satellites: Joint Expectations from Astrophysics and Supersymmetry*, *JCAP* **0906** (2009) 014, [arXiv:0902.4715].

[79] T. Daylan, D. P. Finkbeiner, D. Hooper, T. Linden, S. K. N. Portillo, N. L. Rodd, and T. R. Slatyer, *The Characterization of the Gamma-Ray Signal from the Central Milky Way: A Compelling Case for Annihilating Dark Matter*, arXiv:1402.6703.

[80] **ATLAS** Collaboration, G. Aad et al., *Search for new phenomena in final states with an energetic jet and large missing transverse momentum in pp collisions at $\sqrt{s} = 8$ TeV with the ATLAS detector*, *Eur. Phys. J.* **C75** (2015), no. 7 299, [arXiv:1502.01518].

[81] R. Essig, J. Mardon, M. Papucci, T. Volansky, and Y.-M. Zhong, *Constraining Light Dark Matter with Low-Energy e^+e^- Colliders*, *JHEP* **11** (2013) 167, [arXiv:1309.5084].

[82] P. Agrawal and V. Rentala, *Identifying dark matter interactions in monojet searches*, *JHEP* **05** (2014) 098, [arXiv:1312.5325].

[83] **ATLAS** Collaboration, G. Aad et al., *Search for dark matter in events with a Z boson and missing transverse momentum in pp collisions at* $\sqrt{s}$*=8 TeV with the ATLAS detector*, *Phys. Rev.* **D90** (2014), no. 1 012004, [arXiv:1404.0051].

[84] S. P. Martin, *A Supersymmetry primer*, hep-ph/9709356. [Adv. Ser. Direct. High Energy Phys.18,1(1998)].

[85] I. J. R. Aitchison, *Supersymmetry and the MSSM: An Elementary introduction*, hep-ph/0505105.

[86] H. E. Haber and G. L. Kane, *The Search for Supersymmetry: Probing Physics Beyond the Standard Model*, *Phys. Rept.* **117** (1985) 75–263.

[87] T. Asaka, S. Blanchet, and M. Shaposhnikov, *The nuMSM, dark matter and neutrino masses*, *Phys. Lett.* **B631** (2005) 151–156, [hep-ph/0503065].

[88] T. Asaka and M. Shaposhnikov, *The nuMSM, dark matter and baryon asymmetry of the universe*, *Phys. Lett.* **B620** (2005) 17–26, [hep-ph/0505013].

[89] M. Lindner, D. Schmidt, and A. Watanabe, *Dark matter and* $U(1)'$ *symmetry for the right-handed neutrinos*, *Phys. Rev.* **D89** (2014), no. 1 013007, [arXiv:1310.6582].

[90] N. Okada and O. Seto, *Higgs portal dark matter in the minimal gauged* $U(1)_{B-L}$ *model*, *Phys. Rev.* **D82** (2010) 023507, [arXiv:1002.2525].

[91] L. M. Krauss, S. Nasri, and M. Trodden, *A Model for neutrino masses and dark matter*, *Phys. Rev.* **D67** (2003) 085002, [hep-ph/0210389].

[92] A. Boyarsky, O. Ruchayskiy, and M. Shaposhnikov, *The Role of sterile neutrinos in cosmology and astrophysics*, *Ann. Rev. Nucl. Part. Sci.* **59** (2009) 191–214, [arXiv:0901.0011].

[93] A. Kusenko, F. Takahashi, and T. T. Yanagida, *Dark Matter from Split Seesaw*, *Phys. Lett.* **B693** (2010) 144–148, [arXiv:1006.1731].

[94] **CHARM** Collaboration, F. Bergsma et al., *A Search for Decays of Heavy Neutrinos*, *Phys. Lett.* **B128** (1983) 361.

[95] G. Bernardi et al., *Further Limits On Heavy Neutrino Couplings*, *Phys. Lett.* **B203** (1988) 332.

[96] J. S. Schwinger, *On Quantum electrodynamics and the magnetic moment of the electron*, *Phys. Rev.* **73** (1948) 416–417.

[97] M. Davier, A. Hoecker, B. Malaescu, and Z. Zhang, *Reevaluation of the Hadronic Contributions to the Muon $g-2$ and to alpha(MZ)*, *Eur.Phys.J.* **C71** (2011) 1515, [arXiv:1010.4180].

[98] T. Aoyama, M. Hayakawa, T. Kinoshita, and M. Nio, *Complete Tenth-Order QED Contribution to the Muon $g-2$*, *Phys.Rev.Lett.* **109** (2012) 111808, [arXiv:1205.5370].

[99] C. Gnendiger, D. Stöckinger, and H. Stöckinger-Kim, *The electroweak contributions to $(g-2)_\mu$ after the Higgs boson mass measurement*, *Phys.Rev.* **D88** (2013) 053005, [arXiv:1306.5546].

[100] T. Blum, A. Denig, I. Logashenko, E. de Rafael, B. L. Roberts, et al., *The Muon $(g-2)$ Theory Value: Present and Future*, arXiv:1311.2198.

[101] J. P. Miller, E. d. Rafael, B. L. Roberts, and D. Stckinger, *Muon $(g-2)$: Experiment and Theory*, *Ann.Rev.Nucl.Part.Sci.* **62** (2012) 237–264.

[102] F. S. Queiroz and W. Shepherd, *New Physics Contributions to the Muon Anomalous Magnetic Moment: A Numerical Code*, *Phys. Rev.* **D89** (2014), no. 9 095024, [arXiv:1403.2309].

[103] T. Moroi, *The Muon anomalous magnetic dipole moment in the minimal supersymmetric standard model*, *Phys.Rev.* **D53** (1996) 6565–6575, [hep-ph/9512396].

[104] D. Stockinger, *The Muon Magnetic Moment and Supersymmetry*, *J. Phys.* **G34** (2007) R45–R92, [hep-ph/0609168].

[105] O. Buchmueller et al., *Higgs and Supersymmetry*, *Eur. Phys. J.* **C72** (2012) 2020, [arXiv:1112.3564].

[106] H. Baer, V. Barger, and A. Mustafayev, *Implications of a 125 GeV Higgs scalar for LHC SUSY and neutralino dark matter searches*, *Phys. Rev.* **D85** (2012) 075010, [arXiv:1112.3017].

[107] J. Cao, Z. Heng, D. Li, and J. M. Yang, *Current experimental constraints on the lightest Higgs boson mass in the constrained MSSM*, *Phys. Lett.* **B710** (2012) 665–670, [arXiv:1112.4391].

[108] H. Baer, A. Mustafayev, S. Profumo, A. Belyaev, and X. Tata, *Direct, indirect and collider detection of neutralino dark matter in SUSY models with non-universal Higgs masses*, *JHEP* **07** (2005) 065, [hep-ph/0504001].

[109] H. Baer, A. Mustafayev, S. Profumo, A. Belyaev, and X. Tata, *Neutralino cold dark matter in a one parameter extension of the minimal supergravity model*, *Phys. Rev.* **D71** (2005) 095008, [hep-ph/0412059].

[110] J. R. Ellis, K. A. Olive, and P. Sandick, *Varying the Universality of Supersymmetry-Breaking Contributions to MSSM Higgs Boson Masses*, *Phys. Rev.* **D78** (2008) 075012, [arXiv:0805.2343].

[111] **ATLAS** Collaboration, G. Aad et al., *Observation of a new particle in the search for the Standard Model Higgs boson with the ATLAS detector at the LHC*, *Phys. Lett.* **B716** (2012) 1–29, [arXiv:1207.7214].

[112] **CMS** Collaboration, S. Chatrchyan et al., *Observation of a new boson at a mass of 125 GeV with the CMS experiment at the LHC*, *Phys. Lett.* **B716** (2012) 30–61, [arXiv:1207.7235].

[113] **CDF** Collaboration, T. Aaltonen et al., *Search for $B_s^0 \to \mu^+\mu^-$ and $B^0 \to \mu^+\mu^-$ Decays with CDF II*, *Phys. Rev. Lett.* **107** (2011) 191801, [arXiv:1107.2304]. [Publisher-note107,239903(2011)].

[114] **ATLAS** Collaboration, G. Aad et al., *Search for the decay $B_s^0 \to \mu\mu$ with the ATLAS detector*, *Phys. Lett.* **B713** (2012) 387–407, [arXiv:1204.0735].

[115] J. R. Ellis, K. Enqvist, D. V. Nanopoulos, and K. Tamvakis, *Gaugino Masses and Grand Unification*, *Phys. Lett.* **B155** (1985) 381.

[116] M. Drees, *Phenomenological Consequences of $N = 1$ Supergravity Theories With Nonminimal Kinetic Energy Terms for Vector Superfields*, *Phys. Lett.* **B158** (1985) 409.

[117] S. Mohanty, S. Rao, and D. P. Roy, *Reconciling the muon $g - 2$ and dark matter relic density with the LHC results in nonuniversal gaugino mass models*, *JHEP* **09** (2013) 027, [arXiv:1303.5830].

[118] K. S. Babu, I. Gogoladze, Q. Shafi, and C. S. n, *Muon $g - 2$, 125 GeV Higgs boson, and neutralino dark matter in a flavor symmetry-based MSSM*, *Phys. Rev.* **D90** (2014), no. 11 116002, [arXiv:1406.6965].

[119] S. Baek, N. Deshpande, X. He, and P. Ko, *Muon anomalous $g - 2$ and gauged $L_\mu - L_\tau$ models*, *Phys.Rev.* **D64** (2001) 055006, [hep-ph/0104141].

[120] P. Agrawal, Z. Chacko, and C. B. Verhaaren, *Leptophilic Dark Matter and the Anomalous Magnetic Moment of the Muon*, arXiv:1402.7369.

[121] Y. Bai and J. Berger, *Lepton Portal Dark Matter*, *JHEP* **08** (2014) 153, [arXiv:1402.6696].

[122] G. Blanger, C. Delaunay, and S. Westhoff, *A Dark Matter Relic From Muon Anomalies*, arXiv:1507.06660.

[123] P. Das, S. Kumar Rai, and S. Raychaudhuri, *Anomalous magnetic moment of the muon in a composite model*, hep-ph/0102242.

[124] S. N. Gninenko and N. V. Krasnikov, *The Muon anomalous magnetic moment and a new light gauge boson*, *Phys. Lett.* **B513** (2001) 119, [hep-ph/0102222].

[125] M. Beccaria, F. M. Renard, S. Spagnolo, and C. Verzegnassi, *Bounds on anomalous gauge couplings from past and near future experiments: The Role of the different measurements*, *Phys. Lett.* **B448** (1999) 129–142, [hep-ph/9810323].

[126] D. Chakraverty, D. Choudhury, and A. Datta, *A Nonsupersymmetric resolution of the anomalous muon magnetic moment*, *Phys. Lett.* **B506** (2001) 103–108, [hep-ph/0102180].

[127] R. Casadio, A. Gruppuso, and G. Venturi, *Electromagnetic contributions to lepton $g-2$ in a thick brane world*, *Phys. Lett.* **B495** (2000) 378–383, [hep-th/0010065].

[128] M. L. Graesser, *Extra dimensions and the muon anomalous magnetic moment*, *Phys. Rev.* **D61** (2000) 074019, [hep-ph/9902310].

[129] M. C. Gonzalez-Garcia and S. F. Novaes, *Compositeness effects in the anomalous weak magnetic moment of leptons*, *Phys. Lett.* **B389** (1996) 707–712, [hep-ph/9609393].

[130] K. D. Lane, *New model independent limit on muon substructure*, hep-ph/0102131.

[131] T. Huang, Z. H. Lin, L. Y. Shan, and X. Zhang, *Muon anomalous magnetic moment and lepton flavor violation*, *Phys. Rev.* **D64** (2001) 071301, [hep-ph/0102193].

[132] U. Mahanta, *Constraining new physics in the TeV range by the recent BNL measurement of $(g-2)_\mu$*, *Phys. Lett.* **B511** (2001) 235–239, [hep-ph/0102211].

[133] S. Bar-Shalom, S. Nandi, and A. Soni, *Muon $g-2$ and lepton flavor violation in a two Higgs doublets model for the fourth generation*, *Phys. Lett.* **B709** (2012) 207–217, [arXiv:1112.3661].

[134] C. D. Carone, *Flavor-Nonuniversal Dark Gauge Bosons and the Muon $g-2$*, *Phys. Lett.* **B721** (2013) 118–122, [arXiv:1301.2027].

[135] D. Colladay and V. A. Kostelecky, *Lorentz violating extension of the standard model*, *Phys. Rev.* **D58** (1998) 116002, [hep-ph/9809521].

[136] S. R. Moore, K. Whisnant, and B.-L. Young, *Second Order Corrections to the Muon Anomalous Magnetic Moment in Alternative Electroweak Models*, *Phys. Rev.* **D31** (1985) 105.

[137] G. G. Boyarkina and O. M. Boyarkin, *$(g-2)_\mu$ anomaly, higgs bosons, and heavy neutrinos*, *Phys. Rev.* **D67** (2003) 073023.

[138] **BAIKAL** Collaboration, V. Aynutdinov et al., *Search for a diffuse flux of high-energy extraterrestrial neutrinos with the nt200 neutrino telescope*, *Astropart. Phys.* **25** (2006) 140–150, [astro-ph/0508675].

[139] **NESTOR** Collaboration, G. Aggouras et al., *A measurement of the cosmic-ray muon flux with a module of the NESTOR neutrino telescope*, *Astropart. Phys.* **23** (2005) 377–392.

[140] **IceCube** Collaboration, M. G. Aartsen et al., *Search for a diffuse flux of astrophysical muon neutrinos with the IceCube 59-string configuration*, *Phys. Rev.* **D89** (2014), no. 6 062007, [arXiv:1311.7048].

[141] A. Loeb and E. Waxman, *The Cumulative background of high energy neutrinos from starburst galaxies*, *JCAP* **0605** (2006) 003, [astro-ph/0601695].

[142] X.-C. Chang, R.-Y. Liu, and X.-Y. Wang, *Star-forming galaxies as the origin of the IceCube PeV neutrinos*, *Astrophys. J.* **805** (2015), no. 2 95, [arXiv:1412.8361].

[143] S. Chakraborty and I. Izaguirre, *Diffuse neutrinos from extragalactic supernova remnants: Dominating the 100 TeV IceCube flux*, *Phys. Lett.* **B745** (2015) 35–39, [arXiv:1501.02615].

[144] F. W. Stecker, C. Done, M. H. Salamon, and P. Sommers, *High-energy neutrinos from active galactic nuclei*, *Phys. Rev. Lett.* **66** (1991) 2697–2700. [Erratum: Phys. Rev. Lett.69,2738(1992)].

[145] O. E. Kalashev, A. Kusenko, and W. Essey, *PeV neutrinos from intergalactic interactions of cosmic rays emitted by active galactic nuclei*, *Phys. Rev. Lett.* **111** (2013), no. 4 041103, [arXiv:1303.0300].

[146] O. Kalashev, D. Semikoz, and I. Tkachev, *Neutrinos in IceCube from AGN's*, arXiv:1410.8124.

[147] E. Waxman and J. N. Bahcall, *High-energy neutrinos from cosmological gamma-ray burst fireballs*, *Phys. Rev. Lett.* **78** (1997) 2292–2295, [astro-ph/9701231].

[148] S. Razzaque, *The Galactic Center Origin of a Subset of IceCube Neutrino Events*, *Phys. Rev.* **D88** (2013) 081302, [arXiv:1309.2756].

[149] M. Ahlers and K. Murase, *Probing the Galactic Origin of the IceCube Excess with Gamma-Rays*, *Phys. Rev.* **D90** (2014), no. 2 023010, [arXiv:1309.4077].

[150] B. Wang, X.-H. Zhao, and Z. Li, *Implications of Fermi-LAT observations on the origin of IceCube neutrinos*, *JCAP* **1411** (2014), no. 11 028, [arXiv:1407.2536].

[151] K. Murase, R. Laha, S. Ando, and M. Ahlers, *Testing the Dark Matter Scenario for PeV Neutrinos Observed in IceCube*, *Phys. Rev. Lett.* **115** (2015), no. 7 071301, [arXiv:1503.04663].

[152] B. Feldstein, A. Kusenko, S. Matsumoto, and T. T. Yanagida, *Neutrinos at IceCube from Heavy Decaying Dark Matter*, arXiv:1303.7320.

[153] A. Esmaili and P. D. Serpico, *Are IceCube neutrinos unveiling PeV-scale decaying dark matter?*, arXiv:1308.1105.

[154] Y. Ema, R. Jinno, and T. Moroi, *Cosmic-Ray Neutrinos from the Decay of Long-Lived Particle and the Recent IceCube Result*, *Phys. Lett.* **B733** (2014) 120–125, [arXiv:1312.3501].

[155] T. Higaki, R. Kitano, and R. Sato, *Neutrinoful Universe*, *JHEP* **07** (2014) 044, [arXiv:1405.0013].

[156] A. Bhattacharya, M. H. Reno, and I. Sarcevic, *Reconciling neutrino flux from heavy dark matter decay and recent events at IceCube*, *JHEP* **06** (2014) 110, [arXiv:1403.1862].

[157] L. A. Anchordoqui, V. Barger, H. Goldberg, X. Huang, D. Marfatia, L. H. M. da Silva, and T. J. Weiler, *IceCube neutrinos, decaying dark matter, and the Hubble constant*, arXiv:1506.08788.

[158] C. S. Fong, H. Minakata, B. Panes, and R. Z. Funchal, *Possible Interpretations of IceCube High-Energy Neutrino Events*, *JHEP* **02** (2015) 189, [arXiv:1411.5318].

[159] C. E. Aisati, M. Gustafsson, and T. Hambye, *New Search for Monochromatic Neutrinos from Dark Matter Decay*, arXiv:1506.02657.

[160] C. Rott, K. Kohri, and S. C. Park, *Superheavy dark matter and IceCube neutrino signals: Bounds on decaying dark matter*, *Phys. Rev.* **D92** (2015), no. 2 023529, [arXiv:1408.4575].

[161] A. Bhattacharya, R. Gandhi, and A. Gupta, *The Direct Detection of Boosted Dark Matter at High Energies and PeV events at IceCube*, *JCAP* **1503** (2015), no. 03 027, [arXiv:1407.3280].

[162] J. Kopp, J. Liu, and X.-P. Wang, *Boosted Dark Matter in IceCube and at the Galactic Center*, *JHEP* **04** (2015) 105, [arXiv:1503.02669].

[163] H.-N. He, R.-Z. Yang, Y.-Z. Fan, and D.-M. Wei, *TeV-PeV neutrinos over the atmospheric background: originating from two groups of sources?*, arXiv:1307.1450.

[164] C.-Y. Chen, P. S. B. Dev, and A. Soni, *A Possible Two-component Flux for the High Energy Neutrino Events at IceCube*, arXiv:1411.5658.

[165] S. M. Boucenna, M. Chianese, G. Mangano, G. Miele, S. Morisi, O. Pisanti, and E. Vitagliano, *Decaying Leptophilic Dark Matter at IceCube*, arXiv:1507.01000.

[166] T. Araki, F. Kaneko, Y. Konishi, T. Ota, J. Sato, and T. Shimomura, *Cosmic neutrino spectrum and the muon anomalous magnetic moment in the gauged $L_\mu - L_\tau$ model*, *Phys. Rev.* **D91** (2015), no. 3 037301, [arXiv:1409.4180].

[167] S. L. Glashow, *Resonant Scattering of Antineutrinos*, *Phys.Rev.* **118** (1960) 316–317.

[168] M. D. Kistler, T. Stanev, and H. Yksel, *Cosmic PeV Neutrinos and the Sources of Ultrahigh Energy Protons*, *Phys.Rev.* **D90** (2014), no. 12 123006, [arXiv:1301.1703].

[169] L. A. Anchordoqui, V. Barger, H. Goldberg, J. G. Learned, D. Marfatia, S. Pakvasa, T. C. Paul, and T. J. Weiler, *End of the cosmic neutrino energy spectrum*, *Phys. Lett.* **B739** (2014) 99–101, [arXiv:1404.0622].

[170] F. W. Stecker, S. T. Scully, S. Liberati, and D. Mattingly, *Searching for Traces of Planck-Scale Physics with High Energy Neutrinos*, *Phys. Rev.* **D91** (2015), no. 4 045009, [arXiv:1411.5889].

[171] J. S. Diaz, A. Kostelecky, and M. Mewes, *Testing Relativity with High-Energy Astrophysical Neutrinos*, *Phys.Rev.* **D89** (2014), no. 4 043005, [arXiv:1308.6344].

[172] R. C. Myers and M. Pospelov, *Ultraviolet modifications of dispersion relations in effective field theory*, *Phys. Rev. Lett.* **90** (2003) 211601, [hep-ph/0301124].

[173] E. Ma and G. Rajasekaran, *Softly broken A(4) symmetry for nearly degenerate neutrino masses*, *Phys. Rev.* **D64** (2001) 113012, [hep-ph/0106291].

[174] F. Wilczek, *The $U(1)$ Problem: Instantons, Axions, and Familons*, in *How Far Are We from the Gauge Forces*, p. 0157, 1983.

[175] J. Heeck and W. Rodejohann, *Gauged L_μ - L_τ Symmetry at the Electroweak Scale*, *Phys. Rev.* **D84** (2011) 075007, [arXiv:1107.5238].

[176] **Particle Data Group** Collaboration, K. A. Olive et al., *Review of Particle Physics*, *Chin. Phys.* **C38** (2014) 090001.

[177] A. Freitas, J. Lykken, S. Kell, and S. Westhoff, *Testing the Muon $g-2$ Anomaly at the LHC*, *JHEP* **05** (2014) 145, [arXiv:1402.7065]. [Erratum: JHEP09,155(2014)].

[178] M. Das and S. Mohanty, *Leptophilic dark matter in gauged $L_\mu - L_\tau$ extension of MSSM*, *Phys.Rev.* **D89** (2014), no. 2 025004, [arXiv:1306.4505].

[179] **PAMELA** Collaboration, O. Adriani et al., *PAMELA results on the cosmic-ray antiproton flux from 60 MeV to 180 GeV in kinetic energy*, *Phys. Rev. Lett.* **105** (2010) 121101, [arXiv:1007.0821].

[180] AMS-02 collaboration, *http://www.ams02.org/*, .

[181] S. Baek and P. Ko, *Phenomenology of $U(1)_{L_\mu - L_\tau}$ charged dark matter at PAMELA and colliders*, *JCAP* **0910** (2009) 011, [arXiv:0811.1646].

[182] X.-J. Bi, X.-G. He, and Q. Yuan, *Parameters in a class of leptophilic models from PAMELA, ATIC and FERMI*, *Phys.Lett.* **B678** (2009) 168–173, [arXiv:0903.0122].

[183] W.-L. Guo and Y.-L. Wu, *Enhancement of Dark Matter Annihilation via Breit-Wigner Resonance*, *Phys.Rev.* **D79** (2009) 055012, [arXiv:0901.1450].

[184] M. Ibe, H. Murayama, and T. Yanagida, *Breit-Wigner Enhancement of Dark Matter Annihilation*, *Phys.Rev.* **D79** (2009) 095009, [arXiv:0812.0072].

[185] E. Witten, *An SU(2) Anomaly*, *Phys. Lett.* **B117** (1982) 324–328.

[186] S. Bar-Shalom, S. Nandi, and A. Soni, *Two Higgs doublets with 4th generation fermions - models for TeV-scale compositeness*, *Phys. Rev.* **D84** (2011) 053009, [arXiv:1105.6095].

[187] X.-G. He and G. Valencia, *An extended scalar sector to address the tension between a fourth generation and Higgs searches at the LHC*, *Phys. Lett.* **B707** (2012) 381–384, [arXiv:1108.0222].

[188] C. L. Ong, *A Study of a Model With Horizontal Gauge Symmetry at One Loop Level*, *Phys. Rev.* **D22** (1980) 2886.

[189] M. Cirelli, G. Corcella, A. Hektor, G. Hutsi, M. Kadastik, et al., *PPPC 4 DM ID: A Poor Particle Physicist Cookbook for Dark Matter Indirect Detection*, *JCAP* **1103** (2011) 051, [arXiv:1012.4515].

[190] P. Ciafaloni, D. Comelli, A. Riotto, F. Sala, A. Strumia, et al., *Weak Corrections are Relevant for Dark Matter Indirect Detection*, *JCAP* **1103** (2011) 019, [arXiv:1009.0224].

[191] I. Moskalenko and A. Strong, *Production and propagation of cosmic ray positrons and electrons*, *Astrophys.J.* **493** (1998) 694–707, [astro-ph/9710124].

[192] A. W. Strong, I. V. Moskalenko, and V. S. Ptuskin, *Cosmic-ray propagation and interactions in the Galaxy*, *Ann.Rev.Nucl.Part.Sci.* **57** (2007) 285–327, [astro-ph/0701517].

[193] **Fermi-LAT** Collaboration, A. Abdo et al., *The Spectrum of the Isotropic Diffuse Gamma-Ray Emission Derived From First-Year Fermi Large Area Telescope Data*, *Phys.Rev.Lett.* **104** (2010) 101101, [arXiv:1002.3603].

[194] J. P. Leveille, *The Second Order Weak Correction to (G-2) of the Muon in Arbitrary Gauge Models*, *Nucl.Phys.* **B137** (1978) 63.

[195] S. Khalil, H.-S. Lee, and E. Ma, *Generalized Lepton Number and Dark Left-Right Gauge Model*, *Phys.Rev.* **D79** (2009) 041701, [arXiv:0901.0981].

[196] A. Aranda, J. Lorenzo Diaz-Cruz, J. Hernandez-Sanchez, and E. Ma, *Dark Left-Right Gauge Model: $SU(2)_R$ Phenomenology*, *Phys. Rev.* **D81** (2010) 075010, [arXiv:1001.4057].

[197] E. Ma, *Particle Dichotomy and Left-Right Decomposition of E(6) Superstring Models*, *Phys. Rev.* **D36** (1987) 274.

[198] K. S. Babu, X.-G. He, and E. Ma, *New Supersymmetric Left-Right Gauge Model: Higgs Boson Structure and Neutral Current Analysis*, *Phys. Rev.* **D36** (1987) 878.

[199] R. N. Mohapatra and J. C. Pati, *A Natural Left-Right Symmetry*, *Phys. Rev.* **D11** (1975) 2558.

[200] G. Senjanovic and R. N. Mohapatra, *Exact Left-Right Symmetry and Spontaneous Violation of Parity*, *Phys.Rev.* **D12** (1975) 1502.

[201] R. N. Mohapatra and G. Senjanovic, *Neutrino Mass and Spontaneous Parity Violation*, *Phys.Rev.Lett.* **44** (1980) 912.

[202] N. Deshpande, J. Gunion, B. Kayser, and F. I. Olness, *Left-right symmetric electroweak models with triplet Higgs*, *Phys.Rev.* **D44** (1991) 837–858.

[203] J. C. Pati and A. Salam, *Lepton Number as the Fourth Color*, *Phys. Rev.* **D10** (1974) 275–289. [Erratum: Phys. Rev.D11,703(1975)].

[204] L. Bergstrom, T. Bringmann, and J. Edsjo, *New Positron Spectral Features from Supersymmetric Dark Matter - a Way to Explain the PAMELA Data?*, *Phys.Rev.* **D78** (2008) 103520, [arXiv:0808.3725].

[205] J. R. Ellis, T. Falk, and K. A. Olive, *Neutralino - Stau coannihilation and the cosmological upper limit on the mass of the lightest supersymmetric particle*, *Phys.Lett.* **B444** (1998) 367–372, [hep-ph/9810360].

[206] T. Nihei, L. Roszkowski, and R. Ruiz de Austri, *Exact cross-sections for the neutralino slepton coannihilation*, *JHEP* **0207** (2002) 024, [hep-ph/0206266].

[207] Q.-H. Cao, E. Ma, and G. Shaughnessy, *Dark Matter: The Leptonic Connection*, *Phys.Lett.* **B673** (2009) 152–155, [arXiv:0901.1334].

[208] K. Griest and D. Seckel, *Three exceptions in the calculation of relic abundances*, *Phys. Rev.* **D43** (1991) 3191–3203.

[209] J. Edsjo and P. Gondolo, *Neutralino relic density including coannihilations*, *Phys. Rev.* **D56** (1997) 1879–1894, [hep-ph/9704361].

[210] M. Garny, A. Ibarra, M. Pato, and S. Vogl, *Closing in on mass-degenerate dark matter scenarios with antiprotons and direct detection*, *JCAP* **1211** (2012) 017, [arXiv:1207.1431].

[211] M. Garny, A. Ibarra, M. Pato, and S. Vogl, *Internal bremsstrahlung signatures in light of direct dark matter searches*, *JCAP* **1312** (2013) 046, [arXiv:1306.6342].

[212] T. Bringmann, X. Huang, A. Ibarra, S. Vogl, and C. Weniger, *Fermi LAT Search for Internal Bremsstrahlung Signatures from Dark Matter Annihilation*, *JCAP* **1207** (2012) 054, [arXiv:1203.1312].

[213] S. Blanchet and J. Lavalle, *Diffuse gamma-ray constraints on dark matter revisited. I: the impact of subhalos*, *JCAP* **1211** (2012) 021, [arXiv:1207.2476].

[214] **Fermi-LAT** Collaboration, M. Ackermann et al., *Limits on Dark Matter Annihilation Signals from the Fermi LAT 4-year Measurement of the Isotropic Gamma-Ray Background*, *JCAP* **1509** (2015), no. 09 008, [arXiv:1501.05464].

[215] **HESS** Collaboration, F. Aharonian et al., *The energy spectrum of cosmic-ray electrons at TeV energies*, *Phys. Rev. Lett.* **101** (2008) 261104, [arXiv:0811.3894].

[216] **HESS** Collaboration, F. Aharonian et al., *Probing the ATIC peak in the cosmic-ray electron spectrum with H.E.S.S*, *Astron. Astrophys.* **508** (2009) 561, [arXiv:0905.0105].

[217] M. D. Kistler and J. M. Siegal-Gaskins, *Gamma-ray signatures of annihilation to charged leptons in dark matter substructure*, *Phys. Rev.* **D81** (2010) 103521, [arXiv:0909.0519].

[218] G. Belanger, F. Boudjema, and A. Pukhov, *micrOMEGAs : a code for the calculation of Dark Matter properties in generic models of particle interaction*, arXiv:1402.0787.

[219] P. Brun, T. Delahaye, J. Diemand, S. Profumo, and P. Salati, *The cosmic ray lepton puzzle in the light of cosmological N-body simulations*, *Phys. Rev.* **D80** (2009) 035023, [arXiv:0904.0812].

[220] CMS collaboration, *https://cms-physics.web.cern.ch/cms-physics/public/HIG-12-005-pas.pdf.*

[221] **ATLAS** Collaboration, G. Aad et al., *Search for doubly-charged Higgs bosons in like-sign dilepton final states at $\sqrt{s} = 7$ TeV with the ATLAS detector*, *Eur. Phys. J.* **C72** (2012) 2244, [arXiv:1210.5070].

[222] **CMS** Collaboration, S. Chatrchyan et al., *Search for a light charged Higgs boson in top quark decays in pp collisions at $\sqrt{s} = 7$ TeV*, *JHEP* **07** (2012) 143, [arXiv:1205.5736].

[223] ATLAS collaboration, *http://cds.cern.ch/record/1595533/files/ATLAS-CONF-2013-090.pdf.*

[224] **CMS** Collaboration, S. Chatrchyan et al., *Search for heavy narrow dilepton resonances in pp collisions at $\sqrt{s} = 7$ TeV and $\sqrt{s} = 8$ TeV*, *Phys. Lett.* **B720** (2013) 63–82, [arXiv:1212.6175].

[225] **ATLAS** Collaboration, G. Aad et al., *Search for high-mass dilepton resonances in pp collisions at $\sqrt{s} = 8$ TeV with the ATLAS detector*, *Phys. Rev.* **D90** (2014), no. 5 052005, [arXiv:1405.4123].

[226] **L3** Collaboration, P. Achard et al., *Search for doubly charged Higgs bosons at LEP*, *Phys. Lett.* **B576** (2003) 18–28, [hep-ex/0309076].

[227] S. Doplicher, K. Fredenhagen, and J. E. Roberts, *The Quantum structure of space-time at the Planck scale and quantum fields*, *Commun. Math. Phys.* **172** (1995) 187–220, [hep-th/0303037].

[228] M. Visser, *Lorentz symmetry breaking as a quantum field theory regulator*, *Phys.Rev.* **D80** (2009) 025011, [arXiv:0902.0590].

[229] V. A. Kostelecky and S. Samuel, *Spontaneous Breaking of Lorentz Symmetry in String Theory*, *Phys. Rev.* **D39** (1989) 683.

[230] P. Horava, *Quantum Gravity at a Lifshitz Point*, *Phys.Rev.* **D79** (2009) 084008, [arXiv:0901.3775].

[231] D. Mattingly, *Modern tests of Lorentz invariance*, *Living Rev. Rel.* **8** (2005) 5, [gr-qc/0502097].

[232] S. Liberati, *Tests of Lorentz invariance: a 2013 update*, *Class. Quant. Grav.* **30** (2013) 133001, [arXiv:1304.5795].

[233] F. W. Stecker, *Diffuse Fluxes of Cosmic High-Energy Neutrinos*, *Astrophys. J.* **228** (1979) 919–927.

[234] J. G. Learned and T. J. Weiler, *A Relational Argument for a ∼PeV Neutrino Energy Cutoff*, arXiv:1407.0739.

[235] S. Mohanty and S. Rao, *Neutrino processes with power law dispersion relations*, *Phys. Rev.* **D85** (2012) 102005, [arXiv:1112.2981].

[236] A. Kostelecky and M. Mewes, *Neutrinos with Lorentz-violating operators of arbitrary dimension*, *Phys. Rev.* **D85** (2012) 096005, [arXiv:1112.6395].

[237] J. S. Diaz, *Neutrinos as probes of Lorentz invariance*, *Adv. High Energy Phys.* **2014** (2014) 962410, [arXiv:1406.6838].

[238] F. W. Stecker and S. T. Scully, *Propagation of Superluminal PeV IceCube Neutrinos: A High Energy Spectral Cutoff or New Constraints on Lorentz*

Invariance Violation, *Phys. Rev.* **D90** (2014), no. 4 043012, [arXiv:1404.7025].

[239] L. Maccione, S. Liberati, and D. M. Mattingly, *Violations of Lorentz invariance in the neutrino sector after OPERA*, *JCAP* **1303** (2013) 039, [arXiv:1110.0783].

[240] V. A. Kostelecky and N. Russell, *Data Tables for Lorentz and CPT Violation*, *Rev. Mod. Phys.* **83** (2011) 11–31, [arXiv:0801.0287].

[241] P. A. Bolokhov and M. Pospelov, *Classification of dimension 5 Lorentz violating interactions in the standard model*, *Phys. Rev.* **D77** (2008) 025022, [hep-ph/0703291].

[242] T. A. Jacobson, S. Liberati, D. Mattingly, and F. W. Stecker, *New limits on Planck scale Lorentz violation in QED*, *Phys. Rev. Lett.* **93** (2004) 021101, [astro-ph/0309681].

[243] T. Jacobson, S. Liberati, and D. Mattingly, *Lorentz violation at high energy: Concepts, phenomena and astrophysical constraints*, *Annals Phys.* **321** (2006) 150–196, [astro-ph/0505267].

[244] S. Sahu and L. S. Miranda, *Some possible sources of IceCube TeV?PeV neutrino events*, *Eur. Phys. J.* **C75** (2015), no. 6 273, [arXiv:1408.3664].

[245] G. F. Giudice, S. Sibiryakov, and A. Strumia, *Interpreting OPERA Results on Superluminal Neutrino*, *Nucl.Phys.* **B861** (2012) 1–16, [arXiv:1109.5682].

[246] J. Bijnens, G. Ecker, and J. Gasser, *Radiative semileptonic kaon decays*, *Nucl. Phys.* **B396** (1993) 81–118, [hep-ph/9209261].

[247] V. S. Berezinsky and G. T. Zatsepin, *Cosmic rays at ultrahigh-energies (neutrino?)*, *Phys. Lett.* **B28** (1969) 423–424.

[248] K. Greisen, *End to the cosmic ray spectrum?*, *Phys. Rev. Lett.* **16** (1966) 748–750.

[249] G. T. Zatsepin and V. A. Kuzmin, *Upper limit of the spectrum of cosmic rays*, *JETP Lett.* **4** (1966) 78–80. [Pisma Zh. Eksp. Teor. Fiz.4,114(1966)].

[250] R. Engel, D. Seckel, and T. Stanev, *Neutrinos from propagation of ultrahigh-energy protons*, *Phys. Rev.* **D64** (2001) 093010, [astro-ph/0101216].

[251] F. Staub, *SARAH*, arXiv:0806.0538.

[252] **CMS** Collaboration, V. Khachatryan et al., *Search for heavy neutrinos and W bosons with right-handed couplings in proton-proton collisions at $\sqrt{s} = 8$ TeV*, *Eur. Phys. J.* **C74** (2014), no. 11 3149, [arXiv:1407.3683].

[253] C. Hati, G. Kumar, and N. Mahajan, *$\bar{B} \to D^{(*)}\tau\bar{\nu}$ excesses in ALRSM constrained from B, D decays and $D^0 - \bar{D}^0$ mixing*, *JHEP* **01** (2016) 117, [arXiv:1511.03290].

[254] **LHCb** Collaboration, R. Aaij et al., *Measurement of the ratio of branching fractions $\mathcal{B}(\bar{B}^0 \to D^{*+}\tau^-\bar{\nu}_\tau)/\mathcal{B}(\bar{B}^0 \to D^{*+}\mu^-\bar{\nu}_\mu)$*, *Phys. Rev. Lett.* **115** (2015), no. 11 111803, [arXiv:1506.08614]. [Addendum: Phys. Rev. Lett.115,no.15,159901(2015)].

[255] **BaBar** Collaboration, J. P. Lees et al., *Measurement of an Excess of $\bar{B} \to D^{(*)}\tau^-\bar{\nu}_\tau$ Decays and Implications for Charged Higgs Bosons*, *Phys. Rev.* **D88** (2013), no. 7 072012, [arXiv:1303.0571].

[256] **Belle** Collaboration, M. Huschle et al., *Measurement of the branching ratio of $\bar{B} \to D^{(*)}\tau^-\bar{\nu}_\tau$ relative to $\bar{B} \to D^{(*)}\ell^-\bar{\nu}_\ell$ decays with hadronic tagging at Belle*, *Phys. Rev.* **D92** (2015), no. 7 072014, [arXiv:1507.03233].

[257] K. N. Abazajian and M. Kaplinghat, *Detection of a Gamma-Ray Source in the Galactic Center Consistent with Extended Emission from Dark Matter Annihilation and Concentrated Astrophysical Emission*, *Phys. Rev.* **D86** (2012) 083511, [arXiv:1207.6047]. [Erratum: Phys. Rev.D87,129902(2013)].

[258] A. Boyarsky, D. Malyshev, and O. Ruchayskiy, *A comment on the emission from the Galactic Center as seen by the Fermi telescope*, *Phys. Lett.* **B705** (2014) 165–169, [arXiv:1012.5839].

[259] D. Hooper and L. Goodenough, *Dark Matter Annihilation in The Galactic Center As Seen by the Fermi Gamma Ray Space Telescope*, *Phys. Lett.* **B697** (2014) 412–428, [arXiv:1010.2752].

[260] E. Bulbul, M. Markevitch, A. Foster, R. K. Smith, M. Loewenstein, and S. W. Randall, *Detection of An Unidentified Emission Line in the Stacked X-ray spectrum of Galaxy Clusters*, *Astrophys. J.* **789** (2014) 13, [arXiv:1402.2301].

[261] A. Boyarsky, O. Ruchayskiy, D. Iakubovskyi, and J. Franse, *Unidentified Line in X-Ray Spectra of the Andromeda Galaxy and Perseus Galaxy Cluster*, *Phys. Rev. Lett.* **113** (2014) 251301, [arXiv:1402.4119].

[262] J. Zavala, *Galactic PeV neutrinos from dark matter annihilation*, *Phys. Rev.* **D89** (2014), no. 12 123516, [arXiv:1404.2932].

[263] W. Buchmuller, R. Ruckl, and D. Wyler, *Leptoquarks in Lepton - Quark Collisions*, *Phys. Lett.* **B191** (1987) 442–448. [Erratum: Phys. Lett.B448,320(1999)].

[264] I. Dorner, S. Fajfer, A. Greljo, J. F. Kamenik, and N. Konik, *Physics of leptoquarks in precision experiments and at particle colliders*, arXiv:1603.04993.

[265] M. Mannarelli, M. Mitra, F. L. Villante, and F. Vissani, *Non-Standard Neutrino Propagation and Pion Decay*, *JHEP* **01** (2012) 136, [arXiv:1112.0169].

List of Publications

Publications in journals

1. **Gaurav Tomar**, Subhendra Mohanty, and Sandip Pakvasa, *Lorentz Invariance Violation and IceCube Neutrino Events*, JHEP 1511 (2015) 022, doi: 10.1007/JHEP11(2015)022, arXiv:1507.03193.

2. Tanushree Basak, Subhendra Mohanty, and **Gaurav Tomar**, *Explaining AMS-02 positron excess and muon anomalous magnetic moment in dark left-right gauge model*, JHEP 1603 (2016) 062, doi: 10.1007/JHEP03(2016)062, arXiv:1501.06193.

3. **Gaurav Tomar**, and Subhendra Mohanty, *Muon anomalous magnetic moment and positron excess at AMS-02 in a gauged horizontal symmetric model*, JHEP 1411 (2014) 133, doi: 10.1007/JHEP11(2014)133, arXiv:1403.6301.

Conference Papers

1. **Gaurav Tomar**, *Explaining muon magnetic moment and AMS-02 positron excess in a gauged horizontal symmetric model*, XXI DAE-BRNS High Energy Physics Symposium, IIT Guwahati, Assam, India, December 8-12, 2014, Springer Proceedings in Physics, doi: 10.1007/978/3/319/25619/1/66, arXiv:1507.01797.

Publications attached with thesis

1. **Gaurav Tomar**, Subhendra Mohanty, *Muon anomalous magnetic moment and positron excess at AMS-02 in a gauged horizontal symmetric model*, JHEP 1411 (2014) 133, doi: 10.1007/JHEP11(2014)133.

2. **Gaurav Tomar**, Subhendra Mohanty, and Sandip Pakvasa, *Lorentz Invariance Violation and IceCube Neutrino Events*, JHEP 1511 (2015) 022, doi: 10.1007/JHEP11(2015)022.

Published for SISSA by Springer

Received: July 20, 2014
Revised: October 14, 2014
Accepted: November 3, 2014
Published: November 24, 2014

Muon anomalous magnetic moment and positron excess at AMS-02 in a gauged horizontal symmetric model

Gaurav Tomar[a,b] **and Subhendra Mohanty**[a]

[a] *Physical Research Laboratory, Ahmedabad 380009, India*
[b] *Indian Institute of Technology, Gandhinagar 382424, India*

E-mail: tomar@prl.res.in, mohanty@prl.res.in

Abstract: We studied an extension of the standard model with a fourth generation of fermions to explain the discrepancy in the muon $(g-2)$ and explain the positron excess seen in the AMS-02 experiment. We introduce a gauged $\mathrm{SU}(2)_{\mathrm{HV}}$ horizontal symmetry between the muon and the 4th generation lepton families. The 4th generation right-handed neutrino is identified as the dark matter with mass $\sim 700\,\mathrm{GeV}$. The dark matter annihilates only to $(\mu^+\mu^-)$ and $(\nu_\mu^c\,\nu_\mu)$ states via $\mathrm{SU}(2)_{\mathrm{HV}}$ gauge boson. The $\mathrm{SU}(2)_{\mathrm{HV}}$ gauge boson with mass $\sim 1.4\,\mathrm{TeV}$ gives an adequate contribution to the $(g-2)$ of muon and fulfill the experimental constraint from BNL measurement. The higgs production constraints from 4th generation fermions is evaded by extending the higgs sector.

Keywords: Beyond Standard Model, Cosmology of Theories beyond the SM

ArXiv ePrint: 1403.6301

Article funded by SCOAP[3].

doi:10.1007/JHEP11(2014)133

Contents

1 Introduction

There exist two interesting experimental signals namely the muon $(g-2)$, measured at BNL [1, 2] and the excess of positrons measured by AMS-02 [20, 21], which may have a common beyond standard model (SM) explanation.

There is a discrepancy at 3.6σ level between the experimental measurement [1, 2] and the SM prediction [3–9] of muon anomalous magnetic moment,

$$\Delta a_\mu \equiv a_\mu^{\rm Exp} - a_\mu^{\rm SM} = (28.7 \pm 8.0) \times 10^{-10} \tag{1.1}$$

where a_μ is the anomalous magnetic moment in the unit of $e/2m_\mu$. In the standard model, contribution of W boson to the muon anomalous magnetic magnetic moment goes as $a_\mu^W \propto m_\mu^2/M_W^2$ and we have $a_\mu^{\rm SM} = 19.48 \times 10^{-10}$ [10].

In minimal supersymmetric standard model (MSSM) [11, 12], we get contributions to muon $(g-2)$ from neutralino-smuon and chargino-sneutrino loops. In all MSSM diagrams there still exist a m_μ suppression in $(g-2)$, arising from the following cases: (a) in case of bino in the loop, the mixing between the left and right handed smuons is $\propto m_\mu$ (b) in case of wino-higgsino or bino-higgsino in the loop, the higgsino coupling with smuon is $\propto y_\mu$, so there is a m_μ suppression (c) in the case of chargino-sneutrino in the loop, the higgsino-muon coupling is $\propto y_\mu$, which again gives rise to m_μ suppression. Therefor in MSSM $a_\mu^{\rm MSSM} \propto m_\mu^2/M_{\rm SUSY}^2$, where $M_{\rm SUSY}$ is proportional to the mass of the SUSY particle in the loop.

One can evade the muon mass suppression in $(g-2)$ with a horizontal gauge symmetry. In [13] a horizontal $\mathrm{U}(1)_{L_\mu - L_\tau}$ symmetry was used in which muon $(g-2)$ is proportional to m_τ and $a_\mu \propto m_\mu m_\tau / m_{Z'}^2$, where $L_\mu - L_\tau$ gauge boson mass $m_{Z'} \propto 100\,\mathrm{GeV}$ gives the required a_μ. A model independent analysis of the beyond SM particles which can give a contribution to a_μ is studied in [14]. The SM extension needed to explain muon $(g-2)$ has also been related to dark matter [15, 16] and the implication of this new physics in LHC searches has been studied [17]. An explanation of $(g-2)$ from the 4th generation leptons has also been given in [18, 19].

The second experimental signal, which we address in this paper is the excess of positron over cosmic-ray background, which has been observed by AMS-02 experiment [20] upto energy $\sim 425\,\mathrm{GeV}$ [21]. An analysis of AMS-02 data suggests that a dark matter (DM) annihilation interpretation would imply that the annihilation final states are either μ or τ [23, 24]. The dark matter annihilation into $e^{\pm}$ pairs would give a peak in positron signal, which is not seen in the positron spectrum. The branching ratio of τ decay to e is only 17% compared to μ, which makes μ as the preferred source as origin of high energy positrons. The AMS-02 experiment does not observe an excess, beyond the cosmic-ray background, in the antiproton flux [25, 26], indicating a leptophilic dark matter [27, 28, 33].

In this paper, we introduce a 4th generation of fermions and a $\mathrm{SU(2)_{HV}}$ vector gauge symmetry between the 4th generation leptons and the muon families. In our model, the muon $(g-2)$ has a contribution from the 4th generation charged lepton μ', and the $\mathrm{SU(2)_{HV}}$ gauge boson θ^{+},

$$\Delta a_{\mu} \propto \frac{m_{\mu} m_{\mu'}}{M^2_{\theta^{+}}} \tag{1.2}$$

and from the neutral higgs scalars (h, A),

$$\Delta a_{\mu} \propto \frac{m_{\mu}}{m_{\mu'}} \tag{1.3}$$

and from the charged higgs $H^{\pm}$ the contribution is,

$$\Delta a_{\mu} \propto -\frac{m_{\mu} m_{\nu_{\mu'}}}{m^2_{H^{\pm}}} \tag{1.4}$$

In all these cases, there is no quadratic suppression $\propto m_{\mu}^2$ because of the horizontal symmetry. By choosing parameters of the model without any fine tunning, we can obtain the required number $\Delta a_{\mu} = 2.87 \times 10^{-9}$ within 1σ.

In this model, the 4th generation right-handed neutrino $\nu_{\mu' R}$, is identified as dark matter. The dark matter annihilates to the standard model particles through the $\mathrm{SU(2)_{HV}}$ gauge boson θ_3 and with the only final states being $(\mu^{+}\mu^{-})$ and $(\nu_{\mu}^{c}\, \nu_{\mu})$. The stability of DM is maintained by taking the 4th generation charged lepton to be heavier than DM. To explain the AMS-02 signal [20, 21], one needs a cross-section (CS), $\sigma v_{\chi\chi\to\mu^{+}\mu^{-}} = 2.33 \times 10^{-25}\,\mathrm{cm^3/sec}$, which is larger than the CS, $\sigma v_{\chi\chi\to SM} \sim 3 \times 10^{-26}\,\mathrm{cm^3/sec}$, required to get the correct thermal relic density $\Omega h^2 = 0.1199 \pm 0.0027$ [29, 30]. In our model, the enhancement of annihilation CS of DM in the galaxy is achieved by the resonant enhancement mechanism [31–33], which we attain by taking $M_{\theta_3} \simeq 2m_{\chi}$.

This paper is organized as follows: in section 2, we describe the model. In section 3 we discuss the dark matter phenomenology and in section 4, we compute the $(g-2)$ contributions from this model and then give our conclusion in section 5.

Particles	$G_{\rm STD} \times {\rm SU(2)_{HV}}$ quantum numbers
$\psi_{eLi} \equiv (\nu_e, e)$	$(1, 2, -1, 1)$
$\Psi_{Li\alpha} \equiv (\psi_\mu, \psi_{\mu'})$	$(1, 2, -1, 2)$
$\psi_{\tau Li} \equiv (\nu_\tau, \tau)$	$(1, 2, -1, 1)$
$E_{R\alpha} \equiv (\mu_R, \mu'_R)$	$(1, 1, -2, 2)$
$N_{R\alpha} \equiv (\nu_{\mu R}, \nu_{\mu' R})$	$(1, 1, 0, 2)$
e_R, τ_R	$(1, 1, -2, 1)$
$\nu_{eR}, \nu_{\tau R}$	$(1, 1, 0, 1)$
ϕ_i	$(1, 2, 1, 1)$
$\eta^\beta_{i\alpha}$	$(1, 2, 1, 3)$
χ_α	$(1, 1, 0, 2)$

Table 1. Representation of the various fields in the model under the gauge group $G_{\rm STD} \times {\rm SU(2)_{HV}}$.

2 Model

In addition to the three generations of quarks and leptons, we introduce the 4th generation of quarks (c', s') and leptons (ν'_μ, μ') (of both chiralities) in the standard model. We also add three right-handed neutrinos and extend the gauge group of SM by horizontal symmetry denoted by ${\rm SU(2)_{HV}}$, between the 4th generation lepton and muon families. Addition of three right-handed neutrinos ensures that the model is free from SU(2) Witten anomaly [34]. We assume that the quarks of all four generations and the leptons of e and τ families are singlet of ${\rm SU(2)_{HV}}$ to evade the constraints from flavour changing processes. The ${\rm SU(2)_{HV}}$ symmetry can be extended to e and τ families by choosing suitable discrete symmetries, however in this paper we have taken e and τ families to be singlet of ${\rm SU(2)_{HV}}$ for simplicity and discuss the most economical model, which can explain muon $(g-2)$ and AMS-02 positron excess at the same time.

We denote the left-handed muon and 4th generation lepton families by $\Psi_{Li\alpha}$ and their right-handed charged and neutral counterparts by $E_{R\alpha}$ and $N_{R\alpha}$ respectively (here i and α are the ${\rm SU(2)}_L$ and ${\rm SU(2)_{HV}}$ indices respectively and run through the values 1 and 2). The left-handed electron and tau doublets are denoted by ψ_{eLi} and $\psi_{\tau Li}$ and their right-handed counterparts by e_R and τ_R respectively. The gauge fields of ${\rm SU(2)}_L \times {\rm U(1)}_Y \times {\rm SU(2)_{HV}}$ groups are denoted by A^a_μ, B_μ and θ^a_μ $(a = 1, 2, 3)$ with gauge couplings g, g' and g_H respectively.

The leptons transformations under the gauge group, ${\rm SU(3)}_c \times {\rm SU(2)}_L \times {\rm U(1)}_Y \times {\rm SU(2)_{HV}} \equiv G_{\rm STD} \times {\rm SU(2)_{HV}}$ are shown in table 1. From the assigned quantum numbers, it is clear that the ${\rm SU(2)_{HV}}$ gauge bosons connect only the leptons pairs, $\psi_{\mu_L} \leftrightarrow \psi_{\mu'_L}$ and $(\mu_R, \nu_{\mu R}) \leftrightarrow (\mu'_R, \nu'_{\mu R})$. This assignment prevents the flavour changing process like $\mu \to e\gamma$ for which there are stringent bounds, and also ensures the contribution of heavy lepton μ' to the muon $(g-2)$ as shown in figure 4. In our $G_{\rm STD} \times {\rm SU(2)_{HV}}$ model, the gauge couplings of the muon and 4th generation lepton families are,

$$\begin{aligned}\mathcal{L}_\psi = & i\bar{\Psi}_{Li\alpha}\gamma^\mu\left(\partial_\mu - \frac{i}{2}g\tau\cdot A_\mu + ig'B_\mu - \frac{i}{2}g_H\tau\cdot\theta_\mu\right)_{ij;\alpha\beta}\Psi_{Lj\beta} \\ & + i\bar{E}_{R\alpha}\gamma^\mu\left(\partial_\mu + i2g'B_\mu - \frac{i}{2}g_H\tau\cdot\theta_\mu\right)_{\alpha\beta}E_{R\beta} + i\bar{N}_{R\alpha}\gamma^\mu\left(\partial_\mu - \frac{i}{2}g_H\tau\cdot\theta_\mu\right)_{\alpha\beta}N_{R\beta}\end{aligned} \tag{2.1}$$

The "neutral-current" of $\mathrm{SU(2)_{HV}}$ contributes to the annihilation process, $(\nu_{\mu'}\nu_{\mu'}) \to \theta_3^* \to (\mu^+\mu^-), (\nu_\mu^c\ \nu_\mu)$, which is relevant for the AMS-02 and relic density calculations. The "charge-changing" vertex $\mu\mu'\theta^+$, contributes to the $(g-2)$ of the muon.

To evade the bounds on the 4th generation from the higgs production at LHC, we extend the higgs sector (in addition to ϕ_i) by a scalar $\eta_{i\alpha}^\beta$, which is a doublet under SU(2) and triplet under $\mathrm{SU(2)_{HV}}$. As a SU(2) doublet $\eta_{i\alpha}^\beta$ evades 4th generation bounds from the overproduction of higgs in the same way as [35, 36], in that the 125 GeV mass eigenstate is predominantly η which has no Yukawa couplings with the quarks. As $\eta_{i\alpha}^\beta$ is a triplet under $\mathrm{SU(2)_{HV}}$, its Yukawa couplings with the muon and 4th generation lepton families split the masses of the muon and 4th generation leptons. We also introduce a $\mathrm{SU(2)_{HV}}$ doublet χ_α, which generates masses for $\mathrm{SU(2)_{HV}}$ gauge bosons. The quantum numbers of the scalars are shown in table 1. The general potential of this set of scalars $(\phi_i, \eta_{i\alpha}^\beta, \chi_\alpha)$ is given in [37]. Following [37], we take the vacuum expectation values (vevs) of scalars as,

$$\begin{aligned}\langle\phi_i\rangle &= \langle\phi\rangle\delta_{i2} \\ \langle\eta_{i\alpha}^\beta\rangle &= \langle\eta\rangle\delta_{i2}(\delta_{\alpha1}\delta^{\beta1} - \delta_{\alpha2}\delta^{\beta2}) \\ |\langle\chi\rangle|^2 &= |\langle\chi_1\rangle|^2 + |\langle\chi_2\rangle|^2\end{aligned} \tag{2.2}$$

where $\langle\phi_i\rangle$ breaks $\mathrm{SU(2)}_L$, $\langle\chi_\alpha\rangle$ breaks $\mathrm{SU(2)_{HV}}$ and $\langle\eta_{i\alpha}^\beta\rangle$ breaks both $\mathrm{SU(2)}_L$ and $\mathrm{SU(2)_{HV}}$ and generate the TeV scale masses for $\mathrm{SU(2)_{HV}}$ gauge bosons. The mass eigenstates of the scalars will be a linear combination of $\phi_i, \eta_{i\alpha}^\beta$ and χ_α. We shall assume that the lowest mass eigenstate h_1 with the mass ~ 125 GeV is primarily constituted by $\eta_{i\alpha}^\beta$. We shall also assume that the parameters of the higgs potential [37] are tuned such that mixing between h_1 and ϕ_i is small,

$$\langle h_1|\phi_i\rangle \simeq 10^{-2} \tag{2.3}$$

The Yukawa couplings of 4th generation quarks are only with ϕ_i, therefore the 125 GeV Higgs will have very small contribution from the 4th generation quarks loop.

The gauge couplings of the scalar fields $\phi_i, \eta_{i\alpha}^\beta$ and χ_α are given by the Lagrangian,

$$\begin{aligned}\mathcal{L}_s = & |\left(\partial_\mu - \frac{i}{2}g\tau\cdot A_\mu - ig'B_\mu\right)\phi|^2 + |\left(\partial_\mu - \frac{i}{2}g\tau\cdot A_\mu - ig'B_\mu - ig_H T\cdot\theta_\mu\right)\eta|^2 \\ & + |\left(\partial_\mu - \frac{i}{2}g_H\tau\cdot\theta\right)\chi|^2\end{aligned} \tag{2.4}$$

where $\tau_a/2$ $(a = 1,2,3)$ are 2×2 matrix representation for the generators of SU(2) and T_a $(a = 1,2,3)$ are 3×3 matrix representation for the generators of SU(2). After expanding

$\mathcal{L}_s$ around the vevs defined in eq. (2.2), the masses of gauge bosons come,

$$
\begin{aligned}
&M_W^2 = \frac{g^2}{2}(2\langle\eta\rangle^2 + \langle\phi\rangle^2)\,, \qquad M_Z^2 = \frac{g^2}{2}\sec^2\theta_W(2\langle\eta\rangle^2 + \langle\phi\rangle^2)\,, \qquad M_A^2 = 0\,,\\
&M_{\theta^+}^2 = g_H^2\left(4\langle\eta\rangle^2 + \frac{1}{2}\langle\chi\rangle^2\right), \qquad M_{\theta_3}^2 = \frac{1}{2}g_H^2\langle\chi\rangle^2
\end{aligned}
\tag{2.5}
$$

we tune the parameters in the potential such that the vevs of scalars are,

$$
\begin{aligned}
2\langle\eta\rangle^2 + \langle\phi\rangle^2 &= (174\,\mathrm{GeV})^2\\
\langle\chi\rangle &= 22.7\,\mathrm{TeV}
\end{aligned}
\tag{2.6}
$$

for the generation of large masses for 4th generation leptons μ', $\nu_{\mu'}$ and $\mathrm{SU(2)_{HV}}$ gauge bosons θ^+, θ_3. The Yukawa couplings of the leptons are given by,

$$
\begin{aligned}
\mathcal{L}_Y = &-h_1\bar{\psi}_{eLi}\phi_i e_R - \tilde{h}_1\epsilon_{ij}\bar{\psi}_{eLi}\phi^j\nu_{eR} - h_2\bar{\Psi}_{Li\alpha}\phi_i E_{R\alpha} - \tilde{h}_2\epsilon_{ij}\bar{\Psi}_{Li\alpha}\phi^j N_{R\alpha} - k_2\bar{\Psi}_{Li\alpha}\eta^\beta_{i\alpha}E_{R\beta}\\
&- \tilde{k}_2\epsilon_{ij}\bar{\Psi}_{Li\alpha}\eta^{j\beta}_\alpha N_{R\beta} - h_3\bar{\psi}_{\tau Li}\phi_i\tau_R - \tilde{h}_3\epsilon_{ij}\bar{\psi}_{\tau Li}\phi^j\nu_{\tau R} + \mathrm{h.c.}
\end{aligned}
\tag{2.7}
$$

after corresponding scalars take their vevs as defined in eq. (2.2), we obtain

$$
\begin{aligned}
\mathcal{L}_Y = &-h_1\bar{\psi}_{eL2}\langle\phi\rangle e_R - \tilde{h}_1\bar{\psi}_{eL1}\langle\phi\rangle\nu_{eR} - \bar{\Psi}_{L2\alpha}[h_2\langle\phi\rangle + k_2\langle\eta\rangle(\delta_{\alpha 1} - \delta_{\alpha 2})]E_{R\alpha}\\
&- \bar{\Psi}_{L1\alpha}[\tilde{h}_2\langle\phi\rangle + \tilde{k}_2\langle\eta\rangle(\delta_{\alpha 1} - \delta_{\alpha 2})]N_{R\alpha} - h_3\bar{\psi}_{\tau L2}\langle\phi\rangle\tau_R - \tilde{h}_3\bar{\psi}_{\tau L1}\langle\phi\rangle\nu_{\tau R}\\
&- h_1\bar{\psi}_{eLi}\phi'_i e_R - \tilde{h}_1\epsilon_{ij}\bar{\psi}_{eLi}\phi'^j\nu_{eR} - \bar{\Psi}_{Li\alpha}[h_2\phi'_i\delta^\beta_\alpha + k_2\eta'^\beta_{i\alpha}]E_{R\beta}\\
&- \bar{\Psi}_{Li\alpha}[\tilde{h}_2\epsilon_{ij}\phi'^j\delta^\beta_\alpha + \tilde{k}_2\epsilon_{ij}\eta'^{j\beta}_\alpha]N_{R\beta} - h_3\bar{\psi}_{\tau Li}\phi'_i\tau_R - \tilde{h}_3\epsilon_{ij}\bar{\psi}_{\tau Li}\phi'^j\nu_{\tau R} + \mathrm{h.c.}
\end{aligned}
\tag{2.8}
$$

where ϕ'_i and $\eta'^\beta_{i\alpha}$ are the shifted fields. From eq. (2.8), we see that the muon and 4th generation leptons masses get split and are given by,

$$
\begin{aligned}
&m_e = h_1\langle\phi\rangle\,, \qquad m_\tau = h_3\langle\phi\rangle\,, \qquad m_{\nu_e} = \tilde{h}_1\langle\phi\rangle\,, \qquad m_{\nu_\tau} = \tilde{h}_3\langle\phi\rangle\\
&m_\mu = h_2\langle\phi\rangle + k_2\langle\eta\rangle\,, \qquad m_{\nu_\mu} = \tilde{h}_2\langle\phi\rangle + \tilde{k}_2\langle\eta\rangle\,,\\
&m_{\mu'} = h_2\langle\phi\rangle - k_2\langle\eta\rangle\,, \qquad m_{\nu_{\mu'}} = \tilde{h}_2\langle\phi\rangle - \tilde{k}_2\langle\eta\rangle
\end{aligned}
\tag{2.9}
$$

Thus by choosing the suitable values of Yukawas, the required leptons masses can be generated.

3 Dark matter phenomenology

In our model, we identify the 4th generation right-handed neutral lepton ($\nu'_{\mu_R} \equiv \chi$) as the dark matter, which is used to fit AMS-02 data [20, 21]. The only possible channels for DM annihilation are into ($\mu^+\mu^-$) and ($\nu^c_\mu\ \nu_\mu$) pairs (figure 1). In this scenario for getting the correct relic density, we use the Breit-Wigner resonant enhancement [31–33] and take $M_{\theta_3} \simeq 2m_\chi$. The annihilation CS can be tuned to be $\sim 10^{-26}\,\mathrm{cm^3\,s^{-1}}$ with the resonant enhancement, which gives the observed relic density. In principle the dark matter can decay into the light leptons via $\mathrm{SU(2)_{HV}}$ gauge boson θ^+ and scalar $\eta^\beta_{i\alpha}$, but by taking the mass of 4th generation charged leptons μ' larger than χ, the stability of dark matter can be ensured.

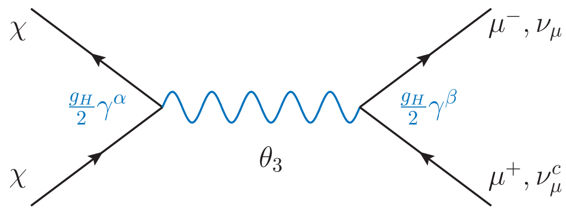

Figure 1. Feynman diagram of dark matter annihilation with corresponding vertex factor.

3.1 Relic density

The dark matter annihilation channels into standard model particles are, $\chi\chi \to \theta_3^* \to \mu^+\mu^-, \nu_\mu^c\nu_\mu$. The annihilation rate of dark matter σv, for a single channel, in the limit of massless leptons, is given by

$$\sigma v = \frac{1}{16\pi} \frac{g_H^4 m_\chi^2}{(s - M_{\theta_3}^2)^2 + \Gamma_{\theta_3}^2 M_{\theta_3}^2} \tag{3.1}$$

where g_H is the horizontal gauge boson coupling, m_χ the dark matter mass, M_{θ_3} and Γ_{θ_3} are the mass and the decay width of $\mathrm{SU(2)_{HV}}$ gauge boson respectively. Since both of the final states (ν_μ, μ) contribute in the relic density, the cross-section of eq. (3.1) is multiplied by a factor of 2 for relic density computation. The contributions to the decay width of θ_3 comes from the decay modes, $\theta_3 \to \mu^+\mu^-, \nu_\mu^c\nu_\mu$. The total decay width is given by,

$$\Gamma_{\theta_3} = \frac{2g_H^2}{48\pi} M_{\theta_3} \tag{3.2}$$

In the non-relativistic limit, $s = 4m_\chi^2(1 + v^2/4)$, then by taking into account the factor of 2, eq. (3.1) simplifies as,

$$\sigma v = \frac{2}{256\pi m_\chi^2} \frac{g_H^4}{(\delta + v^2/4)^2 + \gamma^2} \tag{3.3}$$

where δ and γ are defined as $M_{\theta_3}^2 \equiv 4m_\chi^2(1 - \delta)$, and $\gamma^2 \equiv \Gamma_{\theta_3}^2(1 - \delta)/4m_\chi^2$. If δ and γ are larger than $v^2 \simeq (T/M_\chi)^2$, the usual freeze-out takes place, on the other hand if δ and γ are chosen smaller than v^2 then there is a resonant enhancement of the annihilation CS and a late time freeze-out. We choose $\delta \sim 10^{-3}$ and $\gamma \sim 10^{-4}$, so that we have a resonant annihilation of dark matter. The thermal average of annihilation rate is given as [31–33],

$$\langle \sigma v \rangle (x) = \frac{1}{n_{\mathrm{EQ}}^2} \frac{m_\chi}{64\pi^4 x} \int_{4m_\chi^2}^{\infty} \hat{\sigma}(s) \sqrt{s} K_1\left(\frac{x\sqrt{s}}{m_\chi}\right) ds \tag{3.4}$$

where,

$$n_{\mathrm{EQ}}^2 = \frac{g_i}{2\pi^2} \frac{m_\chi^3}{x} K_2(x) \tag{3.5}$$

$$\hat{\sigma}(s) = 2g_i^2 m_\chi \sqrt{s - 4m_\chi^2}\, \sigma v \tag{3.6}$$

JHEP11(2014)133

and where $x \equiv m_\chi/T$; $K_1(x)$, $K_2(x)$ represent the modified Bessel functions of second type and g_i is the internal degree of freedom of DM particle. Using eq. (3.3), eq. (3.5) and eq. (3.6) in eq. (3.4), it can be written as,

$$\langle\sigma v\rangle(x) = \frac{g_H^4}{512 m_\chi^2}\frac{x^{3/2}}{\pi^{3/2}}\int_0^\infty \frac{\sqrt{z}\,\mathrm{Exp}[-xz/4]}{(\delta+z/4)^2+\gamma^2}dz \tag{3.7}$$

where $z \equiv v^2$. We solve the Boltzmann equation for $Y_\chi = n_\chi/s$,

$$\frac{dY_\chi}{dx} = -\frac{\lambda(x)}{x^2}\left(Y_\chi^2(x) - Y_{\chi\mathrm{eq}}^2(x)\right) \tag{3.8}$$

where

$$\lambda(x) \equiv \left(\frac{\pi}{45}\right)^{1/2} m_\chi M_{\mathrm{Pl}}\left(\frac{g_{*s}}{\sqrt{g_*}}\right)\langle\sigma v\rangle(x) \tag{3.9}$$

and where g_* and g_{*s} are the effective degrees of freedom of the energy density and entropy density respectively, with $\langle\sigma v\rangle$ given in eq. (3.7). We can write the $Y_\chi(x_0)$ at the present epoch as,

$$\frac{1}{Y_\chi(x_0)} = \frac{1}{Y_\chi(x_f)} + \int_{x_f}^{x_s} dx\frac{\lambda(x)}{x^2} \tag{3.10}$$

where the freeze-out x_f is obtained by solving $n_\chi(x_f)\langle\sigma v\rangle = H(x_f)$. We find that $x_f \sim 30$ and the relic density of χ is given by,

$$\Omega = \frac{m_\chi s_0 Y_\chi(x_0)}{\rho_c} \tag{3.11}$$

where $s_0 = 2890\,\mathrm{cm}^{-3}$ is the present entropy density and $\rho_c = h^2 1.9\times10^{-29}\,\mathrm{gm/cm}^3$ is the critical density. We find that by taking $g_H = 0.087$, $\delta \sim 10^{-3}$ and $\gamma \sim 10^{-4}$ in eq. (3.7), we obtain the correct relic density $\Omega h^2 = 0.1199 \pm 0.0027$, consistent with Planck [29] and WMAP [30] data. From g_H and γ we can fix $M_{\theta_3} \simeq 1400\,\mathrm{GeV}$ and $m_\chi \simeq \frac{1}{2}M_{\theta_3} \simeq 700\,\mathrm{GeV}$. There is a large hierarchy between the fourth generation charged fermion mass and the other charged leptons masses. We do not have any theory for the Yukawa couplings and we take the $m_{\mu'}$ mass which fits best the AMS-02 positron spectrum and muon $(g-2)$. A bench mark set of values used in this paper for the masses and couplings is given in table 2.

3.2 Comparison with AMS-02 and PAMELA data

The dark matter in the galaxy annihilates into $\mu^+\mu^-$ and the positron excess seen at AMS-02 [20, 21] appears from the decay of muon. We use publicly available code PPPC4DMID [38, 39] to compute the positron spectrum $\frac{dN_{e^+}}{dE}$ from the decay of μ pairs for 700 GeV dark matter. We then use the GALPROP code [40, 41] for propagation, in which we take the annihilation rate $\sigma v_{\mu^+\mu^-}$, and the positron spectrum $\frac{dN_{e^+}}{dE}$ as an input to the differential injection rate,

$$Q_{e^+}(E,\vec{r}) = \frac{\rho^2}{2m_\chi^2}\langle\sigma v\rangle_{\mu^+\mu^-}\frac{dN_{e^+}}{dE} \tag{3.12}$$

Parameters	Numerical values
g_H	0.087
y_h	0.037
y_A	0.020
$y_{H^\pm}$	0.1
m_χ	700 GeV
$m_{\mu'}$	740 GeV
M_{θ_3}	1400 GeV
M_{θ^+}	1400 GeV
$m_{H^\pm}$	1700 GeV
m_h	125 GeV
m_A	150 GeV
δ	10^{-3}
γ	10^{-4}

Table 2. Bench mark set of values used in the model.

where ρ denotes the density of dark matter in the Milky Way halo, which we take to be the NFW profile [42],

$$\rho_{\rm NFW} = \rho_0 \frac{r_s}{r}\left(1+\frac{r}{r_s}\right)^{-2}, \qquad \rho_0 = 0.4\,{\rm GeV/cm^3}, \qquad r_s = 20\,{\rm kpc} \tag{3.13}$$

In GALPROP code [40, 41], we take the diffusion coefficient $D_0 = 3.6\times10^{28}\,{\rm cm^2\,s^{-1}}$ and Alfven speed $v_A = 15\,{\rm Km\,s^{-1}}$. We choose, $z_h = 4\,{\rm kpc}$ and $r_{\rm max} = 20\,{\rm kpc}$, which are the half-width and maximum size for 2D galactic model respectively. We choose the nucleus spectral index breaks at 9 GeV and spectral index above this is 2.36 and below is 1.82. The normalization flux of electron at 100 GeV is $1.25\times10^{-8}\,{\rm cm^{-2}\,s^{-1}\,sr^{-1}\,GeV^{-1}}$ and for the case of electron, we take breaking point at 4 GeV and its injection spectral index above 4 GeV is $\gamma_1^{\rm el} = 2.44$ and below $\gamma_0^{\rm el} = 1.6$. After solving the propagation equation, GALPROP [40, 41] gives the desired positron flux.

To fit the AMS-02 data, the input annihilation CS required in GALPROP is, $\sigma v_{\chi\chi\to\mu^+\mu^-} = 2.33\times10^{-25}\,{\rm cm^3\,s^{-1}}$. The annihilation CS for μ final state from eq. (3.1) is, $\sigma v \approx 2.8\times10^{-25}\,{\rm cm^3\,s^{-1}}$, which signifies that there is no extra "astrophysical" boost factor needed to satisfy AMS-02 data. The annihilation rate required for relic density was $\langle\sigma v\rangle \sim 3\times10^{-26}\,{\rm cm^3/sec}$ and the factor ~ 10 increase in σv at the present epoch is due to resonant enhancement by taking $m_\chi \simeq \frac{1}{2}M_{\theta_3}$. In figure 2, we plot the output of GALPROP code and compare it with the observed AMS-02 [20, 21] and PAMELA [22] data. We see that our positron spectrum fits the AMS-02 data [20, 21] very well. We also check the photon production from the decay of μ final state by generating the γ-ray spectrum called $\frac{dN_\gamma}{dE}$ from publicly available code PPPC4DMID [38, 39] and propagating it through the GALPROP code [40, 41]. We then compare the output with the observed Fermi-LAT data [43], as shown in figure 3, and find that the γ-ray does not exceed the observed limits.

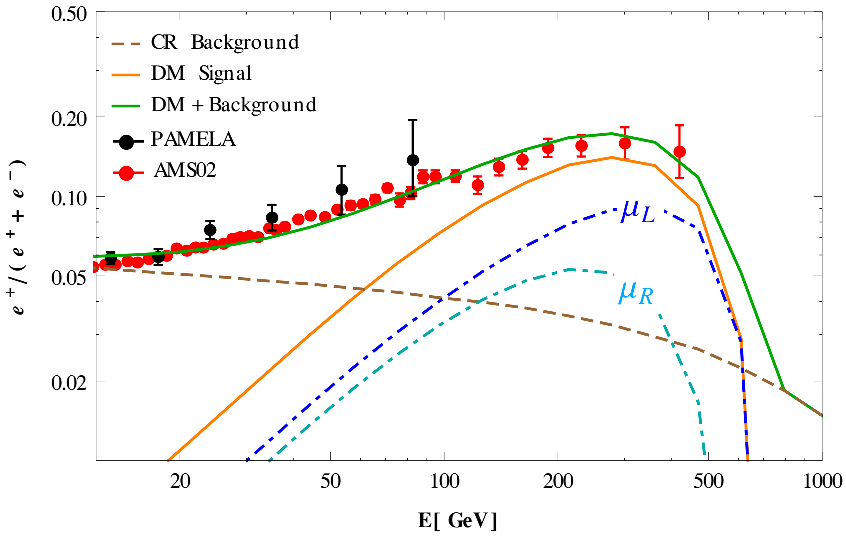

Figure 2. The positron flux spectrum compared with data from AMS-02 [20, 21] and PAMELA [22]. The contributions of different channels (μ_L, μ_R) are shown for comparison.

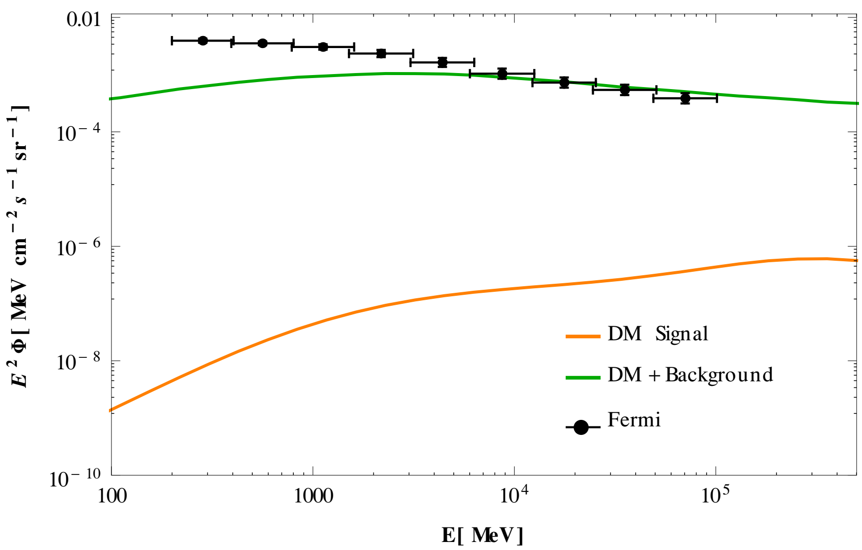

Figure 3. The γ-ray spectrum compared with data from Fermi Lat [43].

There is no annihilation to hadrons, so no excess of antiprotons are predicted, consistent with the PAMELA [25] and AMS-02 [26] data.

4 Muon magnetic moment

The SU$(2)_{\mathrm{HV}}$ horizontal symmetry, which connects muon and 4th generation families, gives extra contributions to muon $(g-2)$. The diagrams that contribute to muon $(g-2)$ with SU$(2)_{\mathrm{HV}}$ charged gauge boson θ^+ and scalar $\eta^{\beta}_{i\alpha}$ are shown in figure 4.

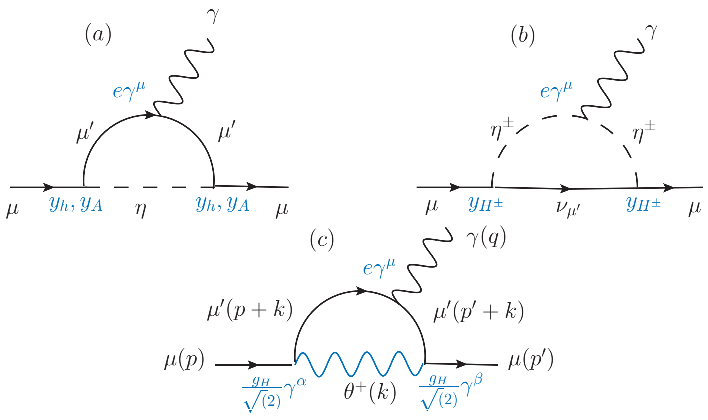

Figure 4. Feynman diagrams of scalar $\eta^{\beta}_{i\alpha}$ and $SU(2)_{HV}$ gauge boson θ^{+}, which give contributions to muon $(g-2)$.

We first calculate the contribution from $SU(2)_{HV}$ gauge boson θ^{+}, which is shown in figure 4(c). For this diagram the vertex factor of the amplitude $\mu(p')\Gamma_{\mu}\mu(p)\epsilon^{\mu}$ is,

$$\Gamma_{\mu} = \frac{eg_H^2}{2}\int\frac{d^4k}{(2\pi)^4}\gamma^{\beta}\frac{(\not{p}' + \not{k} + m_{\mu'})}{(p'+k)^2 - m_{\mu'}^2}\gamma_{\mu}\frac{(\not{p} + \not{k} + m_{\mu'})}{(p+k)^2 - m_{\mu'}^2}\gamma^{\alpha}\frac{g_{\alpha\beta}}{k^2 - M_{\theta+}^2} \tag{4.1}$$

we perform the integration and use the Gorden identity to replace,

$$(p_{\mu} + p'_{\mu}) = 2m_{\mu}\gamma_{\mu} + i\sigma^{\mu\nu}q_{\nu} \tag{4.2}$$

and identify the coefficient of the $i\sigma^{\mu\nu}q_{\nu}$ as the magnetic form factor. The contribution to Δa_{μ} is,

$$[\Delta a_{\mu}]_{\theta+} = \frac{m_{\mu}^2}{16\pi^2}\int_0^1 dx\frac{g_H^2\left(\frac{2m'_{\mu}}{m_{\mu}}(x-x^2) - (x-x^3)\right)}{(1-x)m_{\mu'}^2 - x(1-x)m_{\mu}^2 + xM_{\theta\pm}^2} \tag{4.3}$$

In the limit of $M_{\theta+}^2 \gg m_{\mu'}^2$, we get the anomalous magnetic moment,

$$[\Delta a_{\mu}]_{\theta+} = \frac{g_H^2}{8\pi^2}\left(\frac{m_{\mu}m_{\mu'} - 2/3m_{\mu}^2}{M_{\theta+}^2}\right) \tag{4.4}$$

we note that in eq. (4.4), the first term is dominant which shows $m_{\mu}m_{\mu'}$ enhancement in the muon $(g-2)$.

In our model, the contribution from the neutral higgs η (CP-even h and CP-odd A) is shown in figure 4(a). The $(g-2)$ contribution of this diagram is [44],

$$\begin{aligned}[\Delta a_{\mu}]_{h,A} = &\frac{m_{\mu}^2}{8\pi^2}\int_0^1 dx\frac{y_h^2\left(x^2 - x^3 + \frac{m_{\mu'}}{m_{\mu}}x^2\right)}{m_{\mu}^2x^2 + (m_{\mu'}^2 - m_{\mu}^2)x + m_h^2(1-x)}\\ &+ \frac{m_{\mu}^2}{8\pi^2}\int_0^1 dx\frac{y_A^2\left(x^2 - x^3 - \frac{m_{\mu'}}{m_{\mu}}x^2\right)}{m_{\mu}^2x^2 + (m_{\mu'}^2 - m_{\mu}^2)x + m_A^2(1-x)}\end{aligned} \tag{4.5}$$

where y_h, y_A represent the Yukawa couplings of neutral CP-even and odd higgs respectively and their masses are denoted by m_h and m_A respectively. We shall calculate the contributions from the lightest scalars only, which give the larger contributions in compare to heavy scalars. In the limits $m_{\mu'}^2 \gg m_h^2$, $m_{\mu'}^2 \gg m_A^2$, doing the integration in eq. (4.5) we get the anomalous magnetic moment,

$$[\Delta a_\mu]_{h,A} = \frac{1}{8\pi^2}\left(\frac{3m_\mu m_{\mu'}(y_h^2 - y_A^2) + m_\mu^2(y_h^2 + y_A^2)}{6m_{\mu'}^2}\right) \tag{4.6}$$

In a similar way, the contribution from the mass eigenstate $H^\pm$ of charged higgs $\eta^\pm$, shown in figure 4(b), is given by [44],

$$[\Delta a_\mu]_{H^\pm} = \frac{m_\mu^2}{8\pi^2}\int_0^1 dx \frac{y_{H^\pm}^2\left(x^3 - x^2 + \frac{m_{\nu_{\mu'}}}{m_\mu}(x^2 - x)\right)}{m_\mu^2 x^2 + (m_{H^\pm}^2 - m_\mu^2)x + m_{\nu_{\mu'}}^2(1-x)} \tag{4.7}$$

where $y_{H^\pm}$ and $m_{H^\pm}$ are the Yukawa coupling and mass of the charged higgs respectively. We perform the integration (eq. (4.7)) in the limit $m_{H^\pm}^2 \gg m_{\nu_{\mu'}}^2$, and get the anomalous magnetic moment,

$$[\Delta a_\mu]_{H^\pm} = -\frac{y_{H^\pm}^2}{8\pi^2}\left(\frac{3m_\mu m_{\nu_{\mu'}} + m_\mu^2}{6m_{H^\pm}^2}\right) \tag{4.8}$$

So the complete contribution to muon $(g-2)$ in our model is given as,

$$\Delta a_\mu = [\Delta a_\mu]_{\theta^+} + [\Delta a_\mu]_{h,A} + [\Delta a_\mu]_{H^\pm} \tag{4.9}$$

As discussed before, in our model the lightest CP-even scalar h_1 is mainly composed of η, so we can write,

$$y_h \sim k_2 \cos\alpha_1 \tag{4.10}$$

where α_1 is the mixing angle between CP-even mass eigenstate h_1 and gauge eigenstate η, and k_2 is the Yukawa coupling defined in eq. (2.8). In the similar way, we assume that lightest pseudoscalar A and charged higgs $H^\pm$ are also mainly composed of η, so that we can write

$$y_A \sim k_2 \cos\alpha_2\,, \qquad y_{H^\pm} \sim \tilde{k}_2 \cos\alpha_3 \tag{4.11}$$

where α_2 is the mixing angle between CP-odd scalars and α_3 is the mixing angle between the charged scalars. $\tilde{k}_2$ denotes the Yukawa coupling defined in eq. (2.8).

In the $\mathrm{SU}(2)_H$ gauge boson sector, we take $g_H = 0.087$, $M_{\theta^+} \approx 1400\,\mathrm{GeV}$ ($M_{\theta_3} \approx M_{\theta^+}$), which are fixed from the requirement of correct relic density and we take $m_{\mu'} = 740\,\mathrm{GeV}$, coming from the stability requirement of dark matter ($m_{\mu'} > m_\chi$). After doing numerical calculation, we get $[\Delta a]_{\theta^+} = 3.61 \times 10^{-9}$.

The contribution from (h, A) scalars depend on the parameter $k_2^2\,(\cos^2\alpha_1 - \cos^2\alpha_2)$, which we assume to be $\simeq 10^{-3}$ and obtain $[\Delta a_\mu]_{h,A} = 0.82 \times 10^{-9}$. For the charged scalar contribution, we assume $\tilde{k}_2 \cos\alpha_3 = 0.1$ and $m_{H^\pm} = 1700\,\mathrm{GeV}$ and obtain $[\Delta a_\mu]_{H^\pm} = -1.53 \times 10^{-9}$. Adding the contributions from θ^+, (h, A) and $H^\pm$, we get

$$\Delta a_\mu = 2.9 \times 10^{-9} \tag{4.12}$$

JHEP11(2014)133

which is in agreement with the experimental result [1, 2] within 1σ. To get the desired value of muon $(g-2)$, we have to consider a large hierarchy between the neutral higgs ($m_h \sim 125\,\text{GeV}$, $m_A \sim 150\,\text{GeV}$) and the charged higgs $m_{H^\pm} \sim 1700\,\text{GeV}$. These masses have to arise by appropriate choices of the couplings in the higgs potential of $(\phi_i,\ \eta^\beta_{i\alpha},\ \chi_\alpha)$.

5 Result and discussion

We studied a 4th generation extension of the standard model, where the 4th generation leptons interact with the muon family via $\text{SU}(2)_{\text{HV}}$ gauge bosons. The 4th generation right-handed neutrino is identified as the dark matter. We proposed a common explanation to the excess of positron seen at AMS-02 [20, 21] and the discrepancy between SM prediction [3–9] and BNL measurement [1, 2] of muon $(g-2)$. The $\text{SU}(2)_{\text{HV}}$ gauge boson θ^+ with 4th generation charged lepton μ' and charged higgs $H^\pm$, give the required contribution to muon $(g-2)$ to satisfy the BNL measurement [1, 2] within 1σ. The LHC constraints on 4th generation quarks is evaded by extending the higgs sector as in [35, 36]. In our horizontal $\text{SU}(2)_{\text{HV}}$ gauge symmetry model, we also explain the preferential annihilation of dark matter to $\mu^+\mu^-$ channel over other leptons and predict that there is no antiproton excess, in agreement with PAMELA [25] and AMS-02 [26] data. Since the dark matter has gauge interactions only with the muon family at tree level, we can evade the bounds from direct detection experiments [45, 46] based on scattering of dark matter with the first generation quarks.

References

[1] Muon G-2 collaboration, G.W. Bennett et al., *Final report of the E821 muon anomalous magnetic moment measurement at BNL*, *Phys. Rev.* **D 73** (2006) 072003 [hep-ex/0602035] [inSPIRE].

[2] Muon (g-2) collaboration, G.W. Bennett et al., *An improved limit on the muon electric dipole moment*, *Phys. Rev.* **D 80** (2009) 052008 [arXiv:0811.1207] [inSPIRE].

[3] T. Aoyama, M. Hayakawa, T. Kinoshita and M. Nio, *Complete tenth-order QED contribution to the muon $g-2$*, *Phys. Rev. Lett.* **109** (2012) 111808 [arXiv:1205.5370] [inSPIRE].

[4] C. Gnendiger, D. Stöckinger and H. Stöckinger-Kim, *The electroweak contributions to $(g-2)_\mu$ after the Higgs boson mass measurement*, *Phys. Rev.* **D 88** (2013) 053005 [arXiv:1306.5546] [inSPIRE].

[5] M. Davier, A. Hoecker, B. Malaescu and Z. Zhang, *Reevaluation of the hadronic contributions to the muon $g-2$ and to $\alpha(M_Z^2)$*, *Eur. Phys. J.* **C 71** (2011) 1515 [*Erratum ibid.* **C 72** (2012) 1874] [arXiv:1010.4180] [inSPIRE].

[6] K. Hagiwara, R. Liao, A.D. Martin, D. Nomura and T. Teubner, *$(g-2)_\mu$ and $\alpha(M_Z^2)$ re-evaluated using new precise data*, *J. Phys.* **G 38** (2011) 085003 [arXiv:1105.3149] [inSPIRE].

[7] M. Benayoun, P. David, L. DelBuono and F. Jegerlehner, *An update of the HLS estimate of the muon $g-2$*, *Eur. Phys. J.* **C 73** (2013) 2453 [arXiv:1210.7184] [INSPIRE].

[8] T. Blum et al., *The muon $(g-2)$ theory value: present and future*, arXiv:1311.2198 [INSPIRE].

[9] J.P. Miller, E. de Rafael, B.L. Roberts and D. Stöckinger, *Muon $(g-2)$: experiment and theory*, *Ann. Rev. Nucl. Part. Sci.* **62** (2012) 237 [INSPIRE].

[10] Particle Data Group collaboration, J. Beringer et al., *Review of particle physics*, *Phys. Rev.* **D 86** (2012) 010001 [INSPIRE].

[11] T. Moroi, *The Muon anomalous magnetic dipole moment in the minimal supersymmetric standard model*, *Phys. Rev.* **D 53** (1996) 6565 [*Erratum ibid.* **D 56** (1997) 4424] [hep-ph/9512396] [INSPIRE].

[12] D. Stöckinger, *The muon magnetic moment and supersymmetry*, *J. Phys.* **G 34** (2007) R45 [hep-ph/0609168] [INSPIRE].

[13] S. Baek, N.G. Deshpande, X.G. He and P. Ko, *Muon anomalous $g-2$ and gauged $L_\mu - L_\tau$ models*, *Phys. Rev.* **D 64** (2001) 055006 [hep-ph/0104141] [INSPIRE].

[14] F.S. Queiroz and W. Shepherd, *New physics contributions to the muon anomalous magnetic moment: a numerical code*, *Phys. Rev.* **D 89** (2014) 095024 [arXiv:1403.2309] [INSPIRE].

[15] P. Agrawal, Z. Chacko and C.B. Verhaaren, *Leptophilic dark matter and the anomalous magnetic moment of the muon*, *JHEP* **08** (2014) 147 [arXiv:1402.7369] [INSPIRE].

[16] Y. Bai and J. Berger, *Lepton portal dark matter*, *JHEP* **08** (2014) 153 [arXiv:1402.6696] [INSPIRE].

[17] A. Freitas, J. Lykken, S. Kell and S. Westhoff, *Testing the muon $g-2$ anomaly at the LHC*, *JHEP* **05** (2014) 145 [*Erratum ibid.* **09** (2014) 155] [arXiv:1402.7065] [INSPIRE].

[18] C.D. Carone, *Flavor-nonuniversal dark gauge bosons and the muon $g-2$*, *Phys. Lett.* **B 721** (2013) 118 [arXiv:1301.2027] [INSPIRE].

[19] S. Bar-Shalom, S. Nandi and A. Soni, *Muon $g-2$ and lepton flavor violation in a two Higgs doublets model for the fourth generation*, *Phys. Lett.* **B 709** (2012) 207 [arXiv:1112.3661] [INSPIRE].

[20] AMS collaboration, M. Aguilar et al., *First result from the Alpha Magnetic Spectrometer on the International Space Station: precision measurement of the positron fraction in primary cosmic rays of 0.5–350 GeV*, *Phys. Rev. Lett.* **110** (2013) 141102 [INSPIRE].

[21] AMS collaboration, L. Accardo et al., *High statistics measurement of the positron fraction in primary cosmic rays of 0.5–500 GeV with the Alpha Magnetic Spectrometer on the International Space Station*, *Phys. Rev. Lett.* **113** (2014) 121101 [INSPIRE].

[22] PAMELA collaboration, O. Adriani et al., *An anomalous positron abundance in cosmic rays with energies 1.5–100 GeV*, *Nature* **458** (2009) 607 [arXiv:0810.4995] [INSPIRE].

[23] M. Das and S. Mohanty, *Leptophilic dark matter in gauged $L_\mu - L_\tau$ extension of MSSM*, *Phys. Rev.* **D 89** (2014) 025004 [arXiv:1306.4505] [INSPIRE].

[24] A. De Simone, A. Riotto and W. Xue, *Interpretation of AMS-02 results: correlations among dark matter signals*, *JCAP* **05** (2013) 003 [arXiv:1304.1336] [INSPIRE].

[25] PAMELA collaboration, O. Adriani et al., *PAMELA results on the cosmic-ray antiproton flux from 60 MeV to 180 GeV in kinetic energy*, *Phys. Rev. Lett.* **105** (2010) 121101 [arXiv:1007.0821] [INSPIRE].

[26] AMS-02 collaboration, http://www.ams02.org/.

JHEP11(2014)133

[27] S. Baek and P. Ko, *Phenomenology of* $\mathrm{U}(1)_{L_\mu - L_\tau}$ *charged dark matter at PAMELA and colliders*, *JCAP* **10** (2009) 011 [arXiv:0811.1646] [INSPIRE].

[28] P.S.B. Dev, D.K. Ghosh, N. Okada and I. Saha, *Neutrino mass and dark matter in light of recent AMS-02 results*, *Phys. Rev.* **D 89** (2014) 095001 [arXiv:1307.6204] [INSPIRE].

[29] PLANCK collaboration, P.A.R. Ade et al., *Planck 2013 results. XVI. Cosmological parameters*, *Astron. Astrophys.* **571** (2014) A16 [arXiv:1303.5076] [INSPIRE].

[30] WMAP collaboration, G. Hinshaw et al., *Nine-year Wilkinson Microwave Anisotropy Probe (WMAP) observations: cosmological parameter results*, *Astrophys. J. Suppl.* **208** (2013) 19 [arXiv:1212.5226] [INSPIRE].

[31] M. Ibe, H. Murayama and T.T. Yanagida, *Breit-Wigner enhancement of dark matter annihilation*, *Phys. Rev.* **D 79** (2009) 095009 [arXiv:0812.0072] [INSPIRE].

[32] W.-L. Guo and Y.-L. Wu, *Enhancement of dark matter annihilation via Breit-Wigner resonance*, *Phys. Rev.* **D 79** (2009) 055012 [arXiv:0901.1450] [INSPIRE].

[33] X.-J. Bi, X.-G. He and Q. Yuan, *Parameters in a class of leptophilic models from PAMELA, ATIC and FERMI*, *Phys. Lett.* **B 678** (2009) 168 [arXiv:0903.0122] [INSPIRE].

[34] E. Witten, *An* SU(2) *anomaly*, *Phys. Lett.* **B 117** (1982) 324 [INSPIRE].

[35] S. Bar-Shalom, S. Nandi and A. Soni, *Two Higgs doublets with 4th generation fermions: models for TeV-scale compositeness*, *Phys. Rev.* **D 84** (2011) 053009 [arXiv:1105.6095] [INSPIRE].

[36] X.-G. He and G. Valencia, *An extended scalar sector to address the tension between a fourth generation and Higgs searches at the LHC*, *Phys. Lett.* **B 707** (2012) 381 [arXiv:1108.0222] [INSPIRE].

[37] C.L. Ong, *A study of a model with horizontal gauge symmetry at one loop level*, *Phys. Rev.* **D 22** (1980) 2886 [INSPIRE].

[38] M. Cirelli et al., *PPPC 4 DM ID: a poor particle physicist cookbook for dark matter indirect detection*, *JCAP* **03** (2011) 051 [*Erratum ibid.* **10** (2012) E01] [arXiv:1012.4515] [INSPIRE].

[39] P. Ciafaloni et al., *Weak corrections are relevant for dark matter indirect detection*, *JCAP* **03** (2011) 019 [arXiv:1009.0224] [INSPIRE].

[40] A.W. Strong, I.V. Moskalenko and V.S. Ptuskin, *Cosmic-ray propagation and interactions in the galaxy*, *Ann. Rev. Nucl. Part. Sci.* **57** (2007) 285 [astro-ph/0701517] [INSPIRE].

[41] I.V. Moskalenko and A.W. Strong, *Production and propagation of cosmic ray positrons and electrons*, *Astrophys. J.* **493** (1998) 694 [astro-ph/9710124] [INSPIRE].

[42] J.F. Navarro, C.S. Frenk and S.D.M. White, *The structure of cold dark matter halos*, *Astrophys. J.* **462** (1996) 563 [astro-ph/9508025] [INSPIRE].

[43] FERMI-LAT collaboration, A.A. Abdo et al., *The spectrum of the isotropic diffuse gamma-ray emission derived from first-year Fermi Large Area Telescope data*, *Phys. Rev. Lett.* **104** (2010) 101101 [arXiv:1002.3603] [INSPIRE].

[44] J.P. Leveille, *The second order weak correction to* $(g-2)$ *of the muon in arbitrary gauge models*, *Nucl. Phys.* **B 137** (1978) 63 [INSPIRE].

[45] XENON100 collaboration, E. Aprile et al., *Dark matter results from 225 live days of XENON100 data*, *Phys. Rev. Lett.* **109** (2012) 181301 [arXiv:1207.5988] [INSPIRE].

[46] LUX collaboration, D.S. Akerib et al., *First results from the LUX dark matter experiment at the Sanford Underground Research Facility*, *Phys. Rev. Lett.* **112** (2014) 091303 [arXiv:1310.8214] [INSPIRE].

JHEP11(2014)133

Published for SISSA by Springer

Received: *July 20, 2015*
Revised: *September 9, 2015*
Accepted: *October 14, 2015*
Published: *November 5, 2015*

Lorentz invariance violation and IceCube neutrino events

Gaurav Tomar,[a,b] **Subhendra Mohanty**[a] **and Sandip Pakvasa**[c]

[a] *Physical Research Laboratory, Ahmedabad, 380009 India*
[b] *Indian Institute of Technology, Gandhinagar, 382424 India*
[c] *Department of Physics & Astronomy, University of Hawaii, Honolulu, HI, 96822 U.S.A.*

E-mail: tomar@prl.res.in, mohanty@prl.res.in, pakvasa@phys.hawaii.edu

Abstract: The IceCube neutrino spectrum shows a flux which falls of as E^{-2} for sub PeV energies but there are no neutrino events observed above ~ 3 PeV. In particular the Glashow resonance expected at 6.3 PeV is not seen. We examine a Planck scale Lorentz violation as a mechanism for explaining the cutoff of observed neutrino energies around a few PeV. By choosing the one free parameter the cutoff in neutrino energy can be chosen to be between 2 and 6.3 PeV. We assume that neutrinos (antineutrinos) have a dispersion relation $E^2 = p^2 - (\xi_3/M_{\rm Pl})\ p^3$, and find that both π^+ and π^- decays are suppressed at neutrino energies of order of few PeV. We find that the μ^- decay being a two-neutrino process is enhanced, whereas μ^+ decay is suppressed. The $K^+ \to \pi^0 e^+ \nu_e$ is also suppressed with a cutoff neutrino energy of same order of magnitude, whereas $K^- \to \pi^0 e^- \bar{\nu}_e$ is enhanced. The $n \to p^+ e^- \bar{\nu}_e$ decay is suppressed (while the $\bar{n} \to p^- e^+ \nu_e$ is enhanced). This means that the $\bar{\nu}_e$ expected from n decay arising from $p + \gamma \to \Delta \to \pi^+ n$ reaction will not be seen. This can explain the lack of Glashow resonance events at IceCube. If no Glashow resonance events are seen in the future then the Lorentz violation can be a viable explanation for the IceCube observations at PeV energies.

Keywords: Cosmology of Theories beyond the SM, Neutrino Physics, Beyond Standard Model

ArXiv ePrint: 1507.03193

doi:10.1007/JHEP11(2015)022

Contents

1 Introduction

IceCube collaboration has observed the neutrinos of very high energy going to beyond 2.6 PeV [1–4]. The IceCube data in the energy range 60 TeV to ~ 3 PeV is consistent with E_ν^{-2} neutrino spectrum following $E_\nu^2 dN_\nu/dE_\nu \simeq 1.2 \times 10^{-8}$ GeVcm^{-2}s^{-1}sr^{-1} [2, 3]. A neutrino spectrum sharper than $E^{-2.3}$ does not give a good fit to the data [3]. There are no neutrino events observed above ~ 3 PeV.

In particular, there is no evidence of Glashow resonance [5], $\bar{\nu}_e + e^- \to W^- \to$ shower, which is expected at $E = 6.3$ PeV. Glashow resonance gives rise to an enhanced cross-section for $\bar{\nu}_e$ at resonance energy $E = M_W^2/2m_e = 6.3$ PeV, which increases the detection rate of $\nu_e + \bar{\nu}_e$ by a factor of ~ 10 [2]. This implies that at least three events should have been observed at Glashow resonance, but none were.

The Glashow resonance gives rise to multiple energy peaks at different energies [6]. The first one is at 6.3 PeV and others lie at the $E_{\text{vis}} = E - E_X$, where E_X is the energy in the W decay, which does not contribute to the visible shower [7]. The decay of W into hadrons goes as $W \to \bar{q}q$, giving rise to a peak at 6.3 PeV, while decay into leptons goes as $W \to \bar{\nu}l$, which means W boson will lose half of its energy and so a second peak at 3.2 PeV is expected. In case of τ lepton in the final state, a further decay takes place producing a neutrino and thus a third peak at 1.6 PeV. The events observed by IceCube [1–4] between 1 PeV to ~ 3 PeV range may be associated with the second (leptonic decay of W) and third peak (τ decay), but non-appearance of Glashow resonance hadronic shower from $W \to \bar{q}q$ at 6.3 PeV (dominant peak) makes this idea less attractive. The non observation of the expected signature of Glashow resonance in IceCube data indicates a cutoff of neutrino energies between 2–6.3 PeV [7, 8].

In this paper, we propose a mechanism which can explain why neutrinos above a certain energy may be suppressed in the astrophysical production processes like $\pi \to \mu\nu_\mu$, $K \to \mu\nu_\mu$ etc. We assume that Lorentz violating higher dimensional operators [9, 10] give rise to a modified dispersion relation for the neutrinos (antineutrinos) of the form $E^2 = p^2 + m_\nu^2 - (\xi_n/M_{\rm Pl}^{n-2})\, p^n$ with $n > 2$. Depending on the sign of ξ_n, the neutrinos (antineutrinos) can be either superluminal ($\xi_n < 0$) or subluminal ($\xi_n > 0$). For the superluminal case, it has been shown [11, 12] that the presence of the extra terms in the dispersion results in a suppression of π and K decay widths. The phase space suppression for both the subluminal and superluminal dispersions for meson decay and the Cerenkov process $\nu \to \nu e^+ e^-$ has been noticed in [9, 13–16] with limits on Lorentz violation parameters from IceCube events. A comprehensive listing of Lorentz and CPT violating operators and their experimental constraints is given in [17]. In this paper, we calculate the π, K, μ and n decay processes in a fixed frame (the frame chosen being the one in which the CMBR is isotropic; although the Earth moves at a speed $v_{\rm Earth} \sim 300$ km/sec with respect to the CMBR, the Lorentz correction to the neutrino energy is small as $\beta_{\rm Earth} \sim 10^{-3}$), where the neutrinos (antineutrinos) dispersion relation is $E^2 = p^2 + m_\nu^2 - (\xi_3/M_{\rm Pl})\, p^3$ [10, 18–20]. We will have $\xi_3 > 0$ for neutrinos and $\xi_3 < 0$ for antineutrinos. In the π^+ decay, we find that the $\overline{|M|}^2$ is suppressed at neutrino energy E_ν, where $m_\pi^2 - m_\mu^2 \simeq (\xi_3/M_{\rm Pl})\, p_\nu^3$. This implies that for the leading order Planck suppression ($n = 3$) taking $\xi_3 \sim 0.05$, the π^+ decay is suppressed at $E_\nu \sim 1.3$ PeV. Similarly K^+ decay will be cutoff at $E_\nu \sim 2$ PeV with $m_K^2 - m_\mu^2 \sim (\xi_3/M_{\rm Pl}) p^3$ and neutron decay will be cutoff for p, where $(m_n - m_p)^2 \sim (\xi_3/M_{\rm Pl}) p^3$, which is lower than the Glashow resonance energy. For the π^- decay the $\overline{|M|}^2$ is enhanced but the phase space is suppressed and therefor $\pi^- \to \mu^- \nu_\mu$ is also suppressed. In the case of $\mu^- \to e^- \bar{\nu}_e \nu_\mu$ decay, $\overline{|M|}^2$ is enhanced whereas the phase space suppression is not significant, so the μ^- decay rate is enhanced (while $\mu^+ \to e^+ \nu_e \bar{\nu}_\mu$ decay rate is suppressed). This enhancement is significant at μ^- energies ~ 2 PeV but since the primary source of μ^- is π^- decay which is already cutoff, there will be no observable effect of this enhancement in the neutrino spectrum seen at IceCube. Neutrinos from $K^- \to \mu^- \bar{\nu}_\mu$ and $K^+ \to \mu^+ \nu_\mu$ decays will be cutoff at slightly higher energies. Radiative $\pi^\pm$ decay with a single neutrino in the outgoing state are also suppressed. The three body kaon decay rate are determined by the ξ_3 dependence of $\overline{|M|}^2$ and we find that $K^+ \to \pi^0 \mu^+ \nu_\mu$ decay is suppressed but $K^- \to \pi^0 \mu^- \bar{\nu}_\mu$ decay is enhanced. Neutron beta decay $n \to p^+ e^- \bar{\nu}_e$ gets suppressed in the same way as μ^+ decay. If the source of $\bar{\nu}_e$ is neutron beta-decay [21] then the mechanism proposed in this paper can be used for explaining the absence of Glashow resonance [5] at IceCube. The value of $(\xi_3/M_{\rm Pl}) \sim 0.05\ M_{\rm pl}^{-1}$ used in this paper to explain the cutoff in PeV neutrinos is much smaller than the bound on the dimension-five coefficient, $(a_{\rm of}^{(5)})_{00} < 3.5 \times 10^{-10}\ {\rm GeV}^{-1}$ from SN1987A dispersion [13].

The rest of the paper is organized as follows. In section 2, we calculate the leptonic decay widths of pions and kaons using modified dispersion relation of neutrino and compare them with their standard model counterparts. In section 3 we study $\mu^- \to e^-\bar{\nu}_e\nu_\mu$, $K^+ \to \pi^0 e^+\nu_e$ and $n \to p^+e^-\bar{\nu}_e$ processes with modified neutrino dispersion. We give our conclusion in section 4.

2 Two body decays

2.1 Neutrino velocity with modified dispersion

To calculate the decay widths of pion, kaon and muon, we use the following dispersion relation,

$$E^2 = p^2 + m_\nu^2 - \frac{\xi_n}{M_{\rm Pl}^{n-2}}\, p^n \tag{2.1}$$

which is motivated by Lorentz violating higher dimensional operators [9, 10]. We will take $\xi_n > 0$ for neutrinos and $\xi_n < 0$ for antineutrinos. We use this modified dispersion relation to get the neutrino (antineutrino) velocity, which becomes

$$v = \frac{\partial E}{\partial p} = 1 - \frac{n-1}{2}\, \frac{\xi_n}{M_{\rm Pl}^{n-2}}\, p^{n-2}\,. \tag{2.2}$$

This is clear from eq. (2.2) that we have a subluminal neutrinos and superluminal antineutrinos. In this paper, we will consider the leading order Planck suppressed dispersion relation $E^2 = p^2+m_\nu^2-(\xi_3/M_{\rm Pl})\, p^3$ to compute the primary decay processes which produce neutrinos and antineutrinos. In appendix A, we obtained modified dispersion relations for neutrinos and antineutrinos using dimension 5 operator.

2.2 $\pi^+ \to \mu^+\nu_\mu$

We calculate the pion decay width using the modified dispersion relation for neutrino by taking $n = 3$ case. The amplitude calculation of pion decay process $\pi^+(q) \to \mu^+(p)\nu_\mu(k)$ gives,

$$M = f_\pi V_{ud}\; q^\mu \bar{u}(k)\frac{G_{\rm F}}{\sqrt{2}}\gamma_\mu(1-\gamma_5)v(p) \tag{2.3}$$

where $f_\pi \equiv f(m_\pi^2)$ is a constant factor and V_{ud} is the CKM matrix element. The spin averaged amplitude squared is,

$$\overline{|M|^2} = 2G_{\rm F}^2 f_\pi^2 |V_{ud}|^2 m_\mu^2 F(k)\left[m_\pi^2 - m_\mu^2 - \xi_3' k^3\left(\frac{m_\pi^2}{m_\mu^2}+2\right)\right] \tag{2.4}$$

where $\xi_3' \equiv \xi_3/M_{\rm Pl}$ and the $F(k)$ factor comes from the modified spinor relation of neutrino, as described in eq. (B.9). The decay width of pion is then given by,

$$\begin{aligned}\Gamma =& \frac{G_{\rm F}^2 f_\pi^2 |V_{ud}|^2 m_\mu^2 F(k)}{8\pi E_\pi}\int \frac{k^2\, dk\, d\cos\theta}{E_\nu\sqrt{|\vec{q}-\vec{k}|^2+m_\mu^2}}\delta(E_{\nu_\mu} - E_\pi + \sqrt{|\vec{q}-\vec{k}|^2+m_\mu^2})\\ &\times\left[m_\pi^2 - m_\mu^2 - \xi_3' k^3\left(\frac{m_\pi^2}{m_\mu^2}+2\right)\right]\end{aligned} \tag{2.5}$$

JHEP11(2015)022

after using $E_{\nu_\mu} = F(k)k$, and writing $|\vec{p}| = |\vec{q} - \vec{k}|^2 = k^2 + q^2 - 2kq\cos\theta$, our expression of eq. (2.5) takes the following form

$$\Gamma = \frac{G_F^2 f_\pi^2 |V_{ud}|^2 m_\mu^2}{8\pi E_\pi} \int \frac{k\,dk\,d\cos\theta}{\sqrt{|\vec{q}-\vec{k}|^2 + m_\mu^2}} \delta(E_{\nu_\mu} - E_\pi + \sqrt{|\vec{q}-\vec{k}|^2 + m_\mu^2}) \times \left[m_\pi^2 - m_\mu^2 - \xi_3' k^3 \left(\frac{m_\pi^2}{m_\mu^2} + 2\right)\right] \tag{2.6}$$

from the argument of the delta function in eq. (2.6), we have

$$\sqrt{|\vec{q}-\vec{k}|^2 + m_\mu^2} = E_\pi - E_{\nu_\mu} \tag{2.7}$$

which gives,

$$\cos\theta = \frac{(m_\mu^2 - m_\pi^2 + 2E_\pi k - E_\pi k^2 \xi_3' + k^3 \xi_3')}{2kq}. \tag{2.8}$$

We reduce the δ function in E_{ν_μ} to a δ function in $\cos\theta$ by taking,

$$\left|\frac{d}{d\cos\theta}(E_{\nu_\mu} - E_\pi + \sqrt{|\vec{q}-\vec{k}|^2 + m_\mu^2})\right| = \frac{kq}{\sqrt{k^2 + q^2 - 2kq\cos\theta + m_\mu^2}} \tag{2.9}$$

and substituting in eq. (2.6). We get the pion decay width,

$$\Gamma = \frac{G_F^2 f_\pi^2 |V_{ud}|^2 m_\mu^2}{8\pi E_\pi} \int \frac{dk}{q} \left[m_\pi^2 - m_\mu^2 - \xi_3' k^3 \left(\frac{m_\pi^2}{m_\mu^2} + 2\right)\right]. \tag{2.10}$$

We solve the integration in the limits of k, which are fixed by taking $\cos\theta = \pm 1$ in eq. (2.8),

$$k_{\rm max} = \frac{m_\pi^2 - m_\mu^2 + \xi_3' k_{\rm max}^2 (E_\pi - k_{\rm max})}{2(E_\pi - q)} \tag{2.11}$$

$$k_{\rm min} = \frac{m_\pi^2 - m_\mu^2 + \xi_3' k_{\rm min}^2 (E_\pi - k_{\rm min})}{2(E_\pi + q)} \tag{2.12}$$

solving these equations numerically, we get the allowed limits of neutrino momentum. We solve eq. (2.10) and then compare our result with the standard model result of pion decay in a moving frame, which is

$$\Gamma_{\rm SM}(\pi \to \mu\nu) = \frac{G_F^2 f_\pi^2 |V_{ud}|^2 m_\mu^2 m_\pi^2}{8\pi E_\pi} \left(1 - \frac{m_\mu^2}{m_\pi^2}\right)^2. \tag{2.13}$$

We compute the pion decay rate numerically for superluminal $\bar{\nu}_e$ ($\xi_3 < 0$) and subluminal ν_e ($\xi_3 > 0$) final states and obtain the following:

- For subluminal neutrino final state ($\xi_3 > 0$), the allowed phase space (eq. (2.11)–eq. (2.12)) goes up but the $\overline{|M|^2}$ (eq. (2.4)) is suppressed. There is a net suppression in $\Gamma(\pi^+ \to \mu^+\nu_\mu)$ as shown in figure 1 for $\xi_3 = 1.3 \times 10^{-2}$.

JHEP11(2015)022

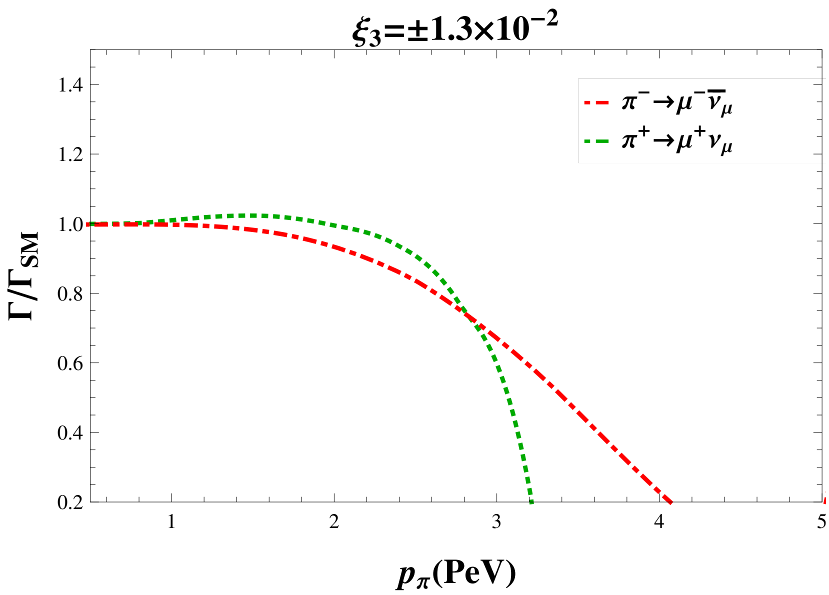

Figure 1. The ratio $\Gamma/\Gamma_{\rm SM}$ for $\pi^+ \to \mu^+\nu_\mu$ and $\pi^- \to \mu^-\bar{\nu}_\mu$ processes in Lorentz invariance violating framework to its standard model prediction for superluminal $\bar{\nu}_\mu$ ($\xi_3 < 0$) and subluminal ν_μ ($\xi_3 > 0$) final states as a function of pion momentum p_π. We considered $\xi_3 = \pm 1.3 \times 10^{-2}$ for corresponding processes.

- For superluminal antineutrino final state ($\xi_3 < 0$), the phase space (eq. (2.11)–eq. (2.12)) is suppressed but the $\overline{|M|^2}$ is enhanced. The net effect however is a suppression in the $\Gamma(\pi^- \to \mu^-\bar{\nu}_\mu)$ for this case also [11], as shown in figure 1 for $\xi_3 = -1.3 \times 10^{-2}$.

In figure 2, for the process $\pi^+ \to \mu^+\nu_\mu$, we show the maximum neutrino energy for different values of ξ_3 using the solution for q in terms of $k_{\rm max}$ and $k_{\rm min}$ from eq. (2.11)–(2.12) in eq. (2.10). We see that for $\xi_3 = 5.0 \times 10^{-2}$, the neutrino spectrum cutoff at $k_{\rm max} = 1.3\,\text{PeV}$. The upper limit of observed neutrino energy provides bound on the Lorentz invariance violation parameter ξ_3. In figure 3, we show the maximum neutrino energy $k_{\rm max}$, as a function of Lorentz invariance violation parameter ξ_3. This is clear from figure 3 that $k_{\rm max}$ goes down as ξ_3 increases.

2.3 $K^+ \to \mu^+\nu_\mu$

In the similar way like pion decay, we calculate the kaon decay width for the process $K^+(q) \to \mu^+(p)\nu_\mu(k)$, using the modified dispersion relation for neutrinos by taking $n = 3$ case. We get the kaon decay width,

$$\Gamma = \frac{G_{\rm F}^2 f_K^2 |V_{us}|^2 m_\mu^2}{8\pi E_K} \int \frac{dk}{q}\left[m_K^2 - m_\mu^2 - \xi_3' k^3 \left(\frac{m_K^2}{m_\mu^2} + 2\right)\right]. \tag{2.14}$$

In the same way like pion, we solve the integration in the limits of k by taking $\cos\theta = \pm 1$ which gives,

$$k_{\rm max} = \frac{m_K^2 - m_\mu^2 + \xi_3' k_{\rm max}^2 (E_K - k_{\rm max})}{2(E_K - q)} \tag{2.15}$$

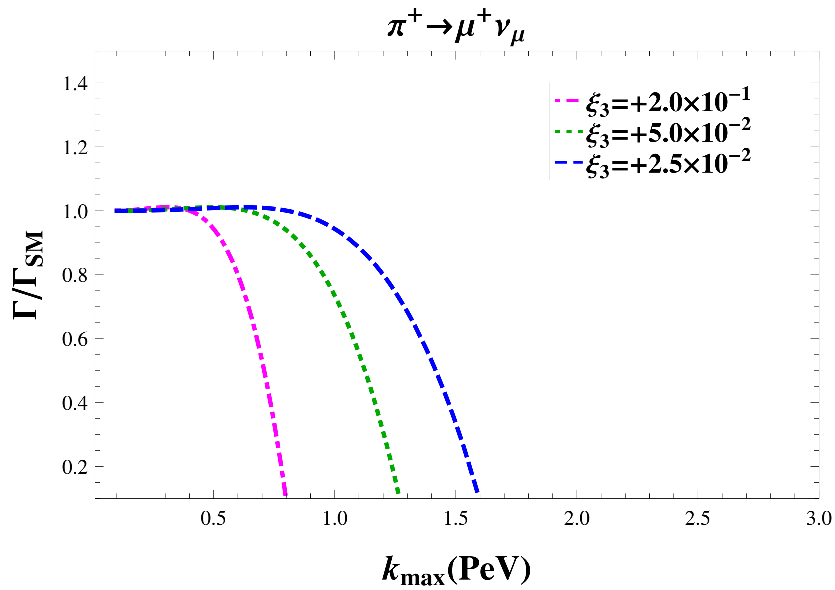

Figure 2. The ratio $\Gamma/\Gamma_{\mathrm{SM}}$ of $\pi^+ \to \mu^+\nu_\mu$ process in Lorentz invariance violating framework to its standard model prediction for subluminal neutrino ($\xi_3 > 0$) as a function of neutrino energy k_{max} with different values of ξ_3.

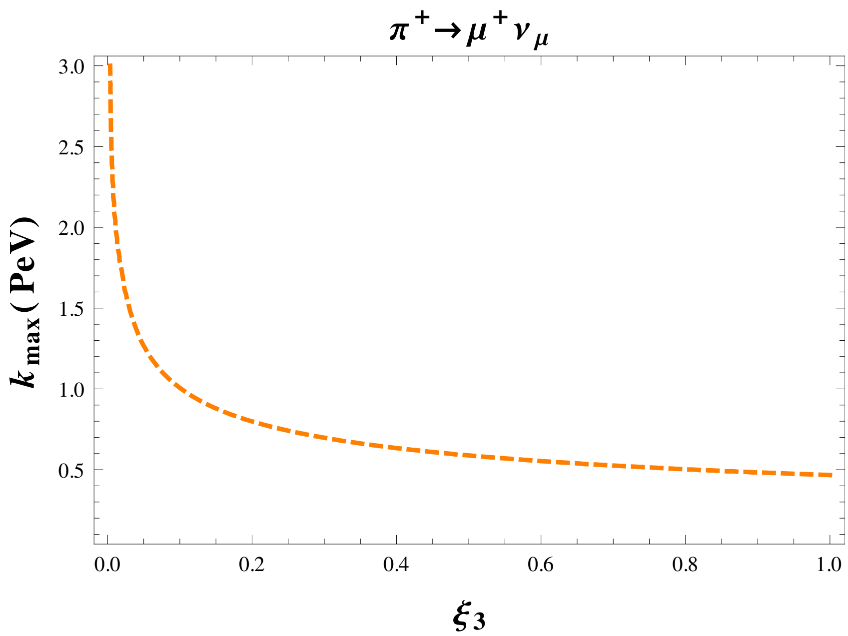

Figure 3. The maximum neutrino energy, k_{max} as a function of Lorentz invariance violation parameter ξ_3.

$$k_{\mathrm{min}} = \frac{m_K^2 - m_\mu^2 + \xi_3' k_{\mathrm{min}}^2 (E_K - k_{\mathrm{min}})}{2(E_K + q)} \tag{2.16}$$

solving these equations numerically, we get the allowed limits of neutrino momentum. We solve eq. (2.14) and then compare our result with the standard model result of kaon decay

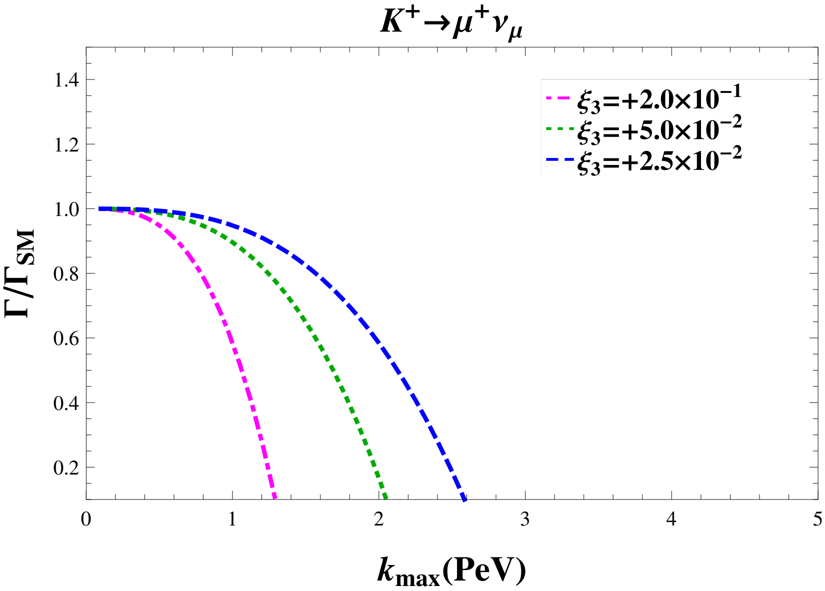

Figure 4. The ratio $\Gamma/\Gamma_{\rm SM}$ of $K^+ \to \mu^+\nu_\mu$ process in Lorentz invariance violating framework to its standard model prediction for subluminal neutrino ($\xi_3 > 0$) as a function of neutrino energy $k_{\rm max}$ with different values of ξ_3.

in a moving frame, which is

$$\Gamma_{\rm SM}(K \to \mu\nu) = \frac{G_{\rm F}^2 f_K^2 |V_{us}|^2 m_\mu^2 m_K^2}{8\pi E_K}\left(1 - \frac{m_\mu^2}{m_K^2}\right)^2 . \tag{2.17}$$

In figure 4, we show the maximum neutrino energy for different values of ξ_3 using the solution for q in terms of $k_{\rm max}$ and $k_{\rm min}$ from eq. (2.15)–(2.16) in eq. (2.14). We see that for $\xi_3 = 5.0 \times 10^{-2}$ the neutrino spectrum cutoff at $k_{\rm max} = 2\,\text{PeV}$.

3 Three body decays

3.1 $\mu^- \to e^-\bar{\nu}_e\nu_\mu$

We compute the muon decay width with subluminal neutrino and superluminal antineutrino in the final state, assuming the dispersion relation for the neutrino (antineutrino), $E_\nu^2 = k^2 - \xi_3' k^3$, where $\xi_3 > 0$ and $\xi_3 < 0$ correspond to subluminal neutrino and superluminal antineutrino respectively. We assume identical ξ_3 for all the species of ν (and $\bar{\nu}$) to avoid an extra source for neutrino oscillations which is not observed [16, 22]. The amplitude for the process $\mu^-(p) \to e^-(k')\bar{\nu}_e(k)\nu_\mu(p')$ is given as,

$$M = \frac{G_{\rm F}}{\sqrt{2}}[\bar{u}(k')\gamma^\mu(1-\gamma_5)v(k)][\bar{u}(p')\gamma_\mu(1-\gamma_5)u(p)] \tag{3.1}$$

where $G_{\rm F}$ is the Fermi constant. After squaring amplitude and solve it using trace technology, we get the spin averaged amplitude,

$$\overline{|M|^2} = 64G_{\rm F}^2(p\cdot k)(p'\cdot k') . \tag{3.2}$$

The decay width of muon is,

$$d\Gamma = \frac{d^3p'}{(2\pi)^3 2E_{\nu_\mu}} \frac{d^3k'}{(2\pi)^3 2E_e} \frac{d^3k}{(2\pi)^3 2E_{\bar{\nu}_e}} \frac{\overline{|M|^2}}{2E_\mu}(2\pi)^4\delta^4(p-p'-k'-k) \tag{3.3}$$

using the squared amplitude from eq. (3.2), we get

$$d\Gamma = \frac{32\ G_{\rm F}^2}{8(2\pi)^5 E_\mu} \frac{d^3k'}{E_e} \frac{d^3p'}{E_{\nu_\mu}} \frac{d^3k}{E_{\bar{\nu}_e}} \delta^4(p-p'-k'-k)(p\cdot k)(p'\cdot k')\,. \tag{3.4}$$

First we write eq. (3.4) as,

$$\Gamma = \frac{32\ G_{\rm F}^2}{8(2\pi)^5 E_\mu} \int \frac{d^3k'}{E_e} p^\alpha k'^\beta I_{\alpha\beta}(p-k') \tag{3.5}$$

where

$$I_{\alpha\beta}(p-k') \equiv \int \frac{d^3k}{E_{\bar{\nu}_e}} \frac{d^3p'}{E_{\nu_\mu}} \delta^4(p-p'-k'-k) k_\alpha p'_\beta \tag{3.6}$$

and then to find out $I_{\alpha\beta}(p-k')$, we use the generic phase space integral formula,

$$\begin{aligned} I_{\alpha\beta} \equiv \int \frac{d^3p}{\sqrt{m_2^2+\vec{p}\cdot\vec{p}}} \frac{d^3q}{\sqrt{m_1^2+\vec{q}\cdot\vec{q}}} \delta^4(k-p-q)p_\alpha q_\beta = \frac{I}{12k^4}(k^2[k^2-(m_1-m_2)^2] \\ [k^2-(m_1+m_2)^2]g_{\alpha\beta} + 2[k^4+k^2(m_1^2+m_2^2)-2(m_1^2-m_2^2)^2]k_\alpha k_\beta) \end{aligned} \tag{3.7}$$

where

$$I = \frac{2\pi}{k^2}\sqrt{[k^2-(m_1-m_2)^2][k^2-(m_1+m_2)^2]}. \tag{3.8}$$

Applying this to our scenario by putting $m_1^2 = m_{\bar{\nu}_e}^2 = \xi_3' k^3$, $m_2^2 = m_{\nu_\mu}^2 = -\xi_3' p'^3$ and taking $k = p'/2 \sim p/4$, we find

$$\begin{aligned} I_{\alpha\beta}(p-k') = \frac{\pi}{6}\left[1+\frac{7}{64}\frac{\xi_3' p^3}{(p-k')^2}\right] \\ \left(\left[(p-k')^2+\frac{7}{32}\xi_3' p^3\right] g_{\alpha\beta} + 2\left[1-\frac{7}{64}\frac{\xi_3' p^3}{(p-k')^2}\right](p-k')_\alpha (p-k')_\beta\right) \end{aligned} \tag{3.9}$$

after contracting $I_{\alpha\beta}$ with the muon and electron momentums which respectively are p and k', we get

$$\begin{aligned} p^\alpha k'^\beta I_{\alpha\beta}(p-k') = \frac{\pi}{6}\left[1+\frac{7}{64}\frac{\xi_3' p^3}{(p-k')^2}\right] \\ \left(\left[(p-k')^2+\frac{7}{32}\xi_3' p^3\right](p\cdot k') + 2\left[1-\frac{7}{64}\frac{\xi_3' p^3}{(p-k')^2}\right](p\cdot p - p\cdot k')(p\cdot k' - k'\cdot k')\right) \end{aligned} \tag{3.10}$$

where,

$$\begin{aligned} p\cdot p &= m_\mu^2 \\ k'\cdot k' &= m_e^2 \approx 0 \\ p\cdot k' &= \vec{k}'(E_\mu - \vec{p}\cos\theta) \\ (p-k')^2 &= m_\mu^2 - 2\vec{k}'(E_\mu - \vec{p}\cos\theta). \end{aligned} \tag{3.11}$$

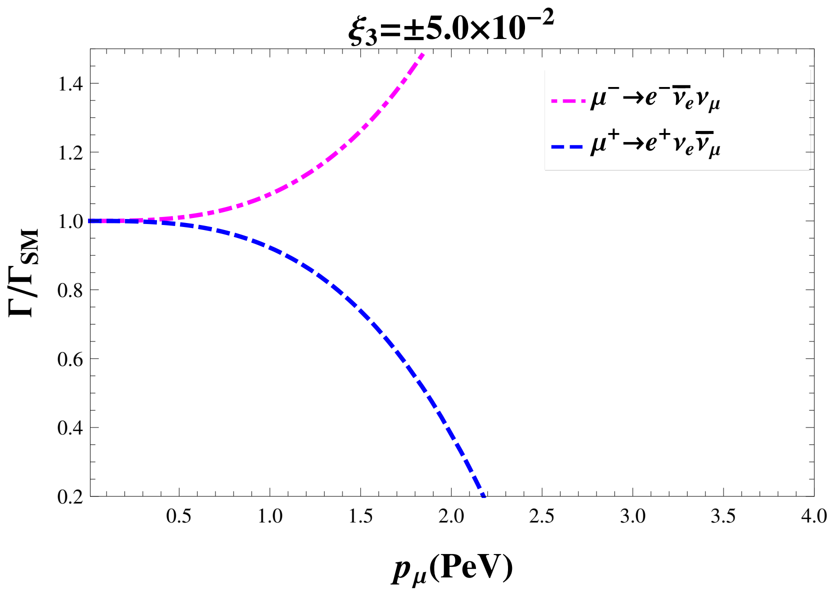

Figure 5. The ratio $\Gamma/\Gamma_{\rm SM}$ for $\mu^+ \to e^+\nu_e\bar{\nu}_\mu$ and $\mu^- \to e^-\bar{\nu}_e\nu_\mu$ processes in Lorentz invariance violating framework to its standard model prediction for superluminal antineutrino ($\xi_3 < 0$) and subluminal neutrino ($\xi_3 > 0$) final states as a function of muon momentum p_μ. Here we considered $\xi_3 = \pm 5.0 \times 10^{-2}$.

The decay width from eq. (3.5) can be written as,

$$\Gamma = \frac{32G_{\rm F}^2}{8(2\pi)^5}\frac{(2\pi)}{E_\mu}\int_{-1}^{1} d\cos\theta \int_0^{m_\mu^2/2(E_\mu - k\cos\theta)} k' dk' p^\alpha k'^\beta I_{\alpha\beta} \tag{3.12}$$

after solving it, we finally get,

$$\Gamma = \frac{G_{\rm F}^2 m_\mu^4}{192\pi^3 E_\mu}\left(m_\mu^2 + \frac{17}{80}\xi_3' p^3\right). \tag{3.13}$$

We compare our result with the standard model prediction of muon decay in a moving frame, which is

$$\Gamma_{\rm SM}(\mu \to e\bar{\nu}_e\nu_\mu) = \frac{G_{\rm F}^2 m_\mu^5}{192\pi^3}\frac{m_\mu}{E_\mu}. \tag{3.14}$$

We compute the muon decay rate for subluminal neutrino ($\xi_3 > 0$) and superluminal antineutrino ($\xi_3 < 0$) and obtain the following:

- The decay rate of the process $\Gamma(\mu^- \to e^-\bar{\nu}_e\nu_\mu)$ is enhanced, as shown in figure 5 for $\xi_3 = \pm 5.0 \times 10^{-2}$.

- The decay rate of the process $\Gamma(\mu^+ \to e^+\nu_e\bar{\nu}_\mu)$ is reduced, as shown in figure 5 for $\xi_3 = \pm 5.0 \times 10^{-2}$.

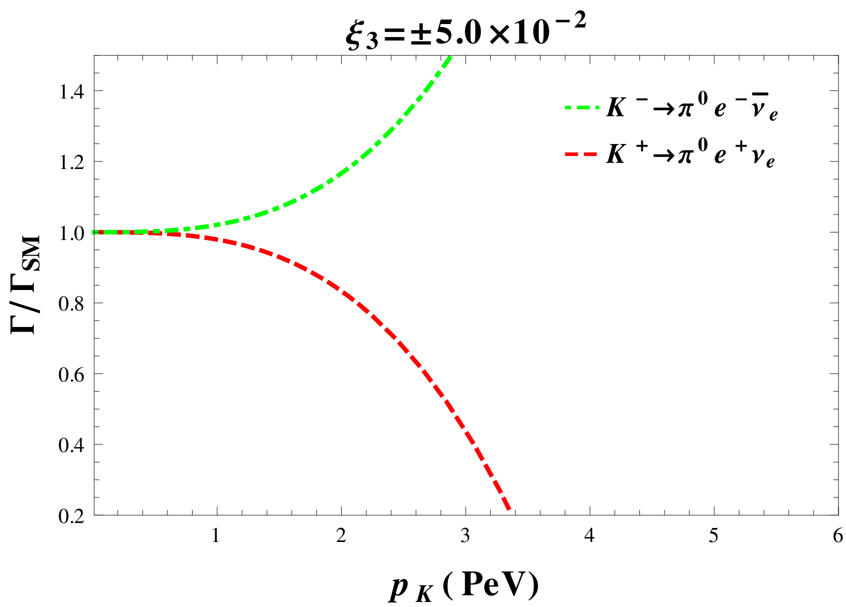

Figure 6. The ratio $\Gamma/\Gamma_{\rm SM}$ for $K^+ \to \pi^0 e^+ \nu_e$ and $K^- \to \pi^0 e^- \bar{\nu}_e$ processes in Lorentz invariance violating framework to its standard model prediction for superluminal $\bar{\nu}_e$ ($\xi_3 < 0$) and subluminal ν_e ($\xi_3 > 0$) final states as a function of kaon momentum p_K. We considered $\xi_3 = \pm 5.0 \times 10^{-2}$ for corresponding processes.

3.2 $K^+ \to \pi^0 e^+ \nu_e$

We also calculate 3-body kaon decay width using the modified dispersion relation for neutrino by taking $n = 3$ case. The amplitude calculation of kaon decay process $K^+(p_K) \to \pi^0(p_\pi) e^+(p_e) \nu_e(p_\nu)$ gives,

$$\overline{|M|^2} = 16 G_{\rm F}^2 |V_{us}|^2 f_+^2 [m_K^2 (p_K \cdot p_\nu + p_\pi \cdot p_\nu) - 2(p_K \cdot p_\nu)(p_K \cdot p_\pi) - 2(p_K \cdot p_\nu)(p_K \cdot p_\nu) - m_K^2 \xi_3' p_\nu^3] \tag{3.15}$$

where f_+ is the kaon form factor. The Decay width of kaon is,

$$d\Gamma = \frac{d^3 p_\pi}{(2\pi)^3 2E_\pi} \frac{d^3 p_{\nu_e}}{(2\pi)^3 2E_{\nu_e}} \frac{d^3 p_e}{(2\pi)^3 2E_e} \frac{\overline{|M|^2}}{2E_K} (2\pi)^4 \delta^4 (p_K - p_\pi - p_{\nu_e} - p_e) \tag{3.16}$$

which gives,

$$\Gamma \simeq \frac{G_{\rm F}^2 |V_{us}|^2 f_+^2 m_K^4}{768 \pi^3 E_K} \left[m_K^2 \left(1 - \frac{8 m_\pi^2}{m_K^2} \right) - \frac{4}{9} p_K^3 \xi_3' \left(1 - \frac{m_\pi^4}{m_K^4} \right) \right]. \tag{3.17}$$

It is clear from eq. (3.17) that the $K^+(K^-)$ decay rate goes down (up) as kaon momentum p_K increases, which is shown in figure 6 for $\xi_3 = \pm 5.0 \times 10^{-2}$.

3.3 $n \to p^+ e^- \bar{\nu}_e$

In the similar way like muon decay, we also calculate the neutron beta decay width using the modified dispersion relation for antineutrino. The spin averaged amplitude squared for the neutron decay process $n(p) \to p^+(k) e^-(k') \bar{\nu}_e(p')$ comes,

$$\overline{|M|^2} = 64 G_{\rm F}^2 (p \cdot p')(k \cdot k') \tag{3.18}$$

using eq. (3.18), we get the following decay width of neutron,

$$d\Gamma = \frac{32\ G_{\rm F}^2}{8(2\pi)^5 E_n}\frac{d^3k}{E_p}\frac{d^3k'}{E_e}\frac{d^3p'}{E_{\bar{\nu}_e}}\delta^4(p-k-k'-p')(p\cdot p')(k\cdot k') \tag{3.19}$$

we solve eq. (3.19) in the similar way like muon decay using generic phase space integral formula (eq. (3.7)). Then we solve the final integral over the electron energy, for which the minimum energy is the rest energy m_e of the electron while the maximum energy is approximately,

$$E_{\rm max} \approx m_n - m_p \tag{3.20}$$

which finally gives,

$$\Gamma \sim \frac{G_{\rm F}^2 (m_n-m_p)^3 m_n}{15\pi^3 E_n}\left[(m_n-m_p)^2 - \frac{5}{16}\xi_3' p^3\right]. \tag{3.21}$$

For $\xi_3 = 0.05$ the neutron decay width goes down at neutrino momentum $p \simeq 0.1\,\mathrm{PeV}$. This implies that antineutrino production from neutron decay will be suppressed and so in our model, it is also possible to explain the absence of Glashow resonance [5]. The decay rate of the charge conjugate process $\bar{n} \to \bar{p}e^+\nu_e$ is enhanced, but since only neutrons are produced in the $p+\gamma \to \Delta \to n+\pi^+$ processes at the source, the enhanced decay of $\bar{n}$ is not relevant to the IceCube events.

4 Conclusion

In this paper we provide a mechanism by which one can account for the lack of antineutrino events at Glashow resonance (6.3 PeV) at IceCube. We show that if the neutrino (antineurino) dispersion is modified by leading order Planck scale suppression $E^2 = p^2 - (\xi_3/M_{\rm Pl})p^3$ (where $\xi_3 > 0$ correspond to neutrinos and $\xi_3 < 0$ correspond to antineutrino), then there is a suppression of the π^+ decay width and corresponding neutrinos will be cutoff at energies $E_\nu = 1.3\,\mathrm{PeV}$ (with $\xi_3 = 0.05$). The neutrinos from Kaon decay $K^+ \to \mu^+\nu_\mu$ will be cutoff at 2 PeV.

- Three body decays like $\mu^- \to e^-\bar{\nu}_e\nu_\mu$ and $K^- \to \pi^0 e^-\bar{\nu}_e$ get enhanced due to different ξ_3 dependence in their $\overline{|M|^2}$, whereas three body decay widths of μ^+ and K^+ get suppressed.

- Neutron decay $n \to p^+e^-\bar{\nu}_e$ gets suppressed in the similar way as μ^+ decay. So if the source of $\bar{\nu}_e$ is neutron beta-decay then the mechanism proposed in this paper can be used to explain the absence of Glashow resonance at IceCube.

- Radiative three body decays like $\pi^\pm \to e^\pm\nu\gamma$ and $\pi^\pm \to \mu^\pm\nu\gamma$ are factorized to the $\overline{|M|^2}$ for two body decays $\pi^\pm \to e^\pm\nu$ and $\pi^\pm \to \mu^\pm\nu$ times α_{em} [23, 24] and these are also suppressed like two body decay processes.

The enhancement in μ^- decay will be significant at muon energies of 2 PeV and if the primary source of μ^- is π^- decay then there will be no observable consequence of this in

IceCube events. However such enhancement of the μ^- decay rate would be observable for μ^- produced not from π^- decay but e.g. via pair production e.g. in $e^+e^- \to \mu^+\mu^-$. The precise numerical values depend on the choice of the parameter ξ_3, but obviously a cutoff between $\sim 3\,\text{PeV}$ and $6.3\,\text{PeV}$ can be easily obtained in this model. We conclude that if neutrinos at Glashow resonance energies are not observed at IceCube then explanations in terms of new physics such as Lorentz violating modified neutrino dispersion relation become attractive. The fact that neutron decay into $p + e + \bar{\nu}_e$ is suppressed has the following implications. The conventional π/K decay neutrinos from astrophysical sources have cutoff in the range of $\sim 3\,\text{PeV}$. However the B-Z neutrinos which arise in GZK process have two components [25], the higher energy neutrinos from π/K will be more suppressed compared to the lower energy n decay to $\bar{\nu}_e$. But both components of GZK process will be suppressed at $E_\nu > 3\,\text{PeV}$.

Acknowledgments

One of us (S.P.) would like to thank Prof. Subhendra Mohanty and PRL for hospitality and support while this work was started, and to acknowledge the hospitality of Prof. Georg Raffelt and MPI, Munich while this work was continued. S.M. would like to thank Alan Kostelecky for valuable discussion.

A Dispersion relation

The cubic dispersion relation we used for neutrinos and antineutrinos can be obtained from the dimension 5 operator [9, 10],

$$\mathcal{L}_{\text{LV}} = \frac{1}{M_{\text{Pl}}}\bar{\psi}(\eta_1 \not{n} + \eta_2 \not{n}\gamma_5)(n\cdot\partial)^2\psi \tag{A.1}$$

where n_μ is a fixed four vector that specifies the preferred frame. Both the vector and axial-vector terms in eq. (A.1) are CPT violating in addition to being Lorentz violating. The Lagrangian gives the equation of motion,

$$i\not{\partial}\psi = -\frac{1}{M_{\text{Pl}}}(\eta_1 \not{n} + \eta_2 \not{n}\gamma_5)(n\cdot\partial)^2\psi \tag{A.2}$$

where we have taken $E \gg m$. This leads to the following dispersion relation for left and right handed particles ψ,

$$E^2 = p^2 + 2(\eta_1 \pm \eta_2)\frac{p^3}{M_{\text{Pl}}} \tag{A.3}$$

where $+$ and $-$ signs correspond to ψ_{R} and ψ_{L} respectively. Now taking the charge conjugation of eq. (A.1), we find

$$\mathcal{L}_{\text{LV}} = \frac{1}{M_{\text{pl}}}\bar{\psi}^c(-\eta_1 \not{n} + \eta_2 \not{n}\gamma_5)(n\cdot\partial)^2\psi^c \tag{A.4}$$

where we used charge conjugation properties viz. $C^{-1}\gamma_\mu C = -\gamma_\mu$ and $C^{-1}\gamma_\mu\gamma_5 C = \gamma_\mu\gamma_5$. The operator (eq. (A.4)) gives the following dispersion relation for left and right handed antiparticle ψ^c,

$$E^2 = p^2 + 2(-\eta_1 \pm \eta_2)\frac{p^3}{M_{\rm Pl}} \tag{A.5}$$

where the $+$ sign is for $\psi^c_{\rm R}$ and $-$ sign is for $\psi^c_{\rm L}$. Therefor for the case of left-handed neutrinos $\nu_{\rm L}$, we will have the dispersion relation,

$$E^2 = p^2 + 2(\eta_1 - \eta_2)\frac{p^3}{M_{\rm Pl}} \tag{A.6}$$

and for antineutrinos $\nu^c_{\rm R}$ we have,

$$E^2 = p^2 - 2(\eta_1 - \eta_2)\frac{p^3}{M_{\rm Pl}}\,. \tag{A.7}$$

We have dispersion relation for neutrinos and antineutrinos $E^2 = p^2 - (\xi_3/M_{\rm Pl})p^3$, where $\xi_3 = -2(\eta_1 - \eta_2)$ for neutrinos and $\xi_3 = 2(\eta_1 - \eta_2)$ for antineutrinos.

B Spinors relation

We assume that all the particles expect neutrinos follow the standard energy-momentum relation i.e.,

$$E_i = \sqrt{p_i^2 + m_i^2}, \tag{B.1}$$

where m_i and p_i are the mass and momentum of different particles ($i = e, \mu, \tau$ etc.). The neutrinos follow the modified dispersion relation given in eq. (2.1). There exist very stringent bounds [22], which suggest that neutrino flavor is independent of their dispersion relation, so we assumed the universal dispersion relation for different flavor of neutrinos. We also define,

$$F(p) \equiv \frac{E}{p} = 1 - \frac{\xi_n p^{n-2}}{2M_{\rm Pl}^{n-2}}, \tag{B.2}$$

where the function $F(p)$ is the measure of the deviation of neutrino dispersion relation from the standard one [26]. In this framework, the modified Dirac equation for neutrino can be written as,

$$(i\gamma^0\partial_0 - iF(p)\vec{\gamma}\cdot\vec{\partial})\psi(x) = 0 \tag{B.3}$$

where we have neglected the neutrino mass for simplification. Now we replace the Dirac field ψ in terms of the linear combination of plane waves i.e.,

$$\psi(x) = u(p)e^{-ip\cdot x} \tag{B.4}$$

using it, we get the following form of Dirac equation,

$$(\gamma^0 E - F(p)\vec{\gamma}\cdot\vec{p})u(p) = 0. \tag{B.5}$$

Clearly, the positive energy solution of this equation will satisfy,

$$E(p) = F(p)p, \tag{B.6}$$

we used these results in the derivation of the spinors sum of neutrinos, which comes,

$$\sum_{s=1,2} u^s(p)\bar{u}^s(p) = \begin{pmatrix} 0 & \tilde{p}\cdot\sigma \\ \tilde{p}\cdot\bar{\sigma} & 0 \end{pmatrix} \tag{B.7}$$

where we assumed neutrino to be massless and defined $\tilde{p} = (E, F(p)p)$. Following the Dirac algebra, we get the following result for spinor sum,

$$\sum_{s=1,2} u^s(p)\bar{u}^s(p) = \gamma^\mu \tilde{p}_\mu \equiv F(p)\gamma^\mu p_\mu \tag{B.8}$$

where we used the result of eq. (B.6) for further simplification. For antiparticle when $m = 0$, there is an overall negative sign in eq. (B.5) and following the same procedure we obtain the same result,

$$\sum_{s=1,2} v^s(p)\bar{v}^s(p) = F(p)\gamma^\mu p_\mu\,. \tag{B.9}$$

References

[1] IceCube collaboration, M.G. Aartsen et al., *First observation of PeV-energy neutrinos with IceCube*, Phys. Rev. Lett. **111** (2013) 021103 [arXiv:1304.5356] [INSPIRE].

[2] IceCube collaboration, M.G. Aartsen et al., *Evidence for High-Energy Extraterrestrial Neutrinos at the IceCube Detector*, Science **342** (2013) 1242856 [arXiv:1311.5238] [INSPIRE].

[3] IceCube collaboration, M.G. Aartsen et al., *Observation of High-Energy Astrophysical Neutrinos in Three Years of IceCube Data*, Phys. Rev. Lett. **113** (2014) 101101 [arXiv:1405.5303] [INSPIRE].

[4] IceCube collaboration, *34th International Cosmic Ray Conference (ICRC 2015)*, The Hague, The Netherlands, July 30–6 Augost 2015 [INSPIRE] and online at http://icrc2015.nl/.

[5] S.L. Glashow, *Resonant Scattering of Antineutrinos*, Phys. Rev. **118** (1960) 316 [INSPIRE].

[6] M.D. Kistler, T. Stanev and H. Yüksel, *Cosmic PeV Neutrinos and the Sources of Ultrahigh Energy Protons*, Phys. Rev. **D 90** (2014) 123006 [arXiv:1301.1703] [INSPIRE].

[7] L.A. Anchordoqui et al., *End of the cosmic neutrino energy spectrum*, Phys. Lett. **B 739** (2014) 99 [arXiv:1404.0622] [INSPIRE].

[8] J.G. Learned and T.J. Weiler, *A Relational Argument for a ∼ PeV Neutrino Energy Cutoff*, arXiv:1407.0739 [INSPIRE].

[9] J.S. Diaz, A. Kostelecky and M. Mewes, *Testing Relativity with High-Energy Astrophysical Neutrinos*, Phys. Rev. **D 89** (2014) 043005 [arXiv:1308.6344] [INSPIRE].

[10] R.C. Myers and M. Pospelov, *Ultraviolet modifications of dispersion relations in effective field theory*, Phys. Rev. Lett. **90** (2003) 211601 [hep-ph/0301124] [INSPIRE].

JHEP11(2015)022

[11] S. Mohanty and S. Rao, *Neutrino processes with power law dispersion relations*, *Phys. Rev.* **D 85** (2012) 102005 [arXiv:1112.2981] [INSPIRE].

[12] F.W. Stecker, S.T. Scully, S. Liberati and D. Mattingly, *Searching for Traces of Planck-Scale Physics with High Energy Neutrinos*, *Phys. Rev.* **D 91** (2015) 045009 [arXiv:1411.5889] [INSPIRE].

[13] A. Kostelecky and M. Mewes, *Neutrinos with Lorentz-violating operators of arbitrary dimension*, *Phys. Rev.* **D 85** (2012) 096005 [arXiv:1112.6395] [INSPIRE].

[14] J.S. Diaz, *Neutrinos as probes of Lorentz invariance*, *Adv. High Energy Phys.* **2014** (2014) 962410 [arXiv:1406.6838] [INSPIRE].

[15] F.W. Stecker and S.T. Scully, *Propagation of Superluminal PeV IceCube Neutrinos: A High Energy Spectral Cutoff or New Constraints on Lorentz Invariance Violation*, *Phys. Rev.* **D 90** (2014) 043012 [arXiv:1404.7025] [INSPIRE].

[16] L. Maccione, S. Liberati and D.M. Mattingly, *Violations of Lorentz invariance in the neutrino sector after OPERA*, *JCAP* **03** (2013) 039 [arXiv:1110.0783] [INSPIRE].

[17] V.A. Kostelecky and N. Russell, *Data Tables for Lorentz and CPT Violation*, *Rev. Mod. Phys.* **83** (2011) 11 [arXiv:0801.0287] [INSPIRE].

[18] P.A. Bolokhov and M. Pospelov, *Classification of dimension* 5 *Lorentz violating interactions in the standard model*, *Phys. Rev.* **D 77** (2008) 025022 [hep-ph/0703291] [INSPIRE].

[19] T.A. Jacobson, S. Liberati, D. Mattingly and F.W. Stecker, *New limits on Planck scale Lorentz violation in QED*, *Phys. Rev. Lett.* **93** (2004) 021101 [astro-ph/0309681] [INSPIRE].

[20] T. Jacobson, S. Liberati and D. Mattingly, *Lorentz violation at high energy: Concepts, phenomena and astrophysical constraints*, *Annals Phys.* **321** (2006) 150 [astro-ph/0505267] [INSPIRE].

[21] S. Sahu and L.S. Miranda, *Some possible sources of IceCube TeV-PeV neutrino events*, *Eur. Phys. J.* **C 75** (2015) 273 [arXiv:1408.3664] [INSPIRE].

[22] G.F. Giudice, S. Sibiryakov and A. Strumia, *Interpreting OPERA Results on Superluminal Neutrino*, *Nucl. Phys.* **B 861** (2012) 1 [arXiv:1109.5682] [INSPIRE].

[23] Particle Data Group collaboration, K.A. Olive et al., *Review of Particle Physics*, *Chin. Phys.* **C 38** (2014) 090001 [INSPIRE].

[24] J. Bijnens, G. Ecker and J. Gasser, *Radiative semileptonic kaon decays*, *Nucl. Phys.* **B 396** (1993) 81 [hep-ph/9209261] [INSPIRE].

[25] R. Engel, D. Seckel and T. Stanev, *Neutrinos from propagation of ultrahigh-energy protons*, *Phys. Rev.* **D 64** (2001) 093010 [astro-ph/0101216] [INSPIRE].

[26] M. Mannarelli, M. Mitra, F.L. Villante and F. Vissani, *Non-Standard Neutrino Propagation and Pion Decay*, *JHEP* **01** (2012) 136 [arXiv:1112.0169] [INSPIRE].